Mechanistic insights into ATP hydrolysis by the ABC transporter TAP

Dissertation

zur Erlangung des Doktorgrades
der Naturwissenschaften

vorgelegt beim
Fachbereich Chemische und Pharmazeutische
Wissenschaften (FB 14)
der Johann Wolfgang Goethe-Universität
in Frankfurt am Main

von
Min Chen
aus Jiangxi, China

Frankfurt/M 2004
(DF1)

vom Fachbereich **Chemische und Pharmazeutische Wissenschaften (FB 14)** der Johann Wolfgang Goethe-Universität als Dissertation angenommen.

Dekan: **Prof. Harald Schwalbe**

Gutachter: **Prof. Robert Tampé**

Datum der Disputation: **12-July-2004**

Publications related to this work:

Chen M, Abele R and Tampé: Role of the acidic residue downstream of the Walker B motif of the TAP complex. i*n preparation*.

Chen M, Abele R and Tampé R: Functional non-equivalence of ABC signature motifs in the transporter associated with antigen processing. *J Biol Chem*, submitted.

Chen M, Abele R and Tampé R: Peptides induce ATP hydrolysis at both subunits of the transporter associated with antigen processing. *J Biol Chem* 2003, **278**:29686-29692.

Janas E, Hofacker M, Chen M, Gompf S, van der Does C and Tampé R: The ATP hydrolysis cycle of the nucleotide-binding domain of the mitochondrial ATP-binding cassette transporter Mdl1p. *J Biol Chem* 2003, **278**:26862-26869.

Heintke S, Chen M, Ritz U, Lankat-Buttgereit B, Koch J, Abele R, Seliger B and Tampé R: Functional cysteine-less subunits of the transporter associated with antigen processing (TAP1 and TAP2) by de novo gene assembly. *FEBS Lett* 2003, **533**:42-46.

1. Introduction

1.1 MHC class I antigen presentation pathway

MHC class I molecules present peptides on the cell surface for surveillance by cytotoxic T lymphocytes (Gromme and Neefjes, 2002; Pamer and Cresswell, 1998). This antigen presentation pathway plays a central role in the cellular immune response to viral infected cells. The processes involved in conventional MHC class I antigen processing and presentation are depicted in Fig. 1-1.

In general, MHC class I molecules present peptides derived from endogenous antigens, although exogenous antigens were also shown to be presented by MHC class I molecules on the cell surface of phagesomes or dendritic cells in very recent studies (Ackerman et al., 2003; Guermonprez et al., 2003; Houde et al., 2003). Degradation of

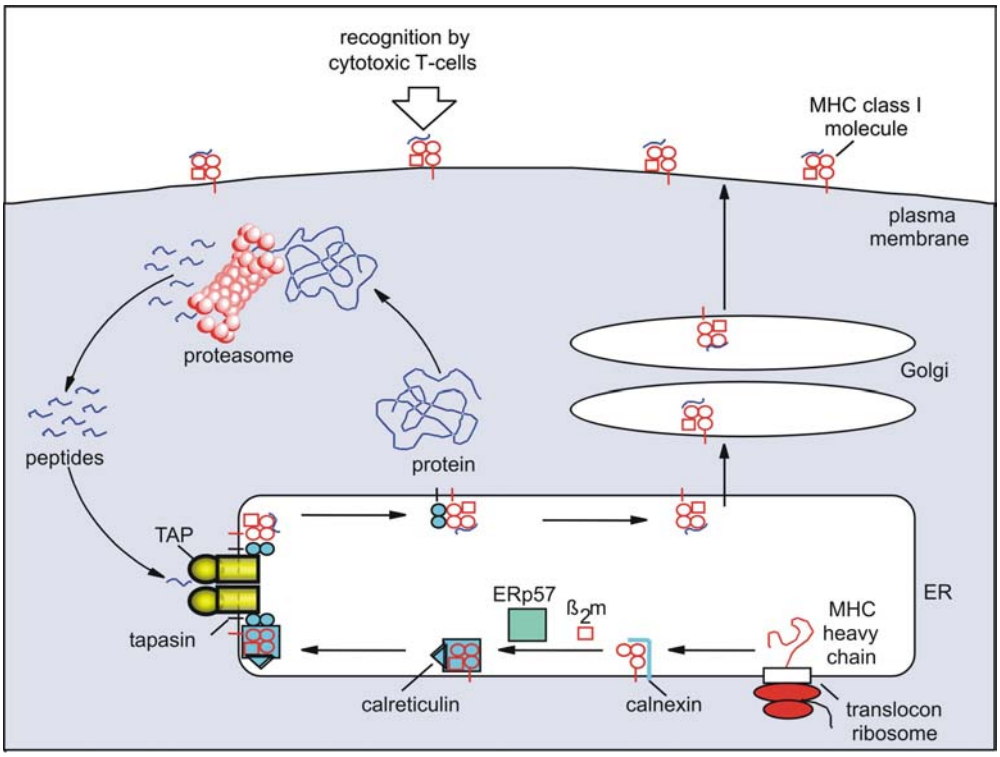

Figure 1-1. MHC class I antigen presentation pathway (Abele and Tampé, 1999). Endogenous antigens are degraded by the proteasome into short peptides. These peptides are transported into the ER lumen by TAP. In the ER, newly synthesized MHC class I heavy chains assemble with β_2m and peptide. This process involves transient interaction with calnexin, calreticulin, ERp57, tapasin and TAP. Upon peptide binding, the MHC complex is released from the ER and transported to the cell surface via the secretory pathway.

cytosolic antigens is essential for generation of MHC class I-presented epitopes. This process is mainly mediated by the proteasome complex (Bochtler et al., 1999; Rock and Goldberg, 1999). The proteasome contains a barrel-shaped 20S core particle that is proteolytically active and can degrade proteins in an ATP-independent fashion (Dick et al., 1994; Eggers et al., 1995). Most intracellular protein degradation, however, appears to be mediated by a larger protein complex that consists of the 20S core decorated by two additional 19S regulatory subunits, forming the 26S particle. The size of the peptides produced by proteosome distributes from 3-30 residues with an optimum length of 6-11 residues (Ehring et al., 1996; Kisselev et al., 1999). Interferon-γ stimulates the formation of the so-called immunoproteasomes (Akiyama et al., 1994; Fruh et al., 1994; Gaczynska et al., 1994; Nandi et al., 1996). This subpopulation of proteasomes cleaves after hydrophobic and basic residues in higher efficiency and increases the production of peptides that favor binding to MHC class I molecules (Aki et al., 1994; Ustrell et al., 1995). Although proteosome-dependent degradation of antigens contributes the majority of peptides for assembly with MHC class I molecules, there is also strong evidence that MHC class I can present peptides produced in the ER (Hammond et al., 1995; Henderson et al., 1992).

Peptides produced in the cytosol must pass through the ER membrane before they can be loaded onto the MHC class I molecules. This process is mediated by the transporter associated with antigen processing (TAP) (Abele and Tampé, 1999), which will be discussed in detail later. MHC class I molecules consist of a glycosylated transmembrane heavy chain (45 kDa) noncovalently associated with a 12 kDa soluble protein, β_2m, and a short peptide usually of 8-10 amino acids. Binding and presentation of peptides by MHC class I molecules are inextricably related to their structure (Madden, 1995). The heavy chain harbors three domains (α1-α3). α1 and α2 domains consist of two α-helices resting on a sheet of eight β-strands, forming the peptide-binding groove. The N- and C- terminal residues of the peptide are anchored to the opposite end of the peptide-binding groove via multiple hydrogen bonds and salt bridges, leaving the side chains of the central portion pointing outside the groove. Nevertheless, exceptions have also been reported that one or both ends of peptides can extend outside of the peptide-binding groove (Collins et al., 1994; Urban et al., 1994).

MHC class I molecules must fold into their native conformation in order to overcome ER quality control and exit ER for cell surface presentation. Many chaperones

are responsible for the correct assembly of MHC class I complexes (Paulsson and Wang, 2003). The newly synthesized MHC heavy chain is first bound to calnexin which ensures the proper folding and assembly of the MHC, thereby reduces its degradation (Hammond et al., 1994). Subsequently, β_2m associates with the heavy chain, and calnexin is exchanged for calreticulin (Peterson et al., 1995). A protein disulfide isomerase, ERp57, is believed to play a role in the formation of disulfide bonds of MHC class I molecules (Lindquist et al., 1998; Morrice and Powis, 1998). The association of the MHC class I- β_2m-calreticulin with TAP is bridged by tapasin (Sadasivan et al., 1996). The TAP, tapasin and MHC class I molecules, together with other chaperones (e.g. ERp57), form the multi-subunit peptide loading complex (PLC) in the ER membrane, which facilitates the loading of peptides onto MHC class I molecules (Hughes and Cresswell, 1998; Williams et al., 2002). Binding of a peptide is essential for the stability and transport of MHC class I molecules from the ER to the cell surface. Following peptide binding and release from the ER, MHC class I complexes are transported to the cell surface through the Golgi apparatus and the trans-Golgi network (TGN). At the plasma membrane, MHC class I molecules display their antigenic peptides for immune surveillance by cytotoxic T-lymphocytes (CTLs). Under normal circumstances, T-cell receptors (TCR) of CTLs do not recognize complexes containing “self” peptides. However, during viral infections or malignant transformations, a different spectrum of peptides is displayed by MHC class I molecules. T cells bearing the appropriate TCR will then recognize the peptide-MHC class I complex and eliminate diseased cells.

1.2 Overview of ABC transporters

The ATP-binding cassette (ABC) transporter superfamily contains membrane proteins that translocate a wide variety of substrates across biological membranes. Members of this family not only accomplish the uptake of nutrients but also are involved in a large variety of processes, such as signal transduction, protein secretion, drug and antibiotic resistance, antigen presentation, bacterial pathogenesis and sporulation (Higgins, 1992; Schneider and Hunke, 1998). ABC transporters have been identified in all organisms (bacteria, archaea and eukarya), and might thus be considered as an ancient protein device for solutes to pass through the lipid bilayer against a concentration gradient.

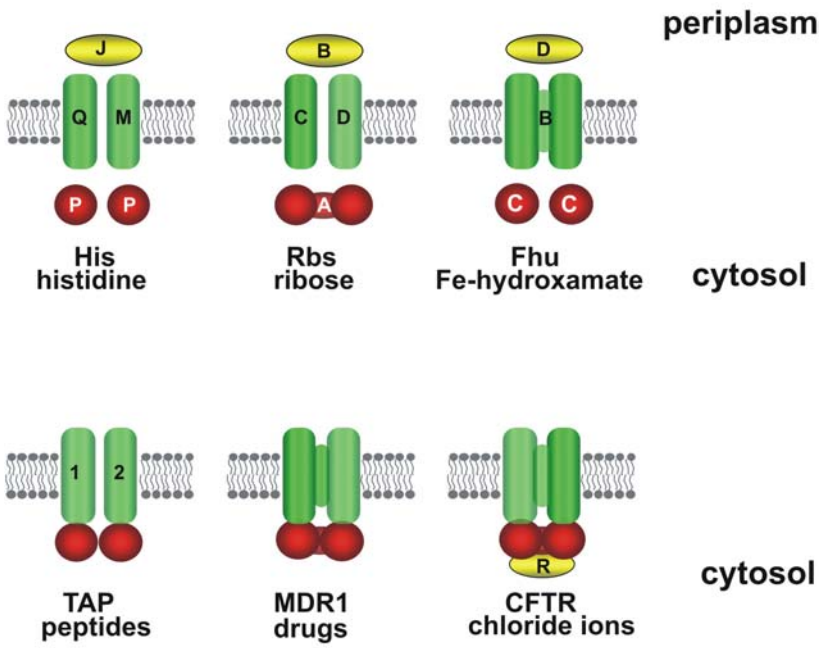

Figure 1-2. Organizations of four-domain structure in ABC transporters (Schmitt and Tampé, 2000). In bacterial import systems, the four domains are usually formed with separate domains (HisP). In some cases either TMDs or NBDs are fused (Flu, Rbs). The extracellular substrate-binding proteins (J, B, D) unique to this subclass are required for efficient uptake of the diluted solutes in the environment. In eukaryotic systems, four domains are generally fused into a polypeptide chain, such as Pgp and CFTR. In CFTR, an additional regulatory domain (R) is located between NBD1 and the following transmembrane domain. In some cases, two half transporters form a full functional complex as a heterodimer (TAP1/TAP2) or homodimer.

Typically, an ABC transporter is composed of four modules: two transmembrane domains (TMD), with each domain spans the membrane six times, and two nucleotide-binding domains (NBD) (Higgins, 1992). In eukaryots, the modules are mostly fused to yield a single polypeptide chain, while bacterial ABC transporters are built up from individual subunits (Fig. 1-2) (Higgins, 1992). In the bacterial importers, an additional substrate-binding protein with a high specificity for its solutes is generally presented in the transporter machinery. The NBDs of ABC transporters always contain two highly conserved motifs: Walker A (GxxGxGKT/S; x: any residues) and Walker B motifs (hhhhD; h: any hydrophobic residues) which are also present in other ATPases. In addition the NBDs also harbors the third characteristic sequence LSGGQ, which is specific to the ABC transporter family and termed C-loop or signature motif. By these criteria, a few proteins containing these three motifs have also been recognized as typical ABC proteins.

These proteins usually do not have a transmembrane domain and serve other functions. In contrast, the TMDs generally share little sequence homology among different ABC transporters and are specialized for the binding and translocation of their different substrates.

ABC transporters work unidirectionally. In bacteria, they are predominantly involved in the import of essential compounds (sugars, vitamins, metal ions, etc). In eukaryotes, most ABC transporters move compounds from the cytoplasm to the outside of the cell or into an intracellular compartment. Most of the known functions of eukaryotic ABC transporters involve the shuttling of hydrophobic compounds either within the cell as part of a metabolic process or outside the cell for transport to other organs or secretion from the body.

1.2.1 Structure of ABC transporters

ABC transporters are large membrane proteins. Earlier efforts have focused on determining the structure of the cytosolic soluble NBD. The first high resolution X-ray crystal structure emerged in 1998, which was the NBD of HisP, a histidine permease

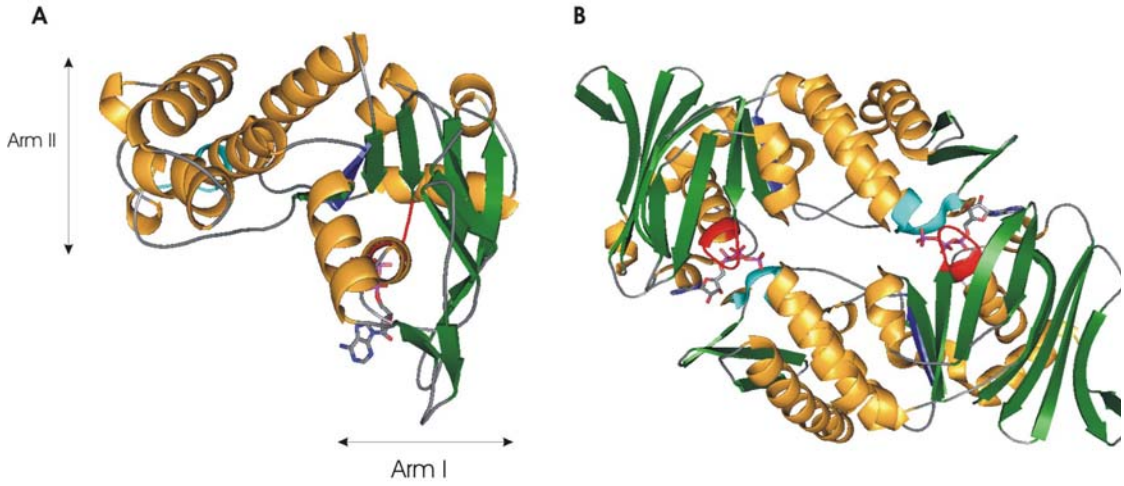

Figure 1-3. Structure of nucleotide-binding domain of ABC transporter. A, Structure of HisP monomer (Hung et al., 1998). The arm I contains the Walker A and Walker B motifs. Arm II contains mainly α-helices. α-Helices are shown in orange and β-sheets in green. The location of conserved motifs are indicated by different colors: Walker A, red; Walker B, blue; C-loop, cyan. The bound ATP is in ball and stick presentation. **B,** Structure of Rad50 dimer (Hopfner et al., 2000). Two monomers are orientated in a "head-to-tail" conformation. Two ATPs are sandwiched between the Walker A and B motifs from one domain and C-loop from the opposite domain.

(Hung et al., 1998). The HisP NBD monomer reveals a two-domain architecture, which are approximately perpendicular to each other (Fig.1-3A). Domain I mainly consists of α/β structure, containing the Walker A and B motifs and the helical domain II, harbors the signature motif. Two other conserved motifs, namely the Q-loop and the H-loop, are located at the interface of the two arms. Binding of a nucleotide is mainly contributed by the interaction between the phosphate moiety and the Walker A motif as well as the aromatic ring and the conserved tyrosine through π-π stacking. The crystal structure was reported as a dimer with the C-loop facing outward. Since then, a number of isolated NBDs have been crystallized in monomeric or dimeric conformation (Diederichs et al., 2000; Gaudet and Wiley, 2001; Hopfner et al., 2000; Karpowich et al., 2001; Smith et al., 2002b; Yuan et al., 2001). Although the structure of all monomers is very similar, publications about the NBD dimers introduced a controversial discussion about the dimer interface (Diederichs et al., 2000; Hopfner et al., 2000; Zhou et al., 2000). Recently, Hunt and co-workers reported MJ0796 structure from *Methanoccocus janaschii* (Smith et al., 2002a). In the crystal structure, the mutated ABC domain adopted a dimer interface that is identical to the one in Rad50 (Fig. 1-3B) showing a head-to-tail orientation. Within the dimer, two ATP molecules were sandwiched between the Walker A motif from one NBD and the signature motif from the other NBD. This dimer interface gained more support from the second MalK structure (Chen et al., 2003a). Further evidences also came from biochemical data obtained from MalK and Pgp (Fetsch and Davidson, 2002; Loo et al., 2002). Thus, the current established belief is that a sandwich dimer with a head-to-tail orientation forms during the transport process, in which key residues of both monomers participate together in binding and hydrolysis of each ATP (Schmitt and Tampé, 2002).

Substrate transport through the biological membrane by ABC transporters is a complex process including the communication between the substrate-binding site and the NBDs as well as the crosstalk between the two NBDs. Recently, the structures of two full length ABC transporters provide detailed information about the domain-domain interactions (Fig. 1-4) (Chang and Roth, 2001; Locher et al., 2002). MsbA from *E. coli*, a lipid flippase, is a close homolog to mammalian P-glycoprotein. MsbA was crystallized as a homodimer. Each monomer contains six transmembrane α-helices, which confirms the commonly proposed six-helices organization of the transmembrane domain of ABC transporters. The transmembrane domain has a cone-like structure with the top of the cone

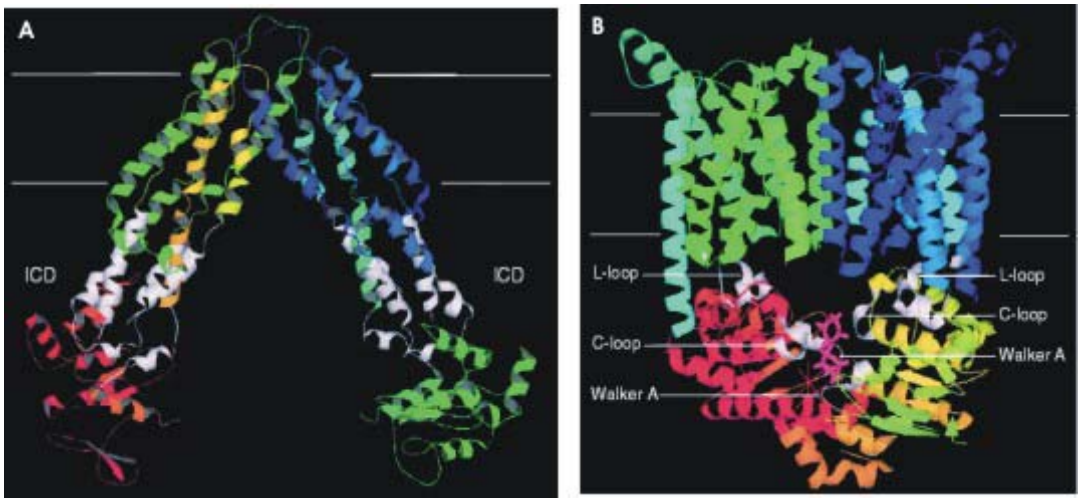

Figure 1-4. Structure of full length ABC transporters. A, Structure of MsbA (Chang and Roth, 2001). The ICD is highlighted in white and the white lines indicate the putative position and dimension of the lipid bilayer. **B,** Structure of BtuCD (Locher et al., 2002). Walker A and C-loop sequences are highlighted in white and labeled. The ligand, cyclotetravanadate, is shown in ball-and-stick representation. Figures were adapted from (Schmitt and Tampé, 2002).

pointing out of the cell. This structure is open at the cytoplasmic side of the membrane. The structure also shows a central chamber, which is easily accessible by substrates from the inner leaflet of the membrane, while excluding substrate from the outer leaflet. A large part of the NBD is invisible in this structure. In addition to the TMD and the NBD, a third domain was identified. The so-called intracellular domain (ICD) is composed of α-helices and located between the NBD and TMD. This arrangement led to the assumption that the ICD acts as a transducer unit, which transmits signals of nucleotide or substrate binding between the NBD and TMD. BtuCD, a protein mediating vitamin B12 uptake in *E.coli*, is the second ABC transporter that has been crystallized. It also shows a dimer structure, however, the transmembrane structure is composed of 10 helices instead of 6 helices per monomer. A large water-filled channel is formed by these 20 helices, which is closed on the cytoplasmic side. The ICD structure in MsbA has not been observed in the BtuCD, while the NBD directly interacts with TMD through so-called "L-loop", which is located between transmembrane helices 6 and 7. This loop folds into two helices and adopts an "L" shape, the sequence of which coincides with the "EAA" motif found in many bacterial ABC transporters (Mourez et al., 1997). The interaction between the NBDs resembles that

of Rad50 and MJ0796 EQ dimers. The structure of the two ABC transporters indicates that diversity in TMD packing might generally exist in ABC transporters in order to cope with a large variety of substrates and the communication between the TMD and NBD might be also different between the exporters and importers (Schmitt and Tampé, 2002).

1.2.2 Transport mechanism of ABC transporters

ABC transporters mediate the translocation of a large variety of solutes across the biological membrane. The detailed mechanisms by which ABC transporters move solute across the cell membrane are still unclear (Higgins, 2001). However, it is believed that substrate binding induces a conformational change in the TMDs which is then transferred to the NBDs to trigger ATP hydrolysis (Higgins, 2001). ABC transporters contain two nucleotide-binding domains, both of which are required for function. It is not fully understood why ABC transporters need two NBDs in one transport machine. An even more complicated question is how the two NBDs coordinate with each other to energize the transport event. Two representative models have been proposed based on the present findings:

In the case of the well studied ABC transporter Pgp, it is supposed to operate in an alternative manner (Sauna and Ambudkar, 2001; Senior et al., 1995). In this model, both NBDs are capable of binding and hydrolyzing ATP (Urbatsch et al., 1995a). There are two ATP hydrolysis events in one single turnover. The transport cycle is initiated by ATP binding to one of the randomly chosen NBD, preventing the other one from doing so. The second ATP binding and hydrolysis event can only occur after the hydrolysis of the first bound ATP. In other words, two ATP hydrolysis events occurred alternatively at each domain, which are functionally equivalent. Several observations provide strong support for this model: (i) the N- and C-terminal NBDs of Pgp have similar ATP binding properties since they are labeled with 8-azido-ATP to the same extent (Senior, 1998; Senior et al., 1998); (ii) vanadate trapping experiments showed that only one mole of MgADP was bound per mole of Pgp after hydrolysis of azido-ATP (Urbatsch et al., 1995b). The same stoichiometry was also found in maltose transport system (Chen et al., 2001; Sharma and Davidson, 2000); (iii) in addition, trapping of either ATP-binding site in the transition state prevents the second site from turning over. A close homologue to Pgp in *Lactococcus lactis*, LmrA seems also to act in an alternating fashion like a two-cylinder engine (van

Veen et al., 2000). However, the sequential mechanism of ATP binding from this model is challenged by a symmetric dimer structure containing two bound ATP molecules (Smith et al., 2002b).

By contrast, two NBDs of several ABC transporters, including MRP1, SUR1, CFTR and TAP do not seem to be functionally identical. In those complexes, nucleotides interact differently with the two NBDs (Aleksandrov et al., 2002; Hou et al., 2000; Karttunen et al., 2001; Matsuo et al., 1999). Mutations of the consensus Walker motifs in the two NBDs of MRP1 and TAP have different effects on substrate transport (Alberts et al., 2001; Daumke and Knittler, 2001; Lapinski et al., 2001). In contrast to Pgp, positive cooperativity in ATP binding has been observed for MRP1 (Hou et al., 2000; Hou et al., 2003). On the other hand, sequence difference in the conserved C-motifs between the two NBDs from these ABC transporters may also provide a hint to unequal functions. In the second nucleotide-binding domain, two critical residues (leucine and glycine) in the common signature motif (LSGGQ) are often substituted by other amino acids forming an irregular sequences xSxGQ. Therefore, this type of C-signature motif is usually called a "degenerated C-loop". Based on these, it was proposed that one NBD in the complex hydrolyses ATP to provide the energy for translocation, while the other one only binds ATP as a regulatory domain (Yang et al., 2003).

The NBDs of ABC transporters presumably undergo the following steps within one ATP hydrolysis cycle: (i) ATP binding, followed by (ii) ATP hydrolysis, (iii) dissociation of P_i, (iiii) release of ADP (Balakrishnan et al., 2003; Schmitt and Tampé, 2002). Three conformational stages are generated following the actions of the NBDs: ATP-associated state, a short-lived transition state in which both ADP and P_i remain bound and an ADP-bound state. It is not known at which stage of the transport cycle the energy is converted into the power stroke, which finally shuttles the substrate across the membrane. In other words, is the binding of ATP, its hydrolysis or the dissociation of inorganic phosphate or ADP the triggering step?

1.3 Transporter associated with antigen presentation

The first indication of peptide transporters was discovered from the studies of various mutant cell lines deficient in cell surface expression of MHC class I molecules, even though the expression levels of MHC class I heavy chain and β_2m are normal

(DeMars et al., 1985). The genes responsible for these defective phenotypes are *tap1* and *tap2* located in the MHC class II locus of human chromosome 6 (Trowsdale et al., 1991). Transfection of these cell lines with cDNA of TAP1 and TAP2 could restore cell surfaces expression of the MHC class I molecules (Attaya et al., 1992; Powis et al., 1991; Spies et al., 1992; Spies and DeMars, 1991). Heterologous expression of TAP1 and TAP2 in insect cells and yeast showed a functional peptide translocation in the absence of factors of the adaptive immune system (Meyer et al., 1994; Urlinger et al., 1997).

1.3.1 Structural organization

TAP1 and TAP2 are localized in the ER or *cis*-Golgi membrane as shown by immunoelectron and immunofluorescence studies (Kleijmeer et al., 1992; Meyer et al., 1994). Both proteins lack an N-terminal signal sequence for ER targeting, suggesting that the insertion of the proteins in the ER membrane may be promoted by an internal signal sequence. The functional peptide transporter is organized as a heterodimer containing TAP1 and TAP2 (Kelly et al., 1992; Spies et al., 1992).

TAP1 and TAP2 belong to the ABC transporter superfamily and are so-called half-size transporters composed of a hydrophobic transmembrane domain (TMD) followed by a highly conserved nucleotide-binding domain (NBD). The sequence identity within the NBDs is 60% whereas within the TMDs of TAP it is only 30%. As mentioned in the structure of ABC transporters, a 2×6 transmembrane helix model was proposed to be the core domain sufficient for substrate translocation. Based on hydrophobicity analysis, the human TAP1 and TAP2 contain 6-10 helix depending on the algorithm used. Sequence alignment with other ABC transporters show weak but significant similarity from TM1 through TM6, excluding the first 175 residues for hTAP1 and 140 for hTAP2. Based on these knowledge, a topological model was proposed for TAP complexes as shown in Fig. 1-5 (Abele and Tampé, 1999). Derived from such a model, the mini-TAP protein which only contains these 6 helices (TM 1-6) for each subunit can process full peptide transport activity (Koch et al., 2004). The hydrophobic N-terminal regions contain probably additional four and three transmembrane helices for TAP1 and TAP2, respectively (TM N1-N4 and TM N1-N3, N stands for N-domain as shown in Fig. 1-5), which were proven to be essential for interaction with tapasin (Koch et al., 2004).

The peptide-binding site of human TAP is contributed by the transmembrane domains of both subunits (Androlewicz et al., 1993; Androlewicz et al., 1994). Mapped by photo-crosslinking experiments, the cytosolic loops between TM4 and TM5 and a C-terminal stretch of approximately 15 amino acids after TM6 are shown to be involved in peptide binding (Nijenhuis and Hammerling, 1996; Nijenhuis et al., 1996). Deletion of some of these amino acids in the TAP1 region resulted in loss of peptide transport (Ritz et al., 2001).

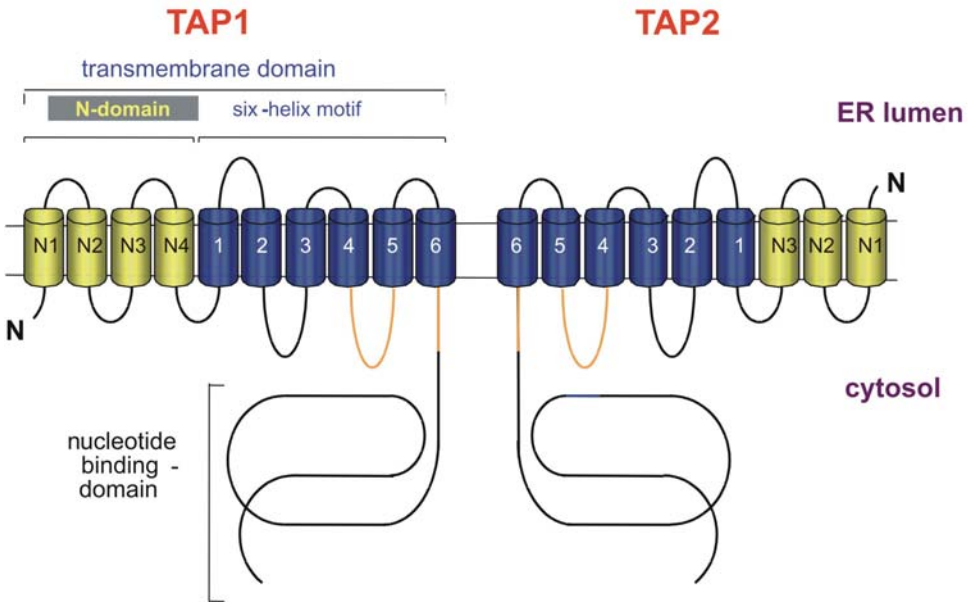

Figure 1-5. Membrane topology of the human TAP complex (Abele and Tampé, 1999). The transmembrane helices are predicted from hydrophobicity plots and sequence alignments with other ABC transporters. The unique N-terminal domains of TAP1 (N1-4) and TAP2 (N1-3) are very hydrophobic, comprising four and three predicted transmembrane helices, respectively (orange cylinders). Orange lines illustrate binding regions for peptides.

1.3.2 Peptide specificity

The first information about substrate specificity of TAP was obtained by comparing the sequence of peptides transported into the ER or bound to MHC class I molecules (Androlewicz et al., 1993; Neefjes et al., 1993b). Peptides of 8-12 amino acids long were observed to be transported most efficiently, whereas van Endert et al. showed an optimal

length for peptide binding is 8-16 amino acids (Koopmann et al., 1996; van Endert et al., 1994). Nevertheless, peptides of 6 or 40 amino acids in length are also transported by TAP albeit in considerable lower efficiency (Koopmann et al., 1996). As previously mentioned, the optimal length of peptides for loading to MHC class I molecules is 8-10 amino acids. TAP transports peptides with similar or slightly larger length suitable for MHC class I binding. ERAAP, ER aminopeptidase associated with antigen processing, is reported to be responsible for further trimming of the transported peptides in the ER (Falk and Rotzschke, 2002; Saric et al., 2002; Serwold et al., 2002; York et al., 2002).

In addition to the size of the peptide, its sequence also determines the efficiency of translocation by TAP. The recognition principle of TAP was resolved by screening combinatorial peptide libraries (Uebel et al., 1997). In this method, the average affinity of a randomized peptide mixture with one residue in common was compared with a totally randomized peptide library. Hence, the influence of each amino acid on the affinity for TAP could be determined. The first three N-terminal and the last C-terminal residues were found to be most critical for peptide-binding specificity (Fig. 1-6A). At the N-terminus, human TAP generally displays preferences for peptides with Lys, Asn and Arg in the first, Arg in the second, and Trp and Tyr in the third position. The C-terminal residue is preferred to be a hydrophobic or basic residue by human TAP. It is noteworthy that the peptide-binding spectrum of TAP and MHC class I molecular overlap in their C-terminal residue, suggesting that the binding principle of TAP and MHC class I molecule coevolved. Furthermore, substrate recognition by TAP is also strictly stereospecific. Introducing the D-amino acids at two opposite terminals of peptides causes complete abrogation of transport (Gromme et al., 1997; Uebel et al., 1997). Acetylation or methylation of the N-terminus or conversion of the C-terminal carboxyl group of a peptide to an amide decreases its translocation efficiency considerably (Momburg et al., 1994; Schumacher et al., 1994). Circular peptides, which lacks of a free termini are generally not a substrate for TAP. Indicated by the structure of MHC class I molecule, the hydrogen bonds between the two termini and MHC class I molecules contribute largely to the free energy of binding. Therefore, TAP was expected to apply an analogous strategy for peptide binding. The residues in the center of the peptide have only a little or no effect on the substrate specificity of TAP. Interestingly, these residues are responsible for the detection of the MHC class I–bound peptide by the T-cell receptor. In conclusion, TAP binds peptides

through the two termini and transports them with maximal diversity in the center of the peptide for T-cell recognition (Fig. 1-6B).

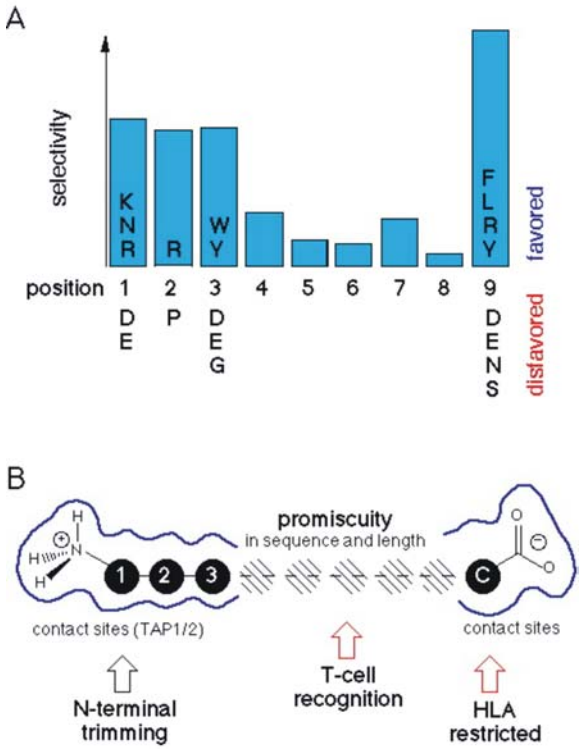

Figure 1-6. Substrate recognition motif of human TAP (Abele and Tampé, 1999). **A**, TAP selectivity is illustrated for positions of the peptide. Favored (upper) and disfavored residues (lower) are given at the individual positions as elucidated using combinatorial peptide libraries. **B**, A model of the substrate-binding pocket is shown in the lower panel.

1.3.3 ATP binding and hydrolysis

ABC transporters hydrolyze ATP to provide the energy for translocation of substrate across the biological membrane. In addition to serve as a energy source, ATP appears to be also an allosteric regulator for TAP (Karttunen et al., 1999). It was found that nucleotides and peptides play a critical role in stabilizing the TAP heterodimer at 37°C (van Endert, 1999). Knittler and colleagues reported that release of the MHC class I molecules from a mutated TAP complex, which could not bind ATP as a result of

mutations in the Walker A site, requires addition of ATP, ADP or even a non-hydrolysable ATP analogue (Knittler et al., 1999). The most surprising observation made in this study was that peptide binding was disrupted in this mutated TAP complex, indicating nucleotide binding plays a critical role in binding of peptide to TAP and the subsequent release of MHC class I molecules (Knittler et al., 1999). However, this concept is contradictory to previous studies on wild-type TAP, in which peptide binding to TAP was not affected by depletion of ATP using apyrase (Androlewicz et al., 1994; Neefjes et al., 1993b).

Peptide transport by TAP strictly requires ATP hydrolysis, as ADP or non-hydrolysable ATP derivatives are unable to support peptide transport (Neefjes et al., 1993b; Uebel et al., 1997; van Endert et al., 1994). Successful reconstitution of partially purified TAP into proteoliposomes has recently allowed direct measurement of the ATPase activity of the peptide transporter (Gorbulev et al., 2001). The Michaelis–Menten constant of ATP hydrolysis (300 μM) is similar to that of other ABC transporters. Moreover, peptides stimulate ATP hydrolysis in a manner that is proportional to their TAP affinity, demonstrating crosstalk between the peptide and nucleotide-binding sites. A single TAP complex was found to hydrolyze about a maximum of five molecules of ATP per second.

Both NBDs seem to be essential for efficient peptide transport. It was found that the rat TAP chimeras containing two identical NBD possessed no peptide transport activity (Daumke and Knittler, 2001); whereas another group still observed a reduced but significant transport activity in similar constructs of human TAP (Arora et al., 2001). In contrast, chimeras with two switched NBDs generally retain the peptide transport ability (Arora et al., 2001; Daumke and Knittler, 2001). However, it is not known whether ATP hydrolysis by TAP1, TAP2, or both is needed for a completion of ATP hydrolysis cycle. In the TAP chimeras having the switched NBDs, the nucleotide binding properties of each individual NBD are conserved independent of the TMD linked with, indicating that NBDs operate as independent modules. The study also showed that the C-terminal tails of the two NBDs are responsible for maintaining their intrinsic property of the NBD (Bouabe and Knittler, 2003).

TAP1 and TAP2 showed distinct roles in the study of peptide transport in different TAP mutants. Mutation of the critical lysine residue at Walker A motif of TAP2 abolishes the peptide transport; by contrast, complexes with the identical mutation at TAP1 showed low but consistent transport activity (Karttunen et al., 2001; Lapinski et al., 2001; Sauna et

al., 2001b). Furthermore, rat TAP complexes bearing the substitution of proline-asparagine (GPNG) with serine-serine (GSSG) of Walker A at TAP2 almost lost the peptide transport ability, whereas TAP1 mutants behaved as wild type protein (Alberts et al., 2001). These results suggest that ATP hydrolysis at TAP1 might not be essential for the peptide transport.

1.3.4 Viral inhibitors

Viruses have evolved several mechanisms to interfere with TAP function in order to evade CTL-mediated immune responses.

The herpes simplex virus (HSV) type 1 and 2 encoding immediate early protein ICP47 blocks release of MHC class I molecules from the ER (Hill et al., 1994; York et al., 1994). ICP47 inhibits binding and translocation of peptides from the cytosol into the ER lumen without interfering with ATP binding (Fruh et al., 1995). ICP47 from HSV type I is an 88 amino acid (9 kDa) cytosolic polypeptide that binds to TAP with high affinity (50 nM) (Ahn et al., 1996; Fruh et al., 1995; Hill et al., 1994). Residues 3-34 are the minimum sequence which can form an active region responsible for TAP binding and subsequent inhibition of TAP function (Galocha et al., 1997; Neumann et al., 1997). Interaction of ICP47 with the TAP complex is species-specific, since murine TAP is not efficiently inhibited by ICP47 from human simplex virus (Ahn et al., 1996; Fruh et al., 1995). In aqueous solution, the active domain of ICP47 (residues 3-34) appears to be mainly unstructured, but in the presence of negatively charged lipid membranes, it adopts an ordered helix-loop-helix structure (Beinert et al., 1997; Pfander et al., 1999). However, the TAP-bound conformation of ICP47 remains to be established. The binding mode of ICP47 to TAP is probably different from that of peptides, as peptides stabilize the TAP heterodimer, whereas ICP47 has a destabilizing effect on TAP in cross-linking studies (Lacaille and Androlewicz, 1998). In addition, N-acetylated peptides cannot bind to TAP (Neefjes et al., 1993a), whereas N-acetylation of ICP47 has no effect on TAP inhibition (Galocha et al., 1997).

The human cytomegalovirus (HCMV) US6 glycoprotein also inhibits TAP-mediated peptide loading of MHC class I molecules (Ahn et al., 1997; Hengel et al., 1997; Lehner et al., 1997). The open reading frame of US6 encodes a 184 amino acid (21 kDa) type I membrane protein composed of a leader sequence (19 aa), an ER-luminal domain

(125 aa), a transmembrane helix (21 aa) and a short cytoplasmic tail (18 aa). The ER-luminal domain of US6 is sufficient for ER retention and inhibition of TAP activity (Ahn et al., 1997; Hengel et al., 1997; Kyritsis et al., 2001). Unlike ICP47 interfering with peptide binding, US6 applies a different strategy to block TAP function. It interacts with TAP from the ER-luminal side, and inhibits ATP binding but not ADP binding to TAP in the cytosol (Hewitt et al., 2001; Kyritsis et al., 2001; Lehner et al., 1997). The mechanism of TAP inhibition by US6 is still largely unknown. It is hypothesized that US6 induces a conformational change in TAP and maintains that conformation, thus it prevents ATP from binding to TAP (Kyritsis et al., 2001).

1.4 Objective

The transport associated with antigen processing (TAP) is essential for translocation of peptides generated by degradation within the ubiquitin-proteasome pathway into the ER, where loading of MHC class I molecules occurs. Up to now, the principle of the substrate recognition and specificity of TAP has been established. Despite this, little is known about the mechanism by which the nucleotide-binding domain hydrolyses ATP to provide the energy for peptide translocation. Thus the goal of the present work is to gain insight into the mechanistic aspect of ATP hydrolysis by the nucleotide-binding domains of TAP.

Firstly, the question whether both nucleotide-binding domains are involved in hydrolyzing ATP was addressed. Although both nucleotide-binding domains of TAP complex are required for peptide transport, no data has directly proven their catalytic functions. Clarifying this point will provide a fundamental view on the function of the two NBDs. An important task was to develop a method to study the ATP hydrolysis properties of each subunit in TAP complex respectively. Consequently, direct evidence of two catalytic NBDs of TAP was presented.

Secondly, biochemical studies of TAP Walker A mutants indicated that the TAP subunits are functional asymmetric in the ATP hydrolysis cycle. The discrepancy in the conserved C-loop of the two NBDs provides the sequence basis for the asymmetry. The question arises: what is the role of the non-equivalent C-loops of TAP1 and TAP2 in inducing asymmetric function of two NBDs? The effect of the mutation in C-loops of

TAP1 and TAP2 was analyzed to deduce the function of the two C-loops in the transport cycle.

Thirdly, the knowledge how ATP binding/hydrolysis is coupled to the structure rearrangement of the transmembrane domain is essential for understanding the translocation mechanism of ABC transporters. To study this coupling process, we mutated the putative catalytic base to identify a low affinity peptide-binding site and its concomitant state of NBDs, which were proposed to occur within the ATP hydrolysis cycle for ABC transporters. In addition, the role of the putative catalytic base in the TAP complex was addressed.

2. Material

2.1 Chemicals

Table 2-1. Chemical list

Chemicals	Company
$AlCl_3$	Sigma-Aldrich GmbH
5-Amino-2,3-dihydro-1,4-phthalazinedione-3-aminophthalhydrazide (Luminol sodium salt)	Sigma-Aldrich GmbH
8-Azido-[γ-^{32}P]ATP or 8-azido-[α-^{32}P]ADP	ICN
8-Azido-biotin-ATP	Affinity labeling technology
Acrylamid 30% (w/v)	National Diagnostics
Adenosine-5'-diphosphate (ADP)	Fluka Chemie GmbH
Adenosine-5'-triphosphate (ATP)	Fluka Chemie GmbH
Apyrase	Sigma-Aldrich GmbH
ATP-agarose (C8 or N6 linked)	Sigma-Aldrich GmbH
BaculoGold™ Transfection Kit	BD bioscience pharmingen
BCA-kit	Pierce
Benzonase	Merck
$BeCl_2$	Sigma-Aldrich GmbH
Biobeads SM-2	New England Biolabs
BSA	Sigma-Aldrich GmbH
Calf intestine alkine phosphatase	Fermentas
Chloramine T	Riedel-de Haen
Concanavalin A-sepharose	Sigma-Aldrich GmbH
D-(+)-desthiobiotin	Sigma-Aldrich GmbH
β-D-decylmaltoside	Calbiochem
DeepVent polymerase	Biolabs
Digitonin	Calbiochem
Dimethylsulfoxide	Fluka Chemie GmbH
4-(4,5-Diphenyl-2-imidazolyl)-benzeneboronic acid (DPA)	Sigma-Aldrich GmbH
Dowex 1 x 8 anion exchange	Sigma-Aldrich GmbH
Enhanced ChemiLuminescence system (ECL)	Amersham Pharmacia
Ethylendiaminetetraacid (EDTA)	Carl Roth GmbH

Ex-Taq polymerase	Takara
Fatal bovine serum	Biochrom AG
Hexokinase	Sigma-Aldrich GmbH
HiTrap desalting column	Amersham Pharmacia
trans-4-Hydroxycinnamic acid (p-Coumaric acid)	Sigma-Aldrich GmbH
Hyperfilm chemiluminescence film	Amersham Pharmacia
Iodoacetamidoflourescein	Molecular Probes
Igepal (NP40)	Sigma-Aldrich GmbH
Isopropyl-ß-D-thiogalactopyranoside (IPTG)	BTS-BioTech Trade& Service GmbH
MultiScreen plates with glass fibre filter, pore size 1.0 µm	Millipore
Megaprime DNA labeling system	Amersham Pharmacia
$Na^{125}I$	Amersham Pharmacia
Nucleospin plasmid kit	Machery-Nagel GmbH & Co. KG, Düren
β-D-Octylglycoside	Calbiochem
Penicillin/Strepmycin (100x)	PAA laboratories GmbH
Pfu DNA polymerase	Promega
Phoshatidylcholine	Avanti Lipids
Phosphatidylethanolamine	Avanti Lipids
Plasmid midi kit	Qiagen GmbH
Pluronic F-68 (10%)	Invitrogen
Polycarbonate filters (200 nm)	Avestin
Polyethylenimine cellulose plates	Merck
Ponceau Red S	Sigma-Aldrich GmbH
Protein A (or G) agarose	Sigma-Aldrich GmbH
Proteinase K	Sigma-Aldrich GmbH
Pwo DNA polymerase	Roche Diagnostics
QIAquick gel extraction kit	Qiagen GmbH
QIAquick spin PCR purification kit	Qiagen GmbH
Restriction enzymes	MBI fermentas
$ScCl_2$	Sigma-Aldrich GmbH
Sephadex G-50 columns	Amersham Pharmacia
Sepharose A	Sigma-Aldrich GmbH
SF900II medium	Invitrogen

Streptactin	IBA GmbH
Streptavidin alkine phosphatase conjugate	IBA GmbH
Superdex 75 30/10	Amersham Pharmacia
Superose 200 HR 11/15	Amersham Pharmacia
Superose 6	Amersham Pharmacia
T4 DNA ligase	MBI Fermentas
N,N,N‘,N‘-Tetramethylethylendiamin (TEMED)	Sigma-Aldrich GmbH
Texas Red	Molecular Probes
Trypan blue solution (0.4%)	Sigma-Aldrich GmbH

2.2 Oligomers

Table 2-2. Primer sequences used for cloning.*

Name	Sequence
TAP1for(BamHI)	GAG CTC GGA TCC GTG ACA ATG GC
TAP1rev1	GGA TCG GCC CTC TAG ATG CAT G
TAP1rev-2	TCG GCC CTC TAG ATG CAT GCT CGA GCG GCC GCC
TAP1-Spel-f (SpeI)	CTC CTG GAC CAC TAG TAT TTC AGG TAT G
TAP1-Cloop-f(Mut sg-AA)	GCT GGG AGC CAG CTG GCA GCG GGT CAG CGA CAG GCA
TAP1-Cloop-r(Mut sg-AA)	TGC CTG TCG CTG ACC CGC TGC CAG CTG GCT CCC AGC
TAP1Mut(GD)PCR1rev	CTG CCT GTC GCT GAT CCC CTG ACA GCT G
TAP1Mut(GV)PCR1rev	CTG CCT GTC GCT GAA CCC CTG ACA GCT G
TAP1Mut(LA)PCR1rev	CTG ACC CCC TGA CGC CTG GCT CCC AGC
TAP1Mut(GD)PCR1for	CAG CTG TCA GGG GAT CAG CGA CAG GCA G
TAP1Mut(GV)PCR1for	CAG CTG TCA GGG GTT CAG CGA CAG GCA G
TAP1Mut(LA)PCR1for	GCT GGG AGC CAG GCG TCA GGG GGT CAG
TAP1 D668Q-F	GTA CTT ATC CTG GAT CAG GCC ACC AGT GCC CTG G
TAP1 D668N-F	GTA CTT ATC CTG GAT AAT GCC ACC AGT GCC CTG G
TAP1 D668Q-r	CCA GGG CAC TGG TGG CCT GAT CCA GGA TAA GTA C
TAP1 D668N-r	CCA GGG CAC TGG TGG CAT TAT CCA GGA TAA GTA C
TAP2nXhoI-f	CAT CAT CTC GAG ATG CGG CTC CCT GCC CTG AGA CC

TAP2XhoI-f	CAT CAT CTC GAG CAT GCG GCT CCC TGC CCT GAG ACC
TAP2-Bsp1407I-f	GCG GAG AAG GTG TAC AAC ACC CGC CAT CAG
TAP2-SphI-r*	GTA GCA TGC TCC TAG AGC TGG GCA AGC TTC
TAP2-Sphl-r	TTT GCG CAT GCT CCT AGA GCT GGG CAA GC
TAP2-Cloop-r(Mut aa-SG)	CGT TGT TTC TGT CCC CCA GAC AGC TGG CTT CCC TTC
TAP2-Cloop-f(Mut aa-SG)	GAA GGG AAG CCA GCT GTC TGG GGG ACA GAA ACA ACG
TAP2Mut(LA)pcr1-r	GTC CCG CAG CCG CCT GGC TTC CCT TCT C
TAP2Mut(LA)PCR2-f	GGA AGC CAG GCG GCT GCG GGA CAG AAA C
TAP2Mut(GV)pcr1-r	TGT TTC TGT ACC GCA GCC AGC TGG CTT C
TAP2Mut(GV)pcr2-f	GCT GGC TGC GGT ACA GAA ACA ACG TC
TAP2Mut(GD)pcr1-r	TGT TTC TGG TCC GCA GCC AGC TGG CTT C
TAP2Mut(GD)pcr2-f	GCT GGC TGC GGA CCA GAA ACA ACG TCT G
TAP2 E632Q-f	GGG TCC TCA TCC TGG ATC AGG CTA CTA GTG CCC TAG
TAP2 E632Q-R	CTA GGG CAC TAG TAG CCT GAT CCA GGA TGA GGA CCC

*The mutation sites or the restriction sites are underlined.

Table 2-3. Primers used for verifying the recombinant Bacmid DNA

Primers	Sequence
TAP2-Bsp1407I-f	GCG GAG AAG GTG TAC AAC ACC CGC CAT CAG
M13-f	TGT AAA ACG ACG GCC AGT
M13-r	CAG GAA ACA GCT ATG ACC

Table 2-4. Primers used for TAP1 sequencing

Primers	Sequence
1F1	CTGCTTTGAA GCCATTAG
1F2	CAGTGCAGTG CTGGAGTTC
1F3	CATTGAGGCT CTGTCG
1F4	ACTCCCTT ACACTTGGAG

1F5	CTCCCTCAG GGCTATGAC
1R1	TGCGGGCAGTGCCGCTGC
RG 4 1B	GCC ATG CGA GAG AAG CTC
RG4 H1	ATG GCT AGC TCT AGG TGT
RG4 H2	CTG GCT GGC TGC TTT GAA
RG4 H3	CTC GGA GAC GCG CCG CCT
RG4 H4	GGA GAC GGA GTT TTT CCA
RG4 H5	AAG TCC AGC CAG GTG GCC
RG4 H5B	AGGTGCGGGAATCTCTGGCA
RG4 H6	TGC AGT TCA CCC AGG CTG
RG4 H7	CTG GGA AGA GCA CAG TGG
RG4 H8	ATG ACA CAG AGG TAG ACG
RG4 H8B	AGG CTG GGA GCC AGC TGT CA
RG4 II	CAC CAG CAG CTC ATG GAG

Table 2-5. Primers used for TAP2 sequencing

Primers	Sequence
RG11 H1	TGA CTG TCT CCC TGA G
RG11 H2	TGG GAG GTG ATT TTG ACC
RG11 H3	GCT CAG CAT ATC GCC TCG
RG11 H4	GCC TTG TAC CTG CTC GTA AG
RG11 H5	GAC AGG CCT GTG CTC AAG GG
RG11 I	CCC TGA AGC AGC CAC AGT
RG11 IB	GGC TGG GGG AGC ACG TGA GG
RG11 II	AGG CTG CAG ACA GTT CAG
RG11 IIB	GAC TTC ATC CAG GAA ATG GA
RG11 R1	CTT CTC CCC TAC ATC TGT
RG11 R2	TCA CCT CAC CAG GAC GTA
RG11 R3	ATC TGC TGC AGC CCA CAG CT
RG11 R4	CAT GTG CAG CAG AGA AAG GA
SeqTAP2-f1	CCC CAG CCA GAG TCG CTT C
SeqTAP2-f3	GTT TTG GGG C CG AGG AGC
SeqTAP2-f4	TCC CAA TCG CCC TGA CAG

SeqTAP2-f5	GAA GCC AGC TGG CTG CGG
SeqTAP2-r1	CCC TGG AGA GCT TCA GCA

2.3 Peptides

Table 2-6. Peptide used in this work

Peptides	Sequence
C4F	RRYCKSTEL (Cysteine labeled with fluoresein)
R9LQK	RRYQKSTEL
D-R9LQK	D-RRYQKSTEL
R9NST	RRYQNSTEL
E9D	EPGNTWDED
ICP47 (2-34)	SWALEMADTFLDTMRVGPRTYADVRDEINKRGR

2.4 Antibodies

Table 2-7. Antibody list

Antibody	Type	Protein	Recognition site
148.3	Monoclonal	TAP1	CYWAMVQAPADAPE
435.3	Monoclonal	TAP2	NBD
429.3	Monoclonal	TAP2	NBD
1P1	Polyclonal	TAP1	GRLTDWILQDGSA
1P2	Polyclonal	TAP1	ETEFFQQNQTGNIMSR
1P3	Polyclonal	TAP1	TVRSFANEEGEAQKFR
1P4	Polyclonal	TAP1	SEKIFEYLDRTPR
2P1	Polyclonal	TAP2	RVIDILGGDFD
2P2	Polyclonal	TAP2	RIREQLFSSLL
2P3	Polyclonal	TAP2	EAVGGLQTVRSFGAEE
2P4	Polyclonal	TAP2	VGAAEKVFSYMDRQPN

3. Methods

3.1 Molecular cloning

3.1.1 E. coli culturing

E. coli DH5α cells were grown in LB-medium (10 g trypton, 5 g yeast extract, 10 g NaCl per liter) at 37°C. If not indicated, 100 μg/ml ampicillin (final concentration) were added after autoclaving. *E. coli* DH10Bac was grown in LB-medium containing 50 μg/ml kanamycin and 10 μg/ml tetracycline. After transformation with pFastBacDual, 7 μg/ml gentamicin was added into the agar plates for selection.

3.1.2 Competent E. coli cells (calcium-mediated)

An overnight culture of *E. coli* DH5α cells was diluted 1:50 in 100 ml LB-medium and grown at 37°C to an OD_{600} of 0.5. The culture was cooled down and the cells were harvested at 1,000 g for 10 min at 4°C. The cell pellet was carefully resuspended in 10ml sterile, ice-cold 0.1 M $CaCl_2$ and incubated on ice for 90 min. After centrifugation the pellet was resuspended in 2 ml ice-cold 0.1 M $CaCl_2$ and 400 μl 87% glycerol. Cell aliquots of 100 μl were frozen in liquid nitrogen and stored at –80°C. To make *E. coli* DH10Bac competent cell, the same procedure was applied except for LB-medium containing 50 μg/ml kanamycin and 10 μg/ml tetracycline.

3.1.3 Transformation of competent E. coli

Competent *E. coli* cells were strictly thawed on ice for 10 min. Plasmid DNA (10ng to 1 μg) was dissolved in 10 μl water, mixed with 100 μl of competent cells and incubated on ice for 30 min. The suspension was transferred to 42°C for 90 sec (heat shock). The cells were regenerated in 1 ml LB-medium for 1 h at 37°C with vigorous shaking. The cell suspension was centrifuged (1,000 g, 10 min, 25°C) and plated on pre-warmed (37°C) LB-agar plates supplemented with the appropriate antibiotics and incubated overnight at 37°C.

3.1.4 DNA preparation, processing and electrophoresis

To obtain highly purified plasmids for sequencing, DNA was isolated by MN Mini kit (MACHEREY-NAGEL GmbH & Co. KG, Germany). For restriction analysis, the plasmids were prepared by alkaline lysis method: cell pellets from 3 ml overnight culture were suspended in 0.3 ml 15 mM Tris-HCl (pH 8.0), 10 mM EDTA, 100 μg/ml RNase A,

followed by gently mixing with 0.3 ml 0.2 M NaOH, 1% SDS for 5 min. After that, 0.3 ml of 3 M potassium acetate (pH 5.5) was slowly added to the mixture. Samples were incubated on ice for 4 min and then centrifuged at 14,000 g for at least 10 min. The supernatant was mixed with 0.8 ml isopropanol and incubated on ice for a minimum of 5 min. Samples were then centrifuged at 14,000 g for 15 min. After removing the supernatant, pellets were washed once with 70% ethanol and dried by air. Finally, DNA pellets were redissolved in 50 µL 5 mM Tris, pH 8.5, which was ready for restriction analysis or cloning.

Restriction enzyme digestion was performed in a DNA to enzyme ratio of 1 µg to 10 units under conditions (temperature and buffer) as suggested by the manufacturer. Before electrophoresis, DNA samples were mixed with loading buffer (10 fold: 40% sucrose (w/v), 0.25% bromphenol blue, xylenecyanol in TE-buffer). DNA fragments were analyzed in 1% agarose gels in TAE-buffer (40 mM Tris-acetate pH 8.0, 1 mM EDTA) and stained with ethidium bromide. DNA fragments were extracted from gel using QIAGEX extraction kit (Qiagen GmbH, Germany).

To reduce religation of vector with blunt ends, dephosphorylation was performed. Routinely, 1-2 µg DNA in a total volume of 50 µl was incubated with 1 unit phosphatase (calf intestine) in 1x manufacturer's reaction buffer for 1 h at 37°C. The enzyme was heat inactivated at 72°C for 10 min.

Ligation was performed by incubating vector DNA with a 3-10 excess of insert DNA with T4-DNA ligase in 1x manufacturer's reaction buffer overnight at 16°C. The total reaction volume of ligation reaction was kept to 20 µL. Before transformation, the sample was incubated at 60°C for 10 min to inactivate T4-DNA ligase.

PCR (Polymerase Chain Reaction) was used to amplify insert DNA using 10 ng plasmid DNA as template. For PCR of high fidelity, Pwo-polymerase (MBI Fermentas GmbH, Germany) or DeepVent (New England Biolabs GmbH, Germany) were used according to manufacturer's instructions.

Clones were checked via restriction analysis. Positive clones were verified by DNA sequencing (Scientific Research & Development GmbH, Germany).

3.1.5 Plasmids construction for generation of baculovirus

The plasmids construction can be divided into three steps (Fig. 3-1):

In the first step, *tap1* and *tap2* wild type cDNA were inserted into pFastBacDual separately. TAP1 was amplified by PCR with the primers (TAP1for and TAP1rev2) taking p46-TAP1 (from Dr. Seliger, Mainz) as template. The PCR product containing BamHI and NotI sites was cloned into the pFastBacDual vector; For TAP2 cloning, primers TAP2nXhoI-f and TAP2-SphI-r and template p46-TAP2 (from Dr. Seliger, Mainz) were used to form pFastBacDual-TAP2. In addition, TAP2 was also inserted into vector pSL1180 using the same restriction sites.

In the second step, mutations were introduced into pFastBacDual-TAP1 and pFastBacDual-TAP2. For generation of TAP C-loop single mutants, three-step overlapping PCR was carried out for the full *tap* gene (Fig. 3-2a). Primer pair used for TAP1 amplification was TAP1for and TAP1rev-2; for TAP2 was TAP2nXhoI-f and TAP2-Sphl-r. Mutagenesis PCR products were exchanged with their wild type fragments in pFastBacDual-TAP1 and pFastBacDul-TAP2. However, extra mutations introduced by PCR became a general problem. Therefore, shorter templates were applied during construction of C-loop exchange mutants, which are between SpeI and NotI restriction sites of tap1 gene and Bsp1407 and SphI sites of tap2 gene. Mutagenesis PCR products were cloned into pFastBacDual-TAP1 and pSL1180-TAP2 by substituting the wild type fragments.

For generation of TAP1 D668Q/N and TAP2 E653Q mutants, quick exchange mutagenesis kit (Stratagene, USA) was used as manufacture's instruction with vectors pFastBacDual-TAP1 and pSL1180-TAP2 as template (Fig.3-2B). After introducing the mutations, the fragments between SpeI and NotI sites of TAP1 as well as Bsp1407 and SphI sites of TAP2 were cut out and exchanged with their wide type in pFastBacDual-TAP1 and pSL1180-TAP2.

In the third step, TAP2 mutant gene fragments were cut from the pSL1180-TAP2 or pBastBacDual-TAP2 using XhoI and SphI and were subsequently ligated into pFastBacDual-TAP1, ending up with pFastBacDual-TAP1/2 bearing double genes.

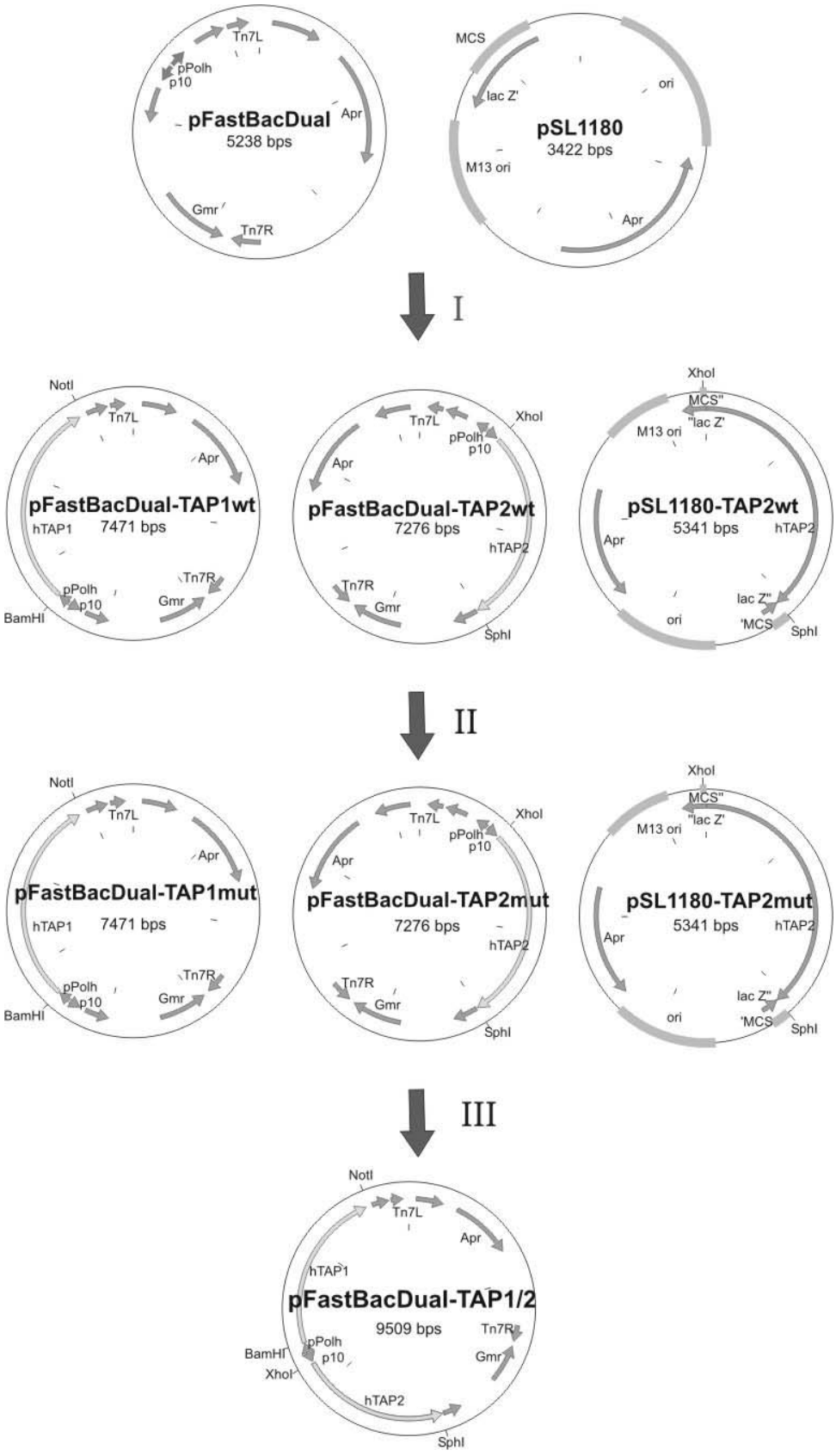
Tn7L
pPolh
p10
pFastBacDual
5238 bps
Apr
Gmr
Tn7R
MCS
lac Z'
ori
pSL1180
3422 bps
M13 ori
Apr
I
NotI
Tn7L
Apr
pFastBacDual-TAP1wt
hTAP1
7471 bps
Tn7R
pPolh
p10
Gmr
BamHI
Tn7L
XhoI
pPolh
p10
Apr
pFastBacDual-TAP2wt
7276 bps
hTAP2
Tn7R
Gmr
SphI
XhoI
MCS"
"lac Z'
M13 ori
pSL1180-TAP2wt
5341 bps
hTAP2
Apr
lac Z"
ori
'MCS
SphI
II
NotI
Tn7L
Apr
pFastBacDual-TAP1mut
hTAP1
7471 bps
Tn7R
pPolh
p10
Gmr
BamHI
Tn7L
XhoI
pPolh
p10
Apr
pFastBacDual-TAP2mut
7276 bps
hTAP2
Tn7R
Gmr
SphI
XhoI
MCS"
"lac Z'
M13 ori
pSL1180-TAP2mut
5341 bps
hTAP2
Apr
lac Z"
ori
'MCS
SphI
III
NotI
Tn7L
Apr
hTAP1
pFastBacDual-TAP1/2
9509 bps
Tn7R
pPolh
p10
Gmr
BamHI
XhoI
hTAP2
SphI

Figure 3-1. Constrution of TAP variants expression vector (previsous page). The construction of TAP expression vector was followed by three steps: **I**, cloning of TAP1 into pFastBacDual via BamHI and NotI, resulting pFastBacDual-TAP1; Cloning of TAP2 into pFastBacDual or pSL1180 via XhoI and SphI, resulting pFastBacDual-TAP2 or pSL1180-TAP2. **II**, based on these vectors, mutagenesis was carried out by PCR (shown by Fig. 3-2). **III**, TAP2 fragment was cut out and insert into pFastBacDual-TAP1, ending up with pFastBacDual-TAP1/2

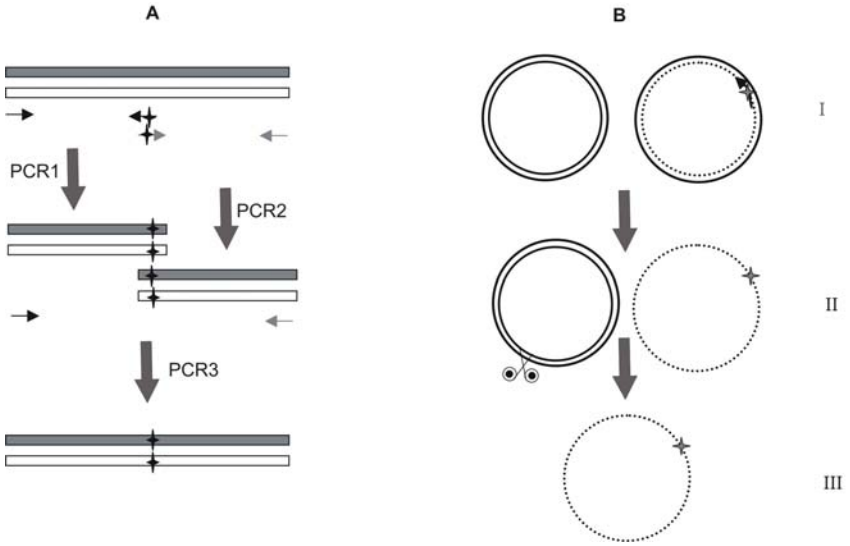

Figure 3-2. Introduction of mutation by PCR. A, three steps overlapping mutagenesis PCR. The gene was subdivided into two parts and amplified by PCR1 and PCR2 respectively. Full-length gene bearing the site-direct mutation was re-synthesized by PCR3. DNA Polymerases creating an 'a'-overhang should be avoided for this method. **B,** quick change mutagenesis. step I: a thermal cycling step to achieve multiple rounds of mutant strand synthesis; step II: digestion of parental DNA via Dpn I; step III: transformation of ssDNA into competent cells.

3.1.6 Transposition in DH10Bac

100 µL of competent DH10Bac cells were thawed on ice. 1 µL of DNA from mini-prep (usually 0.5 µg/µL) was added to the cells and the mixture was incubated on ice for 30 min. Then, cells were heat-shocked at 42°C for 45 seconds and immediately transferred to 4°C for 2 min. 1 ml SOC media was added and cells were subsequently incubated at 37°C for 4 hours. Cells were then spinned down and diluted serially with SOC medium (20g tryptone, 5 g yeast extract, 0.5 g NaCl, 0.186 g KCl in 970 ml H_2O; after autoclaving,

5ml sterile solution of 2 M $MgCl_2$ and 20 ml 1 M glucose were added just before use) to 10^{-1}, 10^{-2} and 10^{-3}. 100 µL mixture of each dilution was plated onto LB agar plates containing 50 µg/ml kanamycin, 7 µg/ml gentamicin, 10 µg/ml tetracycline, 100 µg/ml Bluo-Gal and 40 µg/ml IPTG. Plates were incubated at 37°C for at least 36 hours for development of blue-white colonies. The whites clonies were amplified to isolate the recombinant Bacmids for transfection of insect cells.

3.2 Cell culture

3.2.1 Culture of Raji cells

Human Burkitt lymphoma cells (Raji cells) were propagated in roller bottles at 37°C and 5% CO_2 in RPMI medium 1640 supplemented with 10% FCS, 1 mM sodium pyruvate, and 40 units/ml each of penicillin and streptomycin. Cell density of the culture was generally maintained at $3\sim9\times10^6$ cells/ml.

3.2.2 Monolayer culture of insect Sf9 cells

Spodoptera frugiperda (Sf9) monolayer culture was kept in SF900 II medium (including 10 units/ml Penicilin, 0.1 mg/ml Streptomycin, 0.2% pluromic acid and 5% fetal calf serum). Before passage, medium and floating cells from a confluent monolayer were discarded by aspiration. 10 ml of prewarmed SF900 II medium was added to 75 cm^2 flask. Cells were then detached from the surface by tapping the flask. 2.5 ml of the cell mixture was diluted into a new flask in 10 ml medium and incubated at 27 °C.

3.2.3 Shaker culture of insect Sf9 cells

Sf9 cells were maintained in SF900 II medium for monolayer culture with or without serum. The culture flask was incubated at 27°C in less than 1/4 of the total flask volume until it reaches a cell density of 2×10^6 cells/ml. Then cells were diluted to 0.4×10^6 cells/ml with fresh medium. The cultures must be avoided to reach stationary phase at any time (for cells in Sf-900 II SFM this is a density of 5×10^6 cells/ml).

3.2.4 Transfection of Sf9 cells

2×10^6 Sf9 cells were seeded onto a 60 mm tissue culture plate. Initial cell density should be 50-70% confluent. Cells were incubated at 27°C for 1 hour to allow them to attach firmly onto the plate. Then the culture medium was removed and 1 ml of

transfection buffer A (BaculoGold™) was added to the plate. All areas of the plate should be covered by this buffer. 5 µg bacmid DNA from mini-prep was mixed with 1 ml transfection buffer B. Subsequently the mixture was added to the plates drop by drop. After every two or three drops, the plate should be gently rotated to facilitate the mixing of buffer B with buffer A. Following incubation of the plate at 27°C for 4 hours, the transfection solution was removed and 3 ml of fresh SF900 II medium was added to the cells. The plate was incubated at 27°C for 5-7 days before new recombinant virus (P1 stock) can be harvested.

3.2.5 Amplification of virus

3 ml P1 virus stock harvested from transfection generally has a titre of 1 x 10^7 pfu/ml. Virus were amplified two times before going for infection of cells in a large scale. 10 ml P2 was obtained by infecting 1.2 x 10^6 cells monolayer in 75 cm^2 flask for 5 days with 1 ml P1 stock; after that, 25 ml P3 can be harvested from infection of 3 x 10^7 cells with 3 ml in 175 cm^2 flask for 5 days. All media used for the amplification of virus contained FCS.

3.2.6 Infection of Sf9 cells for protein production

450 ml shaker culture of Sf9 cells were grown at 27°C in serum free medium in a Fernbach flask to a density of 2 x 10^6 cells/ ml. 25 ml of virus stock P3 was added and the culture was continually incubated until 30% cell death rate was achieved. Subsequently cells were harvested by centrifugation at 200 g for 5 min. Cell pellets were washed with 20 ml PBS once and kept frozen at –20°C.

3.2.7 Determination of virus titre by plaque assay

Sf9 cells (1 x 10^6 cells) was seeded into 35 mm petri dishes and incubated at room temperature for 2 hours. Virus stock was diluted in serial from 10^{-1}, 10^{-2} to 10^{-7}. After removal of the medium from the culture, 100 µl virus dilution was added to the dishes, which were incubated at room temperature outside the hood for 1 hour with gentle agitation every 15 min. During incubation, the agarose solution was prepared by combining 8 ml medium with 4 ml 3% low melting agarose (plus 120 µL X-gal 25 mg/ml in DMF). After that, the viral solution was removed and 2 ml of 1% agarose solution was added onto each dish. When the agarose solidified, 1 ml medium was overlaid on it. The

dishes were kept at 27°C for 3-4 days and then stained with 1 ml Neutral Red/PBS solution (1 vol of 0.4% neutral red to 19 vol of PBS). After incubation at 27°C in the dark for 2 hours, the liquid was removed. Incubation of inverted dishes overnight resulted in several white plaques in dark red background. Each plaque is generated by infection of Sf9 cells with an individual baculovirus particle, therefore the total amount of the virus can be determined.

3.3 General biochemical methods

3.3.1 SDS-PAGE (mini gel)

The stacking gel buffer is composed of 0.5 M Tris-HCl, pH 6.8 and 0.4% SDS. The running gel buffer contains 1.5 M Tris-HCl, pH 8.8 and 0.4% SDS. The acrylamide solution consists of 30% acrylamide and 0.8% N,N´-methylenebisacrylamide. Stock aliquots of 10% ammonium peroxodisulphate (APS) are prepared in water and stored at -20°C.

Before electrophoresis the proteins were denatured in 3x sample buffer (150 mM Tris pH 6.8, 6% SDS, 30% glycerol, 0.3% bromphenolblue and freshly added 40 mM DTT). Soluble proteins were incubated for 5 min at 95°C and membrane proteins were incubated for 15 min at 65°C. The SDS electrophoresis was performed at 120 V for 1-1.5 hour in running buffer (25 mM Tris, 192 mM glycine, 0.1% SDS, pH ~8.3).

Table 3-1. Composition of stacking and running gel according to Laemmli (Laemmli, 1970)

	Stacking gel	Running gel		
	5%	7.5%	10%	12%
Acrylamide	6.8 ml	18 ml	24 ml	29 ml
Stacking gel buffer	5 ml	-	-	-
Running gel buffer	-	18 ml	18 ml	18 ml
H_20	28 ml	36 ml	30 ml	25 ml
APS	320 µl	470 µl	470 µl	470 µl
TEMED	32 µl	40 µl	40 µl	40 µl

3.3.2 SDS-PAGE (maxi gel)

To resolve TAP1 and TAP2 subunits with SDS-PAGE, a big gel electrophoresis system (gel size: L×W=30×20 cm) was used. The composition of gel is shown in table 3-2. The stacking gel buffer is composed of 0.5 M Tris-HCl, pH 6.8; the running gel buffer

contains 2 M Tris-HCl, pH 8.8; the acrylamide solution was the same as for the mini gel. Sucrose solution was 60%. The SDS electrophoresis was performed at constant 20 mA for 24 h in running buffer (50 mM Tris, 384 mM glycine, 0.1% SDS, pH ~8.6).

Table 3-2. Composition of stacking and running gel according to Laemmli (Laemmli, 1970)

	Stacking gel 5%	Running gel 11%
Acrylamide	5 ml	29.3 ml
Stacking gel buffer	4ml	-
Running gel buffer	-	16 ml
Sucrose (60%)	7 ml	-
H_20	14 ml	33 ml
SDS (10%)	300 µL	800 µL
APS	150 µL	240 µL
TEMED	15 µL	40 µL

3.3.3 Western blotting

To transfer proteins from the gel onto nitrocellulose, a blotting sandwich was prepared with the following layers: 1) filter paper soaked in transfer buffer (25 mM Tris, 192 mM glycine, 20% methanol, pH 8.2), 2) gel, 3) membrane soaked in transfer buffer (in the case of PVDF membrane, it should be soaked in methanol for 1 min previously), 4) filter paper soaked in transfer buffer. The sandwich was set onto a semidry blotting apparatus (Bio-Rad Laboratories GmbH, Germany) with the nitrocellulose/PVDF membrane facing the anode. The electroblotting was performed at constant current (100 mA per mini gel) for 90 min. To determine the efficiency of the transfer process, the membrane was stained with Ponceau Red (0.1% Ponceau Red S, 5% acetic acid) for 5 min, and washed with water until defined bands were visible. For immunodetection the membrane was blocked with blocking buffer (TBS-T: 10 mM Tris-HCl pH 8.0, 150 mM NaCl, 0.1% (v/v) Triton X-100, including 7% (w/v) skim milk powder and 0.1% (w/v) NaN_3) for at least 30 min at RT or overnight at 4°C. The membrane was incubated at RT for 1 h with the primary antibody diluted in TBS-T buffer. After 3 times washing with TBS-T for 10 min, the membrane was incubated with horseradish peroxidase conjugated second antibodies (1:10,000) for 1 hour. Subsequently, the membrane was washed again 3 times and incubated with 10 ml ECL1 buffer (2.5 mM luminol sodium salt, 0.4 mM

coumaric acid in 100 mM Tris, pH 8.5) for 5 min, followed by 10 ml ECL2 buffer (6.4 µL 30% H_2O_2 in 10 ml 100 mM Tris, pH 8.5) for 30 sec. The chemiluminescent signal was detected by a LumiImager.

3.3.4 Stripping of immunoblots

To develop the same western blot with different antibodies, membranes were stripped with stripping buffer (150 mM glycine, pH 3.0) for 1 hour at room temperature and washed afterwards with TBS, 0.1% Triton X-100 before extensive blocking (at least 1 h) and incubation with the next antibody. For a harsher method, the membrane was incubated in stripping buffer containing 50 mM Tris, pH 6.7, 100 mM mercaptoethenal, 2% SDS (w/v) for 20 min at 50°C before the washing step.

3.4 Biochemical assays for TAP

3.4.1 Preparation of microsomes

Sf9 cell pellets (10^9 cells from 500 ml culture) were thawed and resuspended in 3 volume of cavitation buffer (50 mM Tris, pH 7.5, 250 mM sucrose, 25 mM K_2Ac and 4 mM MgAc) plus 1 mM DTT and protease inhibitors (50 µg/ml AEBSF hydrochloride, 1 µg/ml aprotinin, 10 µg/ml leupeptin, 5 µg/ml pepstatin A and 150 µg/ml benzamidin). After incubation on ice for 30 min, cells were then homogenized by a glass douncer and centrifuged at 200 g for 2 min followed by 700 g for 7 min. The resulting supernatants were loaded on the top of the sucrose gradient, which contained 5 ml 2.7 M sucrose buffer (50 mM Tris, pH 7.5, 2.7 mM sucrose, 150 mM K_2Ac, 5 mM MgAc and 0.5 mM CaAc), overlaid with 6 ml 1.8 M sucrose buffer and 5 ml 0.4 M sucrose buffer. The sucrose gradient was centrifuged at 103,000 g overnight in a SW-28 rotor. The microsomes were harvested from the 1.8 M / 0.4 M sucrose interphase and diluted with 2 volumes of PBS, pH 7.0, 1 mM DTT. The suspension was centrifuged at 160,000 g in Ti50 rotor for 20 min. The pellet was resuspended in 5 ml PBS, pH 7.0, 1 mM DTT, and aliquots were frozen in liquid nitrogen and stored at –80°C. Microsomes from Raji cells were prepared following the same procedure, except that the cavitation buffer contains 10 mM HEPEs, pH 7.4, 5mM $MgCl_2$ and 0.5 mM $CaCl_2$.

3.4.2 Peptide labeling with $Na^{125}I$

Peptides were iodinated using the chloramine T-method (Hunter and Greenwood, 1964). Chloramine T solution (1 mg/ml) and sodium bisulfite (0.17 mg/ml) were freshly prepared in PBS, pH 7.0. The reaction was routinely performed with 1.5 nmol peptide in a total volume of 50 µl and 1 µl (100 µCi) $Na^{125}I$. The reaction was started by addition of 10µl chloramine T. After 5 min incubation at RT the reaction was stopped by addition of 120µl $Na_2S_2O_5$ (sodiumbisulfite). Free iodine was removed by anion exchange chromatography using Dowex 1 x 8 material. Dowex (10 mg) was equilibrated in PBS, pH7.0 containing 0.2% dialyzed BSA and was washed 2 times with PBS buffer without BSA. The Dowex suspension (220 µl) was added to the radiolabeled reaction mix, vortexed and incubated for 5 min at RT. The suspension was applied to an empty spin column and centrifuged for 2 min at full speed. The flow-through contained the radiolabeled peptide in a concentration of 3.75 µM.

3.4.3 Peptide labeling with fluorescein

Iodoacetamidofluorescein stock solution was prepared at 50 mM in DMF. Peptide RRYCKSTEL was dissolved in PBS, pH 6.5, 20% DMF to a concentration of 5 mM. 1.2 molar excess of iodoacetamidofluorescein was immediately added to the peptides and the reaction took place in the dark for 2 hours. The reaction was quenched by adding DTT. Mixture was loaded onto a C18 column (Kontronsorb, C18) equilibriated with 0.1% trifluoroacetic acid solution at the KONTRON HPLC system. After that, free fluorescein was separated from peptides with an acetone gradient running from 0-100% within 50 min at a flow rate of 2 ml/min. The absorption at 490 nm was monitored to localize the fluorescein and peptides. The peak containing fluorescein-labeled peptides was pooled and lyophilized to evaporate all solvents. Peptides were re-dissolved in milliQ water, and the peptide concentration was determined by measuring absorption at 492 nm in Tricine buffer, pH 9.0 (molar extinction coefficients: 75000 cm^{-1} M^{-1}). The purity of the fluorescein-labeled peptides was identified by MS spectrometry.

3.4.4 Peptide binding assay (centrifuge)

Peptide binding to TAP in microsomes was analyzed in AP buffer (PBS, 5 mM $MgCl_2$, pH 7.0). Microsomes (100 µg proteins) were mixed with ^{125}I-labeled peptide R9LQK (for detailed concentration see figure legend) in a volume of 150 µl. The control

sample contained 400-fold excess of unlabeled peptide in the mixture. After 15 min of incubation on ice, 1 ml of AP buffer was added and microsomes were centrifuged at 20,000 *g* for 8 min. After washing with 500 µl of AP buffer, the radioactivity associated with microsomes was quantified by γ-counting.

3.4.5 Peptide binding assay (filter)

The filtration assay was performed using a multiple filtration manifold (Multiscreen Assay System, Millipore) that is capable of handling 96 samples in parallel. The binding reaction took place in multi-well plates in which microsomes (15 µg protein) were mixed with radiolabeled peptide R9LQK at indicated concentration in an AP buffer in a final volume of 50 µL. After incubation on ice for 15 min, the mixture was transferred onto a multiscreen filter (MultiScreen Plates with glass fibre filter, pore size 1.0 µm, Millipore), which was preincubated with 100 µL 0.3% polyethyimine, followed by 100 µL of 0.2% dialysed BSA. Unbound peptide was removed by washing with 150 µl ice-cold AP buffer twice. The filters were air-dried, and radioactivity was quantified by γ-counting. The amount of bound, labeled peptides were corrected for unspecific binding, which was determined in the presence of a 400-fold molar excess of unlabeled peptide R9LQK. To determine the peptide dissociation constant, the data were fitted with Langmuir (1:1) binding equation:

$$B = B_{\max} \times \frac{C}{K_d + C}$$

3.4.6 Peptide binding kinetics

Fluorescein-labeled peptides (C4F) were preincubated in 1 ml AP buffer at 4°C or 27°C. After reaching a stable fuorescence emission signal, microsomes containing TAP were injected into the cuvette. Prior to use, microsomes were depleted of ATP by pretreatment with 1 unit apyrase (Sigma, Germany) for 10 min. The total protein and TAP concentration were around 100 µg/ml and 10 nM, respectively. When binding reached equilibrium as indicated by a stable fluorescent emission signal, a 400-fold molar excess of non-labeled peptide (RRYQKSTEL) was added to induce the dissociation of the peptide. The fluorephore was excited at a wavelength of 470 nm and the emission signal at 515 nm was recorded using a FLUOLOG-3 spectrometer (Instruments S.A., France) equipped with a microstirring device. The time-dependent changes in the fluorescence signal were fitted

by a monoexponential function yielding the observed association and dissociation rate constants, k_{obs} and k_{dis}:

$$F=F_0+\nabla F_{max} \times \exp(-kt)$$

Here the F_0 is the fluorescence signal at the zero time point, the ∇F_{max} is the change of the fluorescence at equilibrium comparing to the starting point (F_0).

3.4.7 Determination of TAP concentration

The amount of TAP in microsomes was considered to be equal to their active peptide-binding sites under saturation condition assuming one peptide-binding site per TAP complex. Microsomes (15 µg proteins) were incubated with 1µM peptides C4F (RRYC(Fluo)KSTEL) or radiolabeled R9LQK on ice for 15 min in 50 µl AP buffer. The mixture was loaded on to the filter plates, which were then washed with AP buffer three times (details see 3.4.5). In the case of using radiolabeled peptides, the radioactivity of filter plates was directly measured. In parallel, the radioactivity of 1 µl peptides (cpm/µl) was measured and the specific radioactivity of this peptide (cpm/mol) can be calculated. After counting the retained radioactivity of the filter plates, the total amount of the peptides (peptide-binding sites) was determined. For fluorescein-labled peptides (C4F), 300 µl PBS, 1% SDS, pH 7.5 was added to the filter plate to solubilize the microsomes as well as the peptides. Filter plate was incubated at room temperature for at least 15 min. Subsequently, the fluorescence emission of the solution was measured in the multi-well plate at 520 nm with the excitation wavelength at 470 nm using FluoroStar fluorometer (BMG Labtechnologies, GmbH, Germany). The C4F peptide was diluted in PBS, 1% SDS, pH 7.5 to a series of defined concentration (0, 10, 20, 40, 80 and 160 nM), which were served as the standard.

3.4.8 Peptide transport

Microsomes (250 µg of proteins) were incubated with 1 µM I^{125}-labeled RRYQNSTEL, 3 mM ATP, or ADP in 50 µl of AP buffer for 2 min at 32°C. The reaction was stopped by adding 500 µl of ice-cold AP buffer supplemented with 10 mM EDTA. After centrifugation, the pellets were solubilized in 900 µl of lysis buffer (20 mM Tris, 150 mM NaCl, 5 mM $MgCl_2$, 1% Igepal, pH 7.5) by incubation for 15 min on ice. The

insoluble material was removed by centrifugation, and the supernatant was incubated with 60 µl of concanavalin A (ConA)-Sepharose (50%, v/v) for 1 hour. After three washing steps, the radioactivity associated with ConA-Sepharose was quantified by γ-counting.

3.4.9 Photocrosslinking of TAP

Microsomes were suspended in 25 µl of photocrosslinking buffer (20 mM HEPES, 140 mM NaCl, 0.1 mM EGTA, 5 mM NaN_3, 1 mM Ouabain, 2 mM Mg^{2+}, 15% glycerol, pH 7.5) containing 1 µM 8-azido-[α-^{32}P]ATP. After 5-min incubation at the indicated temperature, samples were irradiated with UV light for 5 min on ice. 500 µl of ice-cold IP lysis buffer (20 mM Tris, 150 mM NaCl, 1% Igepal, pH 7.5) was added. Subsequently samples were immunoprecipitated (see 3.4.11) and analysed by SDS-PAGE (11%). Gels were dried and exposed to Kodak BIOMAX^{TM} MS films (Kodak GmbH, Germany) with an intensifying screen at -80°C.

3.4.10 Trapping of the TAP complex by ATPase inhibitors

Microsomes were incubated in 25 µl of AP buffer containing 2 µM 8-azido-[α-^{32}P]ATP and 0.5 mM ATPase inhibitors (orthovanadate, BeF_x, AlF_x, or ScF_x) in the presence or absence of peptides for 15 min at 27°C. In this assay, all metal fluorides were prepared by mixing metal chloride and sodium fluoride in a molar ratio of 1 to 100. The reaction was stopped by addition of 1 ml of ice-cold washing buffer (AP containing 10 mM ATP and 0.5 mM ATPase inhibitors). Samples were incubated for 15 min on ice. After centrifugation at 20,000 *g* for 15 min, pellets were resuspended in 50 µl of washing buffer. Finally, samples were irradiated with UV light for 5 min and then subjected to immunoprecipitation (see 3.4.11).

3.4.11 Immunoprecipitation

After photolabeling, TAP was immunoprecipitated either as a complex or as disassembled TAP1 and TAP2 subunits. These two methods differ in the solubilization procedure. In the former case, microsomes were solubilized in 0.9 ml of IP lysis buffer (50 mM Tris, 140 mM NaCl, 1% NP-40, pH 7.5) for 15 min on ice. In the latter case, microsomes were solubilized in 200 µl of IP lysis buffer for 15 min on ice. To disassemble the TAP complex, SDS was added to a final concentration of 0.5%, and incubation was continued for 15 min at 37°C. Finally, 700 µl of ice-cold IP lysis buffer was added. In both

methods, samples were centrifuged at 20,000 *g* for 8 min to remove insoluble material after solubilization. Antibodies (routinely 10 µl) were added to the supernatant and incubated for 2 h on ice. 50 µl of 50% (v/v) protein A/G (for monoclone/polyclonal antibody)-agarose Fast Flow (Sigma) were added, and incubation was continued for 2 h at 4°C. After washing three times with 1 ml of ice-cold IP washing buffer (20 mM Tris, 150 mM NaCl, 0.1% Igepal, pH 7.5), proteins were eluted with SDS sample buffer and applied to SDS-PAGE (11%). Antibodies used were monoclonal antibody 148.3 (anti-TAP1), rabbit antiserum 1p2 (anti-TAP1), and 2p4 (anti-TAP2). The BeF_x-trapped TAP complex was immunoprecipitated by a combination of polyclonal 1p2 and 2p4.

4. Results

4.1 Two catalytically active NBDs of TAP

4.1.1 Introduction

Peptide translocation is strictly dependent on ATP hydrolysis (Neefjes et al., 1993b; Uebel et al., 1997; van Endert et al., 1994). Several groups have most recently addressed the function of the two NBDs in the peptide transport process (van Endert et al., 2002). Exchanging the highly conserved, catalytic active lysine residue of the Walker A site impairs the transport activity strongly. Interestingly, although mutations of this residue in TAP2 fully interrupt peptide transport, TAP1 mutants still show low transport activity, suggesting distinct functions of both subunits during peptide transport (Karttunen et al., 2001; Lapinski et al., 2001; Saveanu et al., 2001). A functional non-equivalence of the two NBDs has also been reported in studies exchanging the NBDs within the TAP complex. The chimera with switched NBDs has substantial higher transport activity than chimeras with two identical NBDs, indicating that two different NBDs are important for TAP function (Arora et al., 2001; Daumke and Knittler, 2001). However, so far it is not clear whether both TAP subunits catalyze ATP hydrolysis. This question could neither be answered by measuring ATPase activity of TAP, nor could mutagenesis studies clarify this point directly.

In this chapter, the ATP hydrolysis properties of the two TAP subunits were studied for the first time by photolabeling with 8-azido-[α-^{32}P]ATP combined with BeF_x trapping. The peptide and ATP binding of TAP complexes in the BeF_x-trapped state were also addressed.

4.1.2 8-Azido-ATP energizes peptide transport as efficiently as ATP

8-Azido-ATP has been used to study the characteristics of binding and/or hydrolysis of ABC transporters such as P-gp, CFTR, and sulfonylurea receptor 1 (SUR1) (Hrycyna et al., 1998; Szabo et al., 1998; Takada et al., 1998; Ueda et al., 1999; Urbatsch et al., 1995a). Before using 8-azido-ATP to probe ATP hydrolysis by TAP, we determined whether this ATP-analog drives peptide transport. Therefore, peptide transport quantified by the amount of glycosylated, radiolabeled peptide was analyzed in the presence of ATP or 8-azido-ATP. The accumulation of peptides in microsomes increases linearly within the

first 2 min (Fig. 4-1A). The initial transport rates were determined at increasing ATP or 8-azido-ATP concentrations and fitted with Michaelis-Menten kinetics (Fig. 4-1B). The apparent K_m values for both nucleotides show only a slight difference, which are 197±35 µM for ATP and 103± 24 µM for 8-azido-ATP, whereas the V_{max} for both nucleotides is equal. From these results, we conclude that 8-azido-ATP support peptide translocation as efficiently as ATP and modification of the C_8 position of the adenine base does not change the properties of the nucleotide during the catalytic cycle.

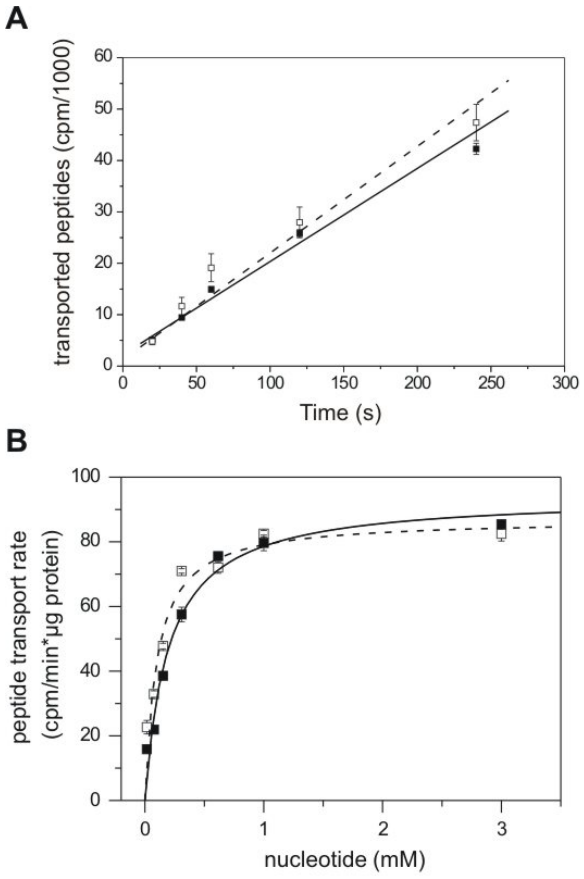

Figure 4-1. TAP-dependent peptide transport in the presence of ATP and 8-azido-ATP. A, Microsomes prepared from insect cells infected with recombinant baculovirus encoding human TAP1 and TAP2 were incubated with 1 µM radiolabeled RRYQNSTEL at 3 mM of ATP (*filled symbols*) or 8-azido-ATP (*open symbols*) at 32°C for different times. Glycosylated peptides were recovered by ConA-Sepharose, and the radioactivity was quantified by using γ-counting. **B,** Peptide uptake of microsomes was measured at various concentrations of ATP (*filled symbols*) or 8-azido-ATP (*open symbols*) for 2 min. The data were fitted with the Michaelis-Menten equation leading to a *Km* value of 197±35 µM for ATP (*solid*) and 103±24 µM for 8-azido-ATP (*dashed line*). Data points and errors were derived from triplicate measurements.

4.1.3 8-Azido-ATP binds specifically to TAP1 and TAP2

Next, we examined the nucleotide binding property of TAP by 8-azido-[α-^{32}P]ATP photocross-linking. After immunoprecipitation, TAP1 and TAP2 (apparent molecular mass, 71 and 75 kDa) were separated by high resolution SDS-PAGE (Fig. 4-2). The identity of the two TAP subunits was confirmed by immuno-precipitation of disassembled TAP1 and TAP2 subunits. The photocross-linking is specific, because it was inhibited by 1 mM ATP. Interestingly, even after immunoprecipitation of the TAP complex with an anti-TAP1 antibody, TAP2 shows stronger photolabeling than TAP1. This preferential labeling of TAP2 was observed both for TAP derived from Raji cells and for TAP expressed in insect cells lacking factors of the MHC loading complex. These results demonstrate that both subunits bind 8-azido-ATP specifically, and TAP2 is photolabeled more efficiently than TAP1.

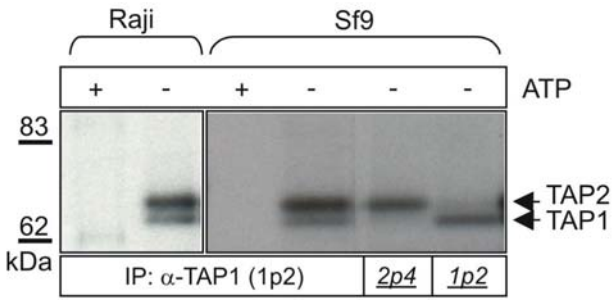

Figure 4-2. 8-Azido-[α-^{32}P]ATP photocross-linking of TAP. Microsome preparations (50 µg of protein) from Raji cells or Sf9 insect cells infected with baculovirus encoding human TAP1/TAP2 were incubated with 1 µM 8-azido-[α-^{32}P]ATP in the presence or absence of 1 mM ATP on ice. Proteins were photolabeled by UV irradiation for 5 min. The two subunits were either co-immunoprecipitated as an intact heterodimeric complex via TAP1-specific antiserum (1p2) or as dissociated subunits via TAP1- or TAP2-specific antibodies (*1p2* and *2p4*). The immunoprecipitated products were analyzed by SDS-PAGE (11%) and visualized by autoradiography.

4.1.4 Magnesium- and temperature-dependent 8-azido-ATP binding

Magnesium is well known to be required for ATP hydrolysis by most ATPases. It has also been shown that Mg^{2+} can have different effects on ATP binding to two subunits

of an ABC transporter (Matsuo et al., 1999). Therefore, we examined the influence of magnesium on 8-azido-[α-^{32}P]ATP photolabeling of the TAP complex. No photolabeling of TAP1 and TAP2 was observed in the absence of magnesium either at 4°C or 37°C, indicating that ATP binding to both TAP subunits is magnesium-dependent (Fig. 4-3*A*). Nucleotide binding to the TAP complex is temperature-dependent. At 4°C, photolabeling preferentially occurred at TAP2. However, at 37°C, TAP1 and TAP2 are equally labeled, and the photolabeling of both subunits is weaker than at 4°C. Peptides slightly stimulate the labeling of both subunits (Fig. 4-3B).

4.1.5 Phosphate analogs trap ADP in TAP1 and TAP2

The contribution of each NBD to the ATPase activity of TAP cannot be directly analyzed by measuring the steady-state release of inorganic phosphate. ATPase inhibitors, such as orthovanadate, BeF_x, AlF_x, or ScF_x, are useful tools to elucidate the mechanism of ATP hydrolysis by forming a stable Mg•ADP•inhibitor complex after ATP hydrolysis and phosphate release arresting the enzyme in the catalytic cycle (Park et al., 1999; Smith and Rayment, 1996; Urbatsch et al., 1995b). Therefore, TAP-containing microsomes were incubated with 8-azido-[α-^{32}P]ATP in the presence of different ATPase inhibitors at 37°C to test their ability to form a trapped Mg•ADP•inhibitor•TAP complex. After trapping, weakly bound nucleotides were removed by washing the microsomes. Photolabeling of TAP1 and TAP2 was observed in the presence of all three metal fluorides, whereas very weak signals were found in the presence of vanadate (Fig. 4-4). No photolabeling was observed in the absence of trapping reagents. Microsomes derived from insect cells infected with baculovirus wild-type also showed no photolabeling. The trapping reaction was peptide-specific, and this is investigated in detail below. These data demonstrate that metal fluorides form a trapped state with ADP within the NBD of TAP1 and TAP2. This state is very stable, because trapped ADP cannot be competed out even by a 1000-fold excess of ATP. In all cases stronger labeling of TAP1 than TAP2 was observed. In summary, the phosphate analogs trap ADP in TAP with the following efficiencies: BeF_x> ScF_x> AlF_x> V_i. complex via TAP1-specific antiserum (1p2) or as dissociated subunits via TAP1- or TAP2-specific antibodies (*1p2* and *2p4*). The immuno-precipitated products were analyzed by SDS-PAGE (11%) and visualized by autoradiography.

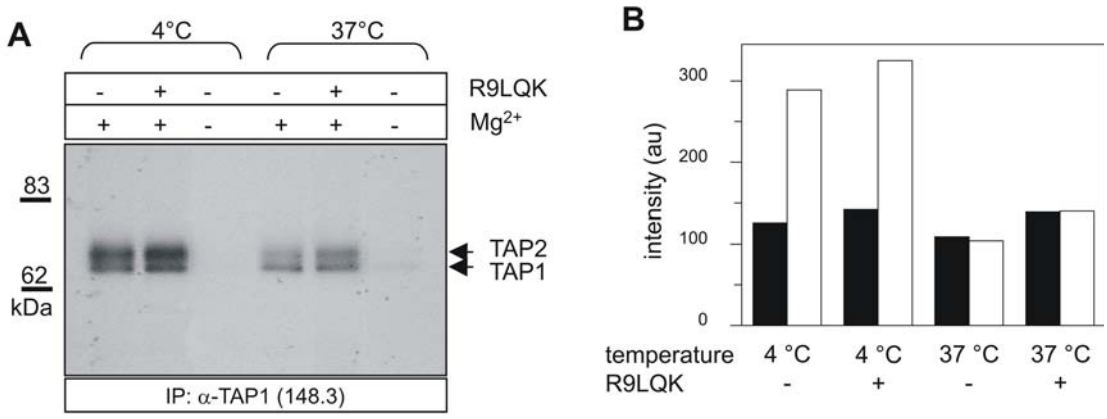

Figure 4-3. Effect of Mg^{2+} and temperature on 8-azido-[α-^{32}P]ATP photocross-linking. ***A*****,** microsomes (100 µg of protein) prepared from Raji cells were incubated with 1 µM 8-azido-[α-^{32}P]ATP in the presence or absence of 1 mM $MgCl_2$ or 1 µM R9LQK for 5 min at 4°C or 37°C. Samples at 37°C were transferred on ice, and all probes were immediately subjected to UV irradiation. The TAP complex was precipitated via anti-TAP1 monoclonal antibody 148.3, separated by SDS-PAGE (11%), and analyzed by autoradiography. ***B*****,** to compare the slight increase in labeling efficiency in the presence of peptide the corresponding TAP1 (*filled bars*) and TAP2 (*open bars*), bands were densitometrically analyzed, and intensities are shown as a histogram.

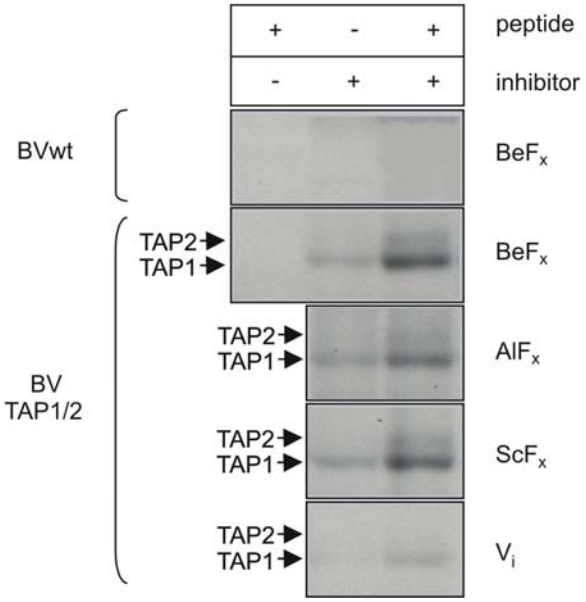

Figure 4-4. Analysis of ATPase inhibitors of TAP. Microsomes (50 µg of protein) from insect cells infected with baculovirus (*BV*) encoding human TAP1/2 or wild type baculovirus were incubated with 2 µM 8-azido-[α-^{32}P]ATP either in the absence or presence of 0.5 mM of different inhibitors (BeF_x, AlF_x, ScF_x, or orthovanadate) and 1 µM peptide R9LQK for 15 min at 27°C. After washing and UV-photocrosslinking, samples were subjected to SDS-PAGE (11%) and visualized by autoradiography.

4.1.6 Peptides induce the formation of a trapped intermediate state

It has been recently demonstrated that ATP hydrolysis is coupled to peptide binding and transport (Gorbulev et al., 2001). However, it remains unclear whether TAP1 or TAP2, or both subunits are involved in ATP hydrolysis. Here, we investigated the effect of various peptides on BeF_x trapping of Mg-8-azido-[α-^{32}P]ADP by incubating TAP with 8-azido-[α-^{32}P]ATP under hydrolyzing conditions. Both subunits were strongly labeled in the presence of the high affinity peptide R9LQK and BeF_x (Fig. 4-5A). A very weak labeling for TAP1 and TAP2 was observed in the presence of the herpes simplex virus protein ICP47, which specifically inhibits peptide binding and thus prevents the peptide-stimulated ATPase activity of TAP (Ahn et al., 1996; Gorbulev et al., 2001). Furthermore, a weak labeling of TAP was found in the presence of the low affinity peptides (K_d>1 mM), E9D and D-R9LQK. In the absence of BeF_x, no labeling of TAP was detected even when high affinity peptides are present. To analyze the peptide-induced formation of a trapped intermediate quantitatively, BeF_x trapping was performed with increasing concentrations of R9LQK. Photolabeling of both TAP subunits was enhanced in a concentration-dependent manner (Fig. 4-5B). The EC_{50} values (peptide concentration required to achieve half-maximal trapping) for TAP1 and TAP2 are very similar with 16 nM and 18 nM, respectively (Fig. 4-5C). These values are in good agreement with the affinity constant of fluoresceinlabeled R9LQK (12 nM) measured under equilibrium binding condition (Neumann and Tampé, 1999). Interestingly, under all trapping conditions, TAP1 was preferentially labeled. Taken together, these data demonstrate that peptides specifically induce BeF_x trapping of both TAP subunits.

Figure 4-5. Peptide-induced BeFx trapping of TAP1 and TAP2. (see picture in next page) Trapping of TAP was performed by incubating Raji microsomes (100 µg of protein) with 2 µM 8-azido-[α-^{32}P]ATP in the presence or absence of 0.5 mM BeF_x and/or 1 µM of different peptides (**A**) or increasing R9LQK concentration (**B**) To investigate the effect of the viral inhibitor ICP47, microsomes were incubated with 20 µM ICP47. The TAP complex was immunoprecipitated by polyclonal antibodies 1p2 and 2p4 and analysed by SDS-PAGE (11%) followed by autoradiography. To determine the EC50 values for peptide-induced trapping, the photolabeling of TAP1 and TAP2 was quantified. The background-corrected intensities were plotted against concentration of R9LQK and fitted with equation $I/I\text{max} = [\text{peptide}]/(EC_{50} + [\text{peptide}])$. The EC_{50} values for trapping of TAP1 (*open circle* and *dashed line*) and TAP2 (*close circles* and *solid line*) are 18 and 16 nM, respectively (**C**).

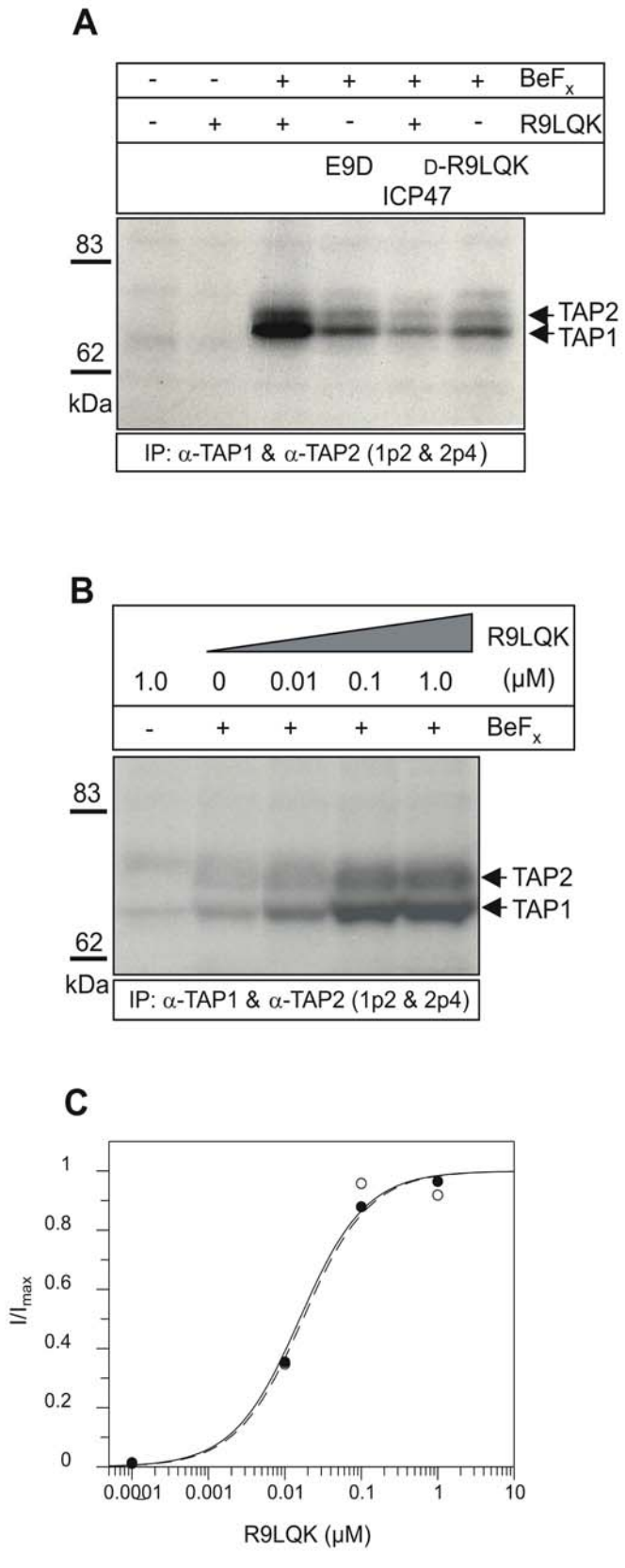
A
- - + + + + BeFx
- + + - + - R9LQK
E9D D-R9LQK
ICP47
83
62
kDa
TAP2
TAP1
IP: α-TAP1 & α-TAP2 (1p2 & 2p4)
B
R9LQK
1.0 0 0.01 0.1 1.0 (μM)
- + + + + BeFx
83
62
kDa
TAP2
TAP1
IP: α-TAP1 & α-TAP2 (1p2 & 2p4)
C
I/Imax
1
0.8
0.6
0.4
0.2
0
0.0001 0.001 0.01 0.1 1 10
R9LQK (μM)

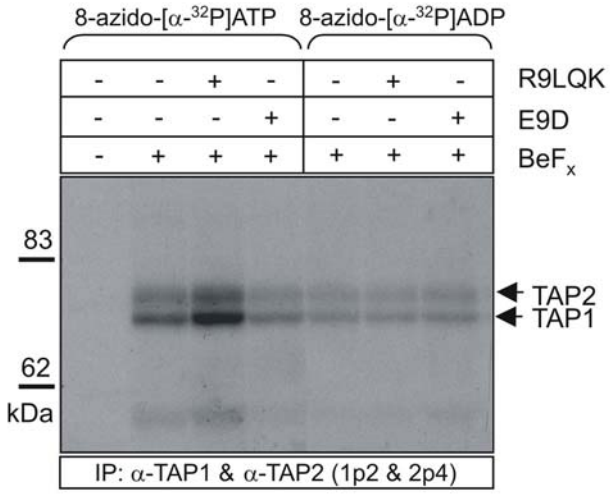

Figure 4-6. Comparison of 8-azido-ATP and 8-azido-ADP trapping with BeF_x. Trapping of TAP was performed by incubating Raji microsomes (100 µg protein) with 2 µM 8-azido-[α-^{32}P]ATP (5µCi) or 2 µM 8-azido-[α-^{32}P]ADP (5 µCi) with or without 0.5 mM BeF_x and 1 µM R9LQK or E9D for 15 min at 27°C. The TAP complex was immunoprecipitated via antibodies 1p2 and 2p4, separated by SDS-PAGE (11%), and visualized by autoradiography.

4.1.7 BeF_x-trapping reflects ATP hydrolysis

Peptide-induced BeF_x trapping of TAP might be due to two different mechanisms: (i) BeF_x substitutes the released phosphate immediately after ATP hydrolysis, forming a stableMg•ADP•BeF_x complex within the NBD (forward reaction); (ii) ATP is hydrolyzed by ATPases present in the microsomal preparation. Trapping is initiated by binding of MgADP to TAP, followed by association of BeF_x and by formation of a stable NBD•Mg•ADP•BeF_x complex (backward reaction). To distinguish between the two pathways, we compared BeF_x trapping in the presence of the 8-azido-[α-^{32}P]ATP and 8-azido-[α-^{32}P]ADP. The concentration as well as the radioactivity of the two nucleotides was kept identical to allow direct comparison of the signal intensities. The high affinity peptide R9LQK strongly stimulates the trapping of TAP with 8-azido-[α-^{32}P]ATP (Fig. 4-6). Moreover, in the case of 8-azido-[α-^{32}P]ADP, the trapping efficiency of TAP is not peptide-dependent and lower than in the presence of 8-azido-[α-^{32}P]ATP. Therefore, we

conclude that efficient BeF_x trapping of TAP occurs only after ATP hydrolysis and that the peptide-induced BeF_x trapping directly reflects ATP hydrolysis during the catalytic cycle of TAP.

4.1.8 BeF_x-trapped state of TAP

To characterize the BeF_x-trapped state of TAP in more detail, peptide and nucleotide binding as well as peptide transport of trapped TAP were analyzed. After incubation of microsomes with BeF_x and ATP for 15 min, peptide transport via TAP was reduced to 20% (Fig. 4-7A). Longer incubation with BeF_x blocked the TAP transport activity completely. However, longer incubation time also impaired TAP function. The stability of the trapping state was examined by monitoring the recovery of peptide transport over time. For this purpose, free BeF_x was removed to facilitate the dissociation of TAP•Mg•ADP•BeF_x complex. It was observed that even after incubation for 45 min on ice, TAP remains in an inhibited state. Longer recovery times were not analyzed, because TAP started to loose activity even at 4°C. Next, we studied the BeF_x-trapped TAP complex with respect to nucleotide and peptide binding. Fig. 4-7B shows that pretreatment of TAP with BeF_x and ATP inhibits the photolabeling with 8-azido-[α-^{32}P]ATP and 8-azido-[α-^{32}P]ADP, demonstrating that the trapped state of TAP can neither bind nor exchange added nucleotides. The weaker photolabeling signal of TAP preincubated with ATP compared with that without ATP results from incomplete dissociation of ATP during the washing step. In contrast to nucleotide binding, BeF_x trapping does not affect peptide binding (Fig. 4-7C). At half-maximal and saturating peptide concentrations, the amount of peptides bound to the trapped and non-trapped state is equal. These data demonstrate that neither the affinity nor the overall amount of the peptide-binding sites was altered. In addition, the same results were obtained when AlF_x and ScF_x were used for trapping (data not shown). Taken together, BeF_x inhibits peptide translocation by trapping TAP in a stable intermediate state to which added nucleotides cannot bind. Importantly, peptide binding to TAP is not affected in this trapped state.

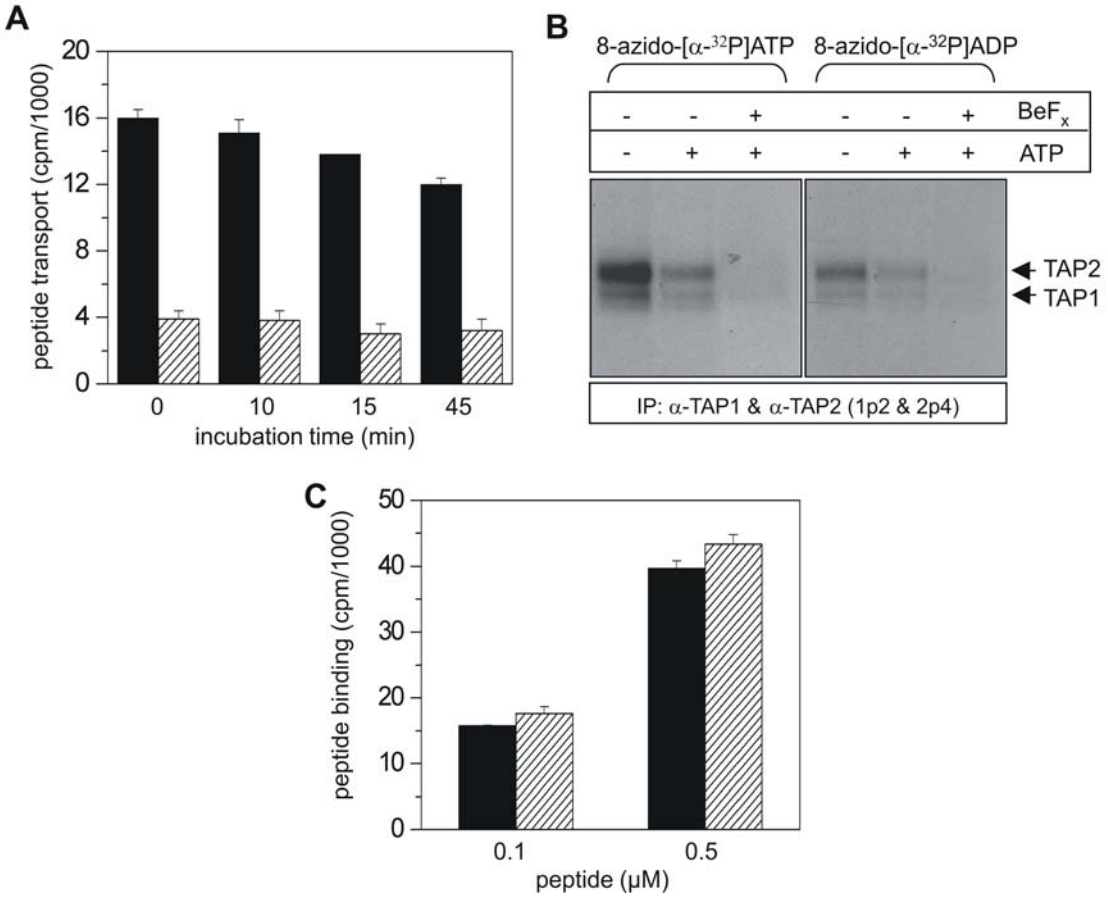

Figure 4-7. Characterization of the BeFx-trapped TAP complex. A, stability of the BeFx-trapped TAP complex. Raji microsomes (250 µg of protein) were incubated with 1 µM R9LQK, 3 mM ATP in the absence (*solid bar*) or presence (*hatched bar*) of 5 mM BeFx at 27°C for 15min. Subsequently, free and un-trapped nucleotides and peptides were removed by washing, and microsomes were resuspended in transport buffer containing 3 mM ATP and incubated on ice. After different time periods, peptide transport was initiated by adding 1 µM radiolabeled RRYQNSTEL and immediately transferring samples to 32°C for 2 min. Translocated peptides were recovered on ConA beads and quantified by γ-counting. **B,** binding of nucleotides to the BeF_x-trapped TAP complex. Raji microsomes (100 µg of proteins) were incubated with 1 µM R9LQK in the presence or absence of 3 mM ATP and/or 5 mM BeF_x (Be:F = 1:10 mol/mol) at 27°C for 15 min. After washing the microsomes to remove all free and loosely bound nucleotide and peptide, microsomes were incubated with 1 µM 8-azido-[α-^{32}P]ATP or 8-azido-[α-^{32}P]ADP for 5 min on ice, followed by UV irradiation. TAP1 and TAP2 were coimmunoprecipitated by a combination of polyclonal antibodies 1p2 and 2p4. **C,** peptide binding to the BeF_x-trapped TAP complex. Raji microsomes (250 µg of proteins) were incubated with 3 mM ATP and 1 µM R9LQK in the absence (*solid bar*) or presence (*hatched bar*) of 5 mM BeF_x (Be:F = 1:10 mol/mol) at 27°C for 15 min. After washing, peptide binding of radiolabeled R9LQK was determined.

4.2 Two non-equivalent C-loops in the NBDs of TAP

4.2.1 Introduction

Peptide transport is strictly ATP-hydrolysis dependent (Neefjes et al., 1993b; Shepherd et al., 1993). Both functional NBDs are required for energizing the peptide transport process (Arora et al., 2001; Daumke and Knittler, 2001; Karttunen et al., 2001; Lapinski et al., 2001; Saveanu et al., 2001). BeF_x trapping studies demonstrated that both NBDs hydrolyze ATP during peptide translocation (Chen et al., 2003b). In addition, the two NBDs behave asymmetrically, the evidence for which came from mutations in the Walker A motif that interrupt peptide transport when introduced in TAP2 but show still low transport activity if placed in TAP1 (Alberts et al., 2001; Karttunen et al., 2001; Lapinski et al., 2001).

Recent structural and biochemical studies demonstrated that the NBDs dimerize in presence of ATP (Chen et al., 2003a; Fetsch and Davidson, 2002; Janas et al., 2003; Loo et al., 2002; Moody et al., 2002; Smith et al., 2002b). Two ATPs are sandwiched at the interface of both NBDs, and positioned by the Walker A/B motifs and the C-loop of the opposite NBD (Fig. 4-8A). In the dimer, the γ-phosphate of ATP is fixed by additional hydrogen bonds to the hydroxyl group of the highly conserved serine and the amide of the invariant glycine of the C-loop (LSGGQ). Although these studies elucidated structural aspects of the symmetric NBD-dimer formation, the functional asymmetry of the NBDs in ABC-transporters cannot be explained.

The functional non-equivalence of the two NBDs of TAP may be reflected in variations of the highly conserved consensus sequences. Notably, all differences from the canonical sequences of ABC-proteins affect the ATP-binding site I, which is built up by the Walker A and B motifs of TAP1 and the C-loop of TAP2 (Fig. 4-8B). Among these changes in the ATP-binding site I, most remarkably, the C-loop of TAP2 contains a " degenerated" sequences LAAGQ instead of conserved LSGGQ. The substitution of the highly conserved serine in the C-loop is unique among all human ABC-transporters (Fig. 4-8C). For this reason, we examined the contribution of the ABC signature motifs to the functional asymmetry of the two TAP subunits by single-site mutations and chimeras.

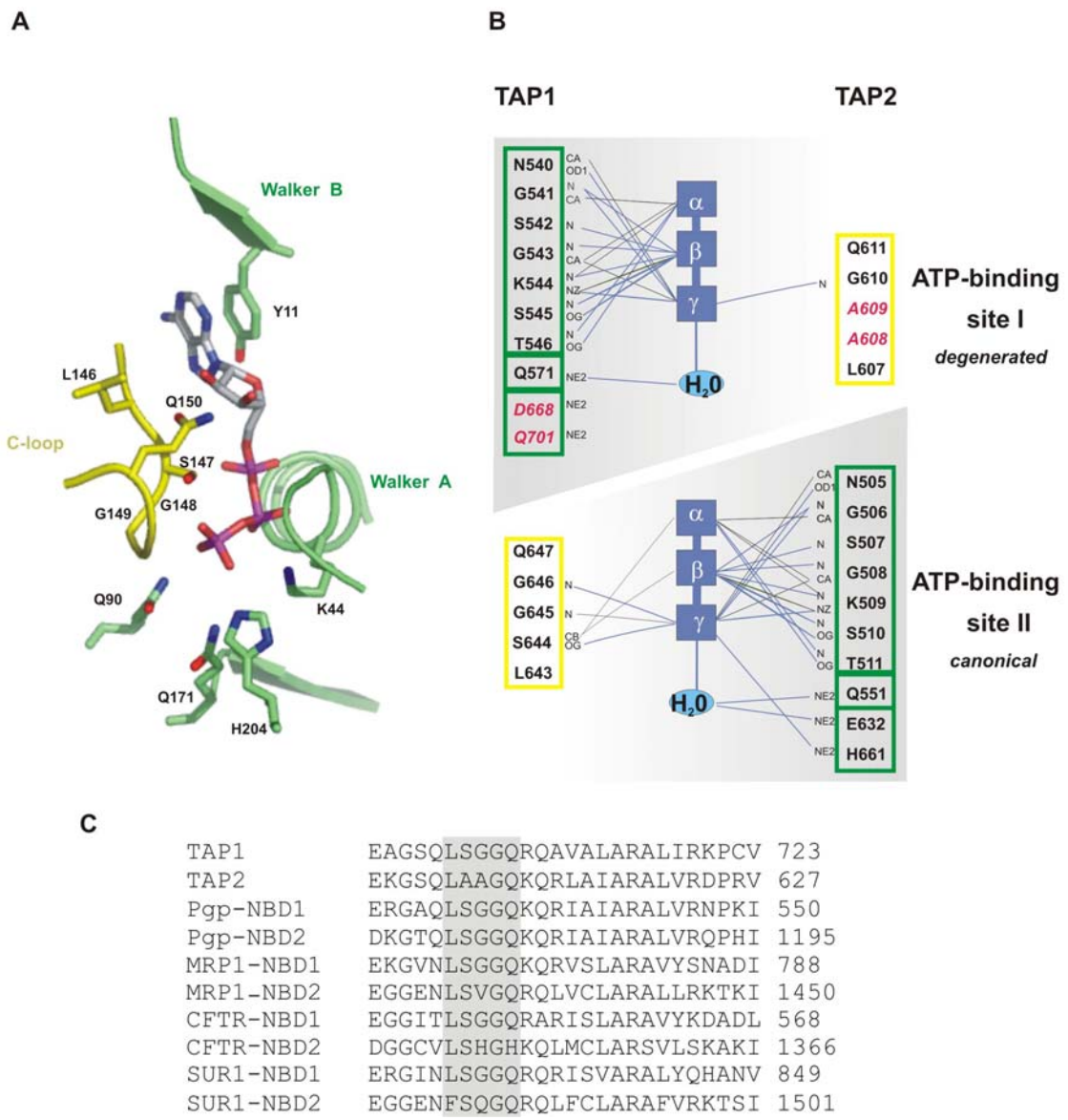

Figure 4-8. Structure of the ATP-binding site. A, X-ray structure of one ATP-binding site of the MJ0769 dimer in complex with Na-ATP (Smith et al., 2002b). One NBD containing Walker A/B sequence is illustrated in green and the second NBD containing the C-loop is depicted in yellow. **B**, Schematic model of the catalytic sites in the ATP-sandwitched dimer of TAP. The interactions between NBDs and the phosphate groups of ATP are adopted from the structure of MJ0796 and Rad50 (Hopfner et al., 2000; Smith et al., 2002b). Van der Waals contacts (≤ 3.6Å) are represented in black lines while H-bonds (≤ 3.3Å) are represented by blue lines. The non-conserved residues at ATP-binding site I are highlighted in red. **C**, Sequence alignment of the C-loops of various human ABC-transporter. The grey frame marks the core sequences of C-loop.

4.2.2 Expression of single site C-loop mutants

Recently, it was shown that NBDs from both subunits (TAP1 and TAP2) are required to assemble a functional TAP transport complex (Arora et al., 2001; Daumke and Knittler, 2001). Moreover, ATP hydrolysis in both subunits is stimulated by peptide binding (Chen et al., 2003b; Gorbulev et al., 2001). However, different peptide transport activities of Walker A mutants indicate a functional asymmetry of both TAP subunits (Alberts et al., 2001; Karttunen et al., 2001; Lapinski et al., 2001). Interesting, TAP1 and TAP2 also show an asymmetry in their C-loop sequences: LSGGQ in TAP1 *versus* LAAGQ in TAP2. The glycine and serine residue of the C-loop (LSGGQ) contacting the γ-phosphate of ATP are highly conserved among members of the ABC superfamily (Fig. 4-8). The other positions (LSGGQ) in the C-loop are however more divergent. To examine the functional relevance of two different C-loops in the functional asymmetry of TAP, we first focused on the leucine and the highly conserved glycine of the C-loop. The leucine, which is not in direct contact with ATP and not as conserved as the remaining residues in the C-loop, was exchanged to alanine. In human ABC-transporters, this leucine is replaced mostly by bulky aromatic amino acids. In addition, the invariant glycine residue was changed to valine or aspartate. In our studies, all mutated half-transporters were combined with a wild type counterpart, which resulted in three pairs of mutants. These six TAP mutants are termed 1LA/2wt vs 1wt/2LA, 1GV/2wt vs 1wt/2GV, 1GD/2wt vs 1wt/2GD (mutated residues of TAP1/TAP2 are underlined). All TAP1 and TAP2 constructs were cloned into one baculovirus to circumvent the problem with double infections, and expressed in Sf9 insect cells under the control of the polyhedrin and p10 promoter, respectively. Three days after infection, cells were harvested and microsomes were prepared. As revealed by immunoblotting, all TAP mutants were expressed in microsomes at comparable level to wt TAP (Fig. 4-9). The small differences in the expression levels were most likely due to variations in microsome preparation or conditions of viral infection. Thus these single-site C-loop mutations do not alter the overall expression level of TAP1 or TAP2.

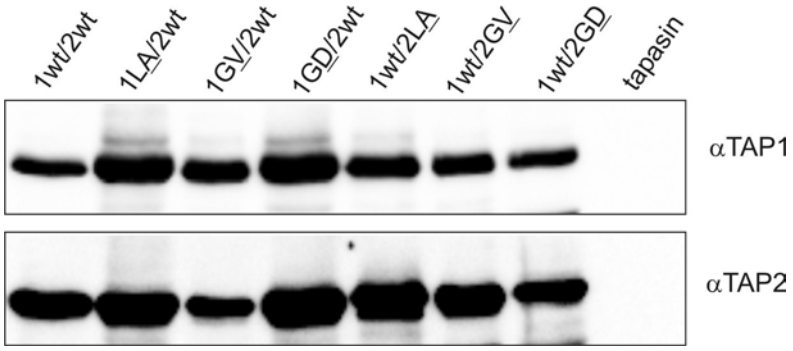

Figure 4-9. Expression of TAP C-loop single substitution mutants. Western Blot analysis of microsome preparations from Sf9 insect cells infected with baculovirus encoding TAP variants. The mouse anti-TAP1 (148.3) and anti-TAP2 (435.3) monoclonal antibodies were used to detect TAP1 and TAP2 protein expression respectively. Cells transfected with baculovirus encoding tapasin were used as negative control.

4.2.3 Peptide binding is not influenced by single C-loop mutations

Peptide binding is a prerequisite for peptide transport (Androlewicz et al., 1994; van Endert et al., 1994). Mutations in the Walker A motif of TAP were shown to influence peptide binding at the TMD (Alberts et al., 2001; Karttunen et al., 2001; Knittler et al., 1999; Saveanu et al., 2001). Therefore, we investigated whether these single-site mutations in the C-loop have an impact on peptide binding. Binding affinities for the high affinity peptide R9LQK (RRYQKSTEL) were determined at 4°C in the absence of nucleotides. As shown in Fig. 4-10, the data can be fitted according to a Langmuir 1:1 binding model for all TAP variants. All mutants have very similar affinities (Tab. 4-1), demonstrating that the C-loop mutations do not modify the structure of the peptide-binding pocket. Moreover, because both subunits are essential for peptide binding, these results prove that these mutations do not interfere with assembly of the heterodimeric TAP complex.

4.2.4 ATP binding is not influenced by single C-loop mutations

In addition to the association with peptides, ATP must bind to energize peptide transport by ATP hydrolysis. Mutations in the Walker A sequence of TAP1 or TAP2 abolished or reduced ATP binding which can explain the defect in peptide transport (Karttunen et al., 2001; Lapinski et al., 2001; Saveanu et al., 2001). The contribution of the

Walker A motif in nucleotide binding can be clearly derived from the x-ray structures of NBDs. However, the effect of C-loop mutations on nucleotide binding is not obvious because singularly expressed TAP subunits bind ATP with similar affinity than the heterodimeric complex (Lapinski et al., 2003). Therefore, nucleotide binding of single C-loop mutants was analyzed by photo-crosslinking with 8-azido-[α-^{32}P]ATP (1 µM, 4°C). All TAP variants can bind 8-azido-[α-^{32}P] ATP, which can be competed out by an excess of unlabeled ATP (Fig. 4-11A). The labeling efficiency of the mutants varies and is lower in comparison to wt TAP. Moreover, the ratio between labeled TAP1 and TAP2 has changed in comparison to wt TAP. To clarify whether these differences are due to changed nucleotide affinities or non-equivalent expression of the two TAP subunits, we compared the expression level of each subunit taking TAP wt as a standard. Fig. 4-11B showed that in comparison to TAP wt, the ratio of the expression level of TAP2 to TAP1 is reduced for all the mutants in dependent of which subunit is mutated. Thus, the stronger labeling at TAP1 subunit in the mutants is likely due to its higher expression level. In summary, the photolabeling efficiency of TAP mutants is relatively lower than wt TAP. Nevertheless, all the C-loop mutants could interact with 8-azido-ATP at a micromolar concentration. Form these studies we concluded that these single-site mutations do not prevent the ATP binding to TAP.

Table 4-1. Peptide dissociation constants of C-loop mutants of TAP

TAP1/TAP2	K_d (µM)	
1wt/2wt	0.27±0.06	wild type
1L<u>A</u>/2wt	0.50±0.09	
1G<u>V</u>/2wt	0.37±0.13	
1G<u>D</u>/2wt	0.36±0.08	single residue
1wt/2L<u>A</u>	0.41±0.10	substitutions
1wt/2G<u>V</u>	0.30±0.07	
1wt/2G<u>D</u>	0.21±0.06	
1SG/2<u>SG</u>	0.34±0.02	
1<u>AA</u>/2AA	0.27±0.03	chimeras
1<u>AA</u>/2<u>SG</u>	0.32±0.05	

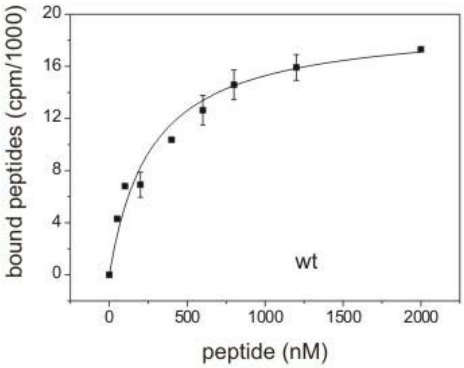
bound peptides (cpm/1000)
peptide (nM)
wt

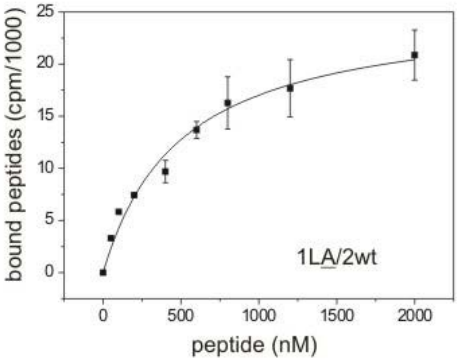
bound peptides (cpm/1000)
peptide (nM)
1LA/2wt

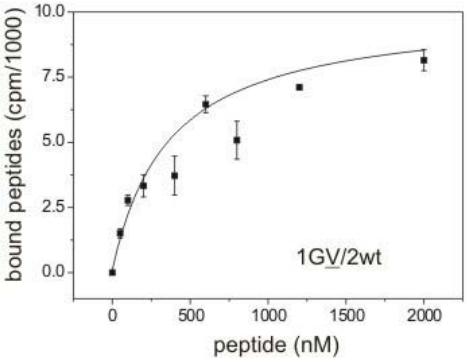
bound peptides (cpm/1000)
peptide (nM)
1GV/2wt

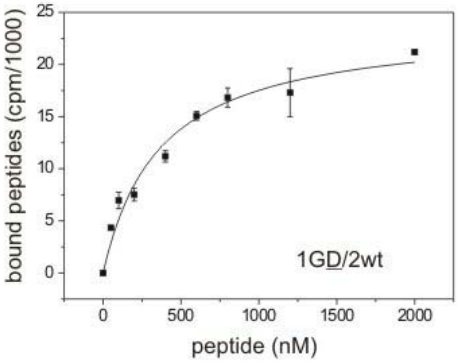
bound peptides (cpm/1000)
peptide (nM)
1GD/2wt

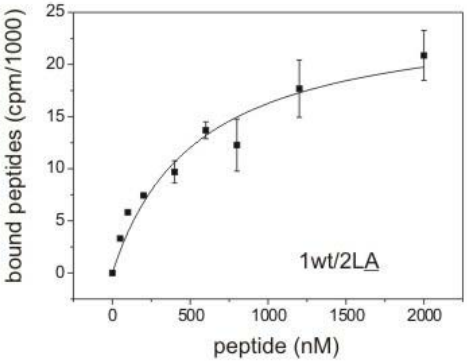
bound peptides (cpm/1000)
peptide (nM)
1wt/2LA

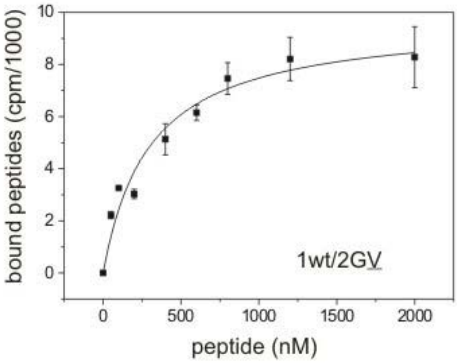
bound peptides (cpm/1000)
peptide (nM)
1wt/2GV

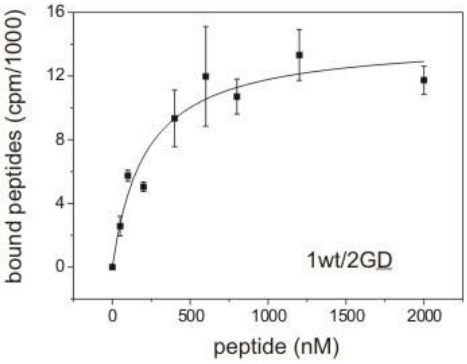
bound peptides (cpm/1000)
peptide (nM)
1wt/2GD

Figure 4-10. Peptide binding of single C-loop mutants of TAP (previous page). Microsomes (15 µg protein) of single C-loop mutants were incubated with increasing concentration of radiolabeled peptide R9LQK (15 min, 4°C). Free peptides were removed by washing and microsome-associated peptides were determined by γ-counting. Specifically bound peptides are plotted against the peptide concentration and fitted by a Langmuir (1:1) binding equation. The peptide affinities are summarized in table 4-1. Data resemble the mean of three measurements.

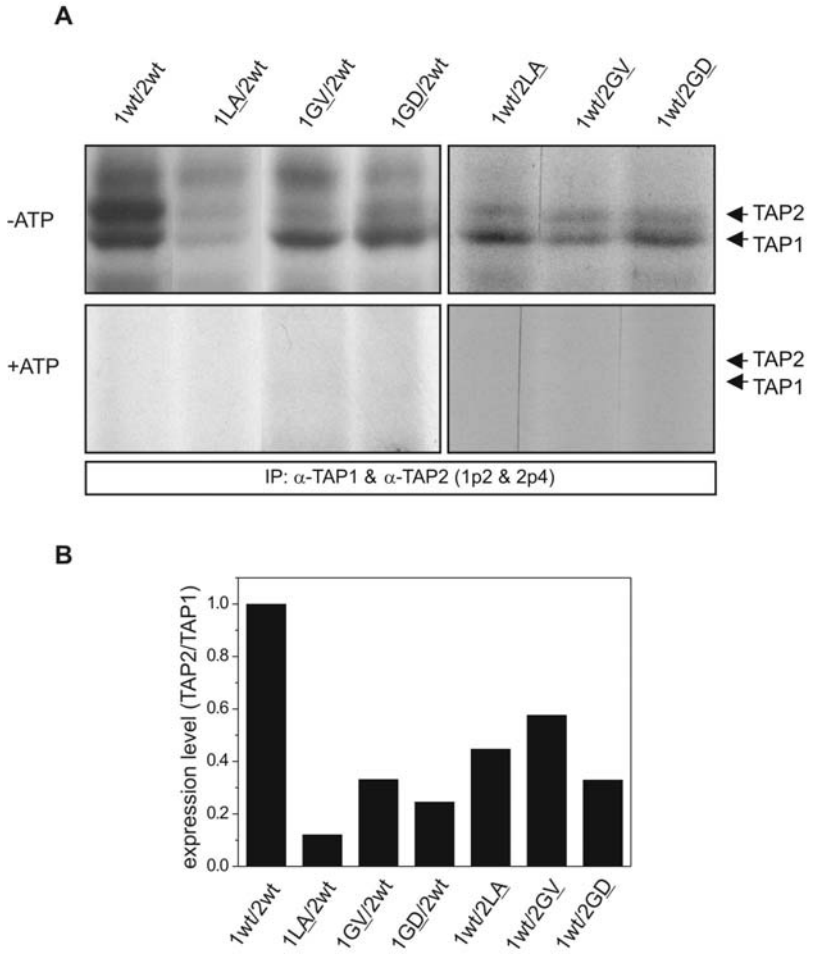

Figure 4-11. ATP binding to single residue substitutions of the C-loop of TAP. A, Microsomes (100 µg protein) containing different single C-loop mutations were incubated with 8-azido-[α-^{32}P]ATP (1 µM) in absence or presence of 1 mM ATP at 4°C. Bound 8-azido-[α-^{32}P]ATP was crosslinked by UV irradiation. Subsequently, TAP was immunoprecipitated with polyclonal antibodies recognizing TAP1 and TAP2 (1p2 and 2p4), separated by SDS-PAGE (11%), and visualized by autoradiography. **B**, Comparison of the expression level of TAP1 and TAP2. The expression level of the two subunits in TAP mutants was detected by western blotting and the signal intensity was analysed by lumi-imager. The ratio of the expression level of TAP2 to TAP1 in these mutants is depicted setting the ratio in wt TAP to 1:1.

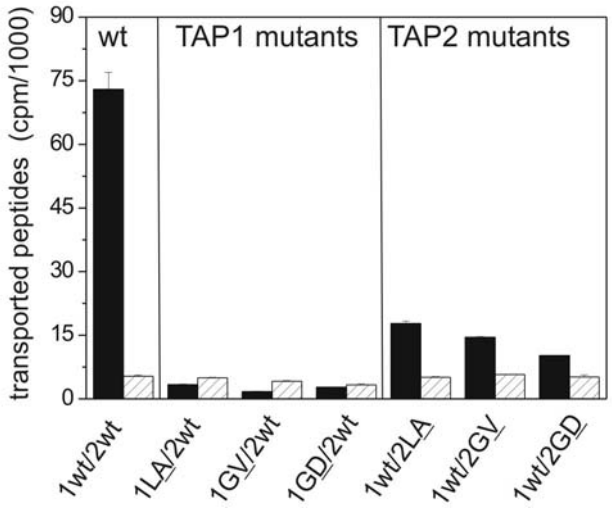

Figure 4-12. Peptide transport of TAP containing single residue substitutions of the C-loop. Microsomes (100 µg protein) containing different C-loop mutations of TAP were incubated with 1 µM radiolabeled RRYQNSTEL in the presence of 3 mM ATP (black) or ADP (hatched) at 32°C for 5 min. Glycosylated peptides were recovered by Con A sepharose and the radioactivity was quantified via γ-counting.

4.2.5 Non-equivalent effect of single C-loop mutants on peptide transport

All C-loop mutants described so far show no significant effect on peptide as well as ATP binding. Finally, the peptide transport function of these mutants was investigated. *In vitro* peptide transport assays were preformed using isolated TAP-containing microsomes and the radiolabeled peptide RRYQNSTEL at 32°C as described (Meyer et al., 1994; Neefjes et al., 1993b). To allow a direct comparison, the TAP concentration, determined by immunoblotting or peptide-binding (B_{max} value), was kept constant in all experiments. In contrast to wt TAP, the mutants did not show any peptide transport activity over a period of 2 min. Transport assays were then extended to 5 min. Even under these prolonged transport periods, the TAP complexes containing TAP1 mutants remained inactive (Fig. 4-12). However, TAP2 mutants transported peptides albeit with much lower efficiency than wt TAP. In addition, there are differences between the mutations introduced in TAP2. The 1wt/2LA TAP complex transports peptides more efficient than 1wt/2GV, whereas 1wt/2GD shows the lowest peptide transport activity. Obviously, the position and the type

of mutation in the C-loop affect the transport in slightly different manner. As these TAP mutants show no difference in peptide as well as ATP binding, the loss of function must be related to disabled ATP hydrolysis or inefficient coupling of ATP hydrolysis to transport. We conclude that C-loop mutations in TAP1 completely abolish the function of the TAP complex, whereas the same substitutions in TAP2 decelerate the transport machinery. These findings further support the idea of the functional non-equivalence of both NBDs of TAP in the overall transport cycle.

4.2.6 Expression of C-loop chimera

Based on the fact that the symmetrical C-loop mutations in TAP1 and TAP2 described so far behaved differently, we focused on residues of the ABC signature motif that vary in TAP1 and TAP2 (L<u>SG</u>GQ *versus* L<u>AA</u>GQ). For this reason, we studied TAP complexes comprising two canonical C-loops motifs (LSGGQ/L<u>SG</u>GQ) named as 1SG/2<u>SG</u>, switched C-loops (L<u>AA</u>GQ/L<u>SG</u>GQ) as 1<u>AA</u>/2<u>SG</u> and two degenerated C-loops (L<u>AA</u>GQ/LAAGQ) as 1<u>AA</u>/2AA (mutated residues are underlined). Microsomes were prepared from insect cells infected with recombinant baculovirus. The expression levels of all C-loop chimeras are very similar (Fig. 4-13), demonstrating that a degenerated C-loop in TAP1 and/or TAP2 does not affect the expression level of TAP.

4.2.7 Peptide and nucleotide binding of C-loop chimera

The behavior of the TAP C-loop chimeras was studied following the same procedures as for the single residue mutants described above. The TAP C-loop chimeras and wt TAP bind peptide with the same affinity (Fig. 4-14/Tab. 4-1). Therefore we conclude that similar to the single residue mutants, the switched C-loop chimeras do not influence peptide binding. As analyzed in 8-azido-[α-^{32}P]ATP photo-crosslinking studies, all TAP C-loop chimeras bind ATP in a competitive manner (Fig. 4-15A). In contrast to wt TAP, TAP1 is stronger labeled than TAP2 for all three chimeras, which is also likely caused by its higher expression level.

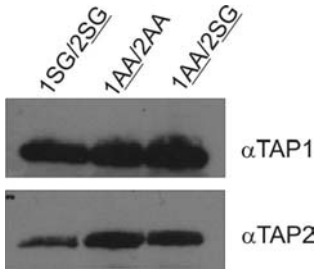

Figure 4-13. Expression of TAP C-loop chimera. Western Blot analysis of microsome preparations from Sf9 insect cells infected with baculovirus encoding TAP variants. The mouse anti-TAP1 (148.3) and anti-TAP2 (435.3) monoclonal antibodies were used to detect TAP1 and TAP2 protein expression, respectively.

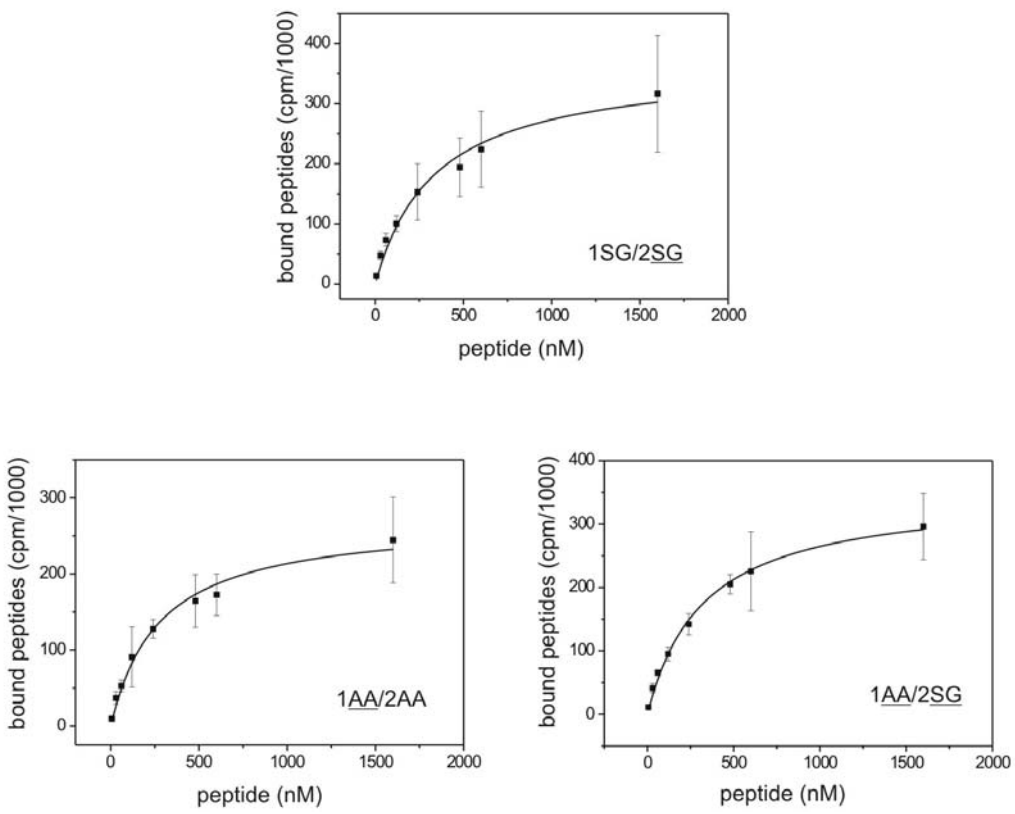

Figure 4-14. Peptide binding of C-loop chimera. Microsomes (15 µg protein) of C-loop chimeras were incubated with increasing concentration of radiolabeled peptide R9LQK (15 min, 4°C). Free peptides were removed by washing and microsome-associated peptides were determined by γ-counting. Specifically bound peptides are plotted against the peptide concentration and fitted by a Langmuir (1:1) binding equation. The peptide affinities are summarized in table 4-1. Data resemble the mean of three measurements.

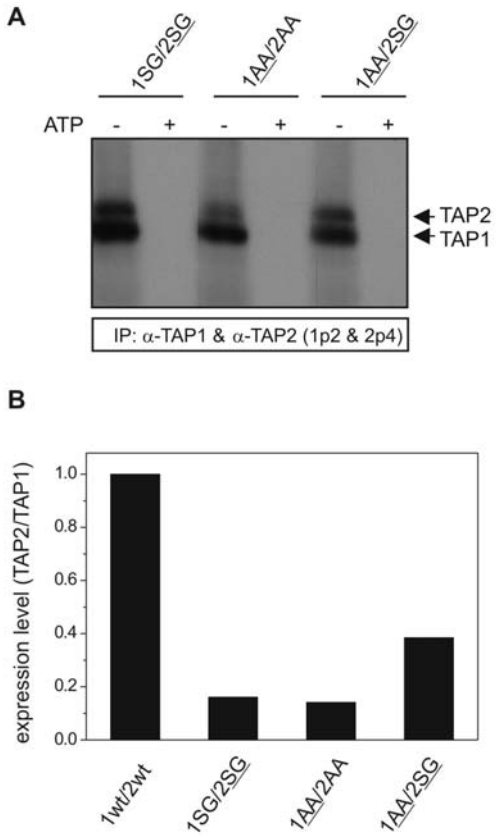

Figure 4-15. ATP binding to C-loop chimera of TAP. A, Microsomes (100 µg protein) containing different single C-loop mutations were incubated with 8-azido-[α-^{32}P]ATP (1 µM) in absence or presence of 1 mM ATP at 4°C. Bound 8-azido-[α-^{32}P]ATP was crosslinked by UV irradiation. Subsequently, TAP was immunoprecipitated with polyclonal antibodies recognizing TAP1 and TAP2 (1p2 and 2p4), separated by SDS-PAGE (11%) and visualized by autoradiography. **B**, **Comparison of the expression level of TAP1 and TAP2.** The procedure is the same as described in figure 4-11B.

4.2.8 Non-identical C-loops induce functional asymmetry

We next investigated the transport activity of the C-loops chimeras. Interestingly, unlike the single residue substitutions of the C-loop described above, all TAP chimeras including the construct having two degenerate C-loops (1AA/2AA) are highly active in peptide translocation. To detect even subtle differences in peptide-translocation activity, initial transport rates were determined. The concentration of functional TAP was normalized by peptide binding (B_{max} value). ATP-dependent peptide translocation into microsomes is peptide-specific and increases linearly over a period of 3 min for all four

TAP variants (Fig. 4-16). However, by analyzing the initial transport rates the differences in peptide transport became obvious (Table 4-2). The 1SG/2SG variant transported peptides with the fastest rate (k = 0.330 cpm/s), which is 115% of the wt TAP. The TAP chimera 1AA/2SG harboring the exchanged C-loop (k = 0.262 cpm/s) translocated peptide as efficiently as wt TAP (k = 0.287 cpm/s).). The most drastic effect showed the TAP complex with two degenerated C-loops with a 50% reduced transport rate in comparison to wt TAP. These results indicate that the C-loop in both TAP subunits controls the peptide-transport rate by tuning the ATP hydrolysis in both ATP-binding sites. In addition, the C-loop is at least partially responsible for the functional asymmetry of both NBDs.

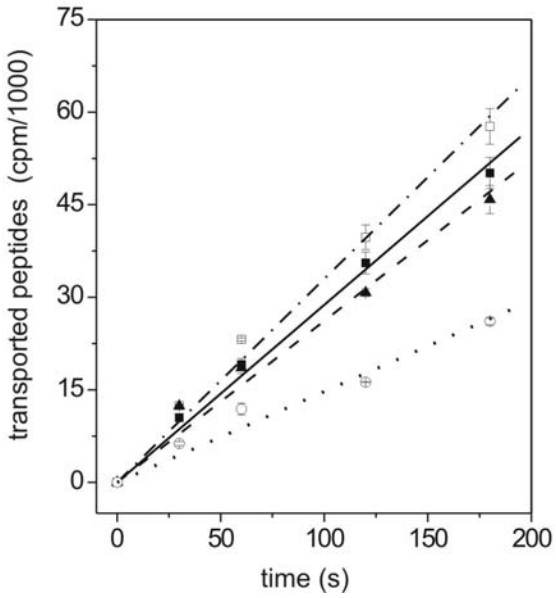

Figure 4-16. Peptide transport of C-loop chimera. The microsomes expressing TAP C-loop chimera were adjusted by their peptide-binding capacity, which were then incubated with 1 µM radiolabeled RRYQNSTEL in the presence of 3 mM ATP or ADP at 32°C over various periods in a total volume of 50 µL. Glycosylated peptides were recovered by Con A sepharose and the radioactivity was quantified via γ-counting. ATP-dependent peptide transport is plotted against time and fitted linearly. The slopes reflect the initial rate constant for peptide transport and are listed in table 4-2. The data points are the mean of three measurements. 1SG/2SG (-·-·- □); 1wt/2wt (—— ■); 1AA/2SG (- - - - ▲); 1AA/2AA (····· ○).

Table 4-2. Peptide transport rates of C-loop chimeras

TAP1/TAP2	k (cpm/s)
1wt/2wt	0.287±0.007
1SG/2SG	0.330±0.010
1AA/2SG	0.262±0.012
1AA/2AA	0.147±0.008

4.2.9 Effect of ATP on the stability of C-loop mutants

The TAP complex undergoes rapid denaturation at 37°C, resulting in a drastically reduced peptide binding and transport activity (van Endert, 1999). Taking peptide-binding ability as readout for TAP function, we analyzed the effect of C-loop mutations on the thermal stability of TAP in the absence of nucleotides. Microsomes containing TAP variants were incubated for 15 min at 37°C and their remaining activities were analyzed by peptide-binding assay. To prevent the interference of the trace-amount ATP or ADP in the microsomes, 1 unit apyrase was added. Here, the peptide binding of each TAP variant at 4°C was defined to 100%. Wild type TAP from Raji cells still showed 65% of peptide-binding capacity after incubation at high temperature, while only 40% peptide-binding sites remained in the wt TAP from Sf9 cells (Fig. 4-17). These results indicate that interaction of the TAP complex with tapasin and MHC class I molecule in Raji cells increases its thermal stability.

In comparison to wt TAP from insect cells, all TAP C-loop single mutants exhibited a reduced stability. The most severe effect was observed for 1LA/2wt, which lost nearly 90% of its peptide-binding ability. Interestingly, two C-loop chimera 1SG/2SG and 1AA/2SG were as stable as wild type TAP; while the C-loop chimera (1AA/2AA) bearing two “degenerated” C-loop resulted in a less stable protein. Taking together, these results demonstrate that the mutation of the highly conserved leucine and glycine in the C-loop from either subunit impair the stability of the TAP complex. Moreover, TAP containing two consensus C-loop (1SG/2SG) or only one consensus C-loop (wt, 1AA/2SG) have similar stability at 37°C. The tolerance of the transporter over high temperature decreases only when the TAP contains two “degenerate ” C-loops.

It was shown by van Endert and his colleagues that ADP and ATP stabilize TAP complexes and maintain its peptide-binding ability at 37°C (Saveanu et al., 2001; van Endert, 1999). Fig 4-17 shows that the presence of 3 mM ATP preserves the peptide-binding ability of all TAP mutants at 37°C, however to different extent. 50% peptide-binding activity remained in all TAP1 C-loop single mutants in the presence of ATP. Interestingly, ATP did not have identical effect on the function of all TAP2 single mutants. It stabilized the TAP2 glycine mutants (1wt/2GV and 1wt/2GD) to the similar level as the wild type, while TAP2 leucine mutant (1wt/2LA) retained only 30% of peptide-binding capacity. For the C-loop chimeras, 1SG/2SG still maintains its 100% peptide-binding ability in the presence of ATP after incubation at 37°C. Under identical condition, the peptide-binding ability of 1AA/2SG is slightly reduced. In comparison, the peptide binding of 1AA/2AA is drastically decreased to 60%. Based on these results, we could draw the following conclusions: i) ATP could only moderately preserve the full function of all TAP1 mutants. ii) the effect of ATP on the stability of TAP2 mutants are diverse. TAP2 glycine mutants retained the full activity in peptide binding but not the leucine mutants. iii) ATP stabilizes TAP chimera containing at least one consensus C-loop to the similar extent as wt TAP.

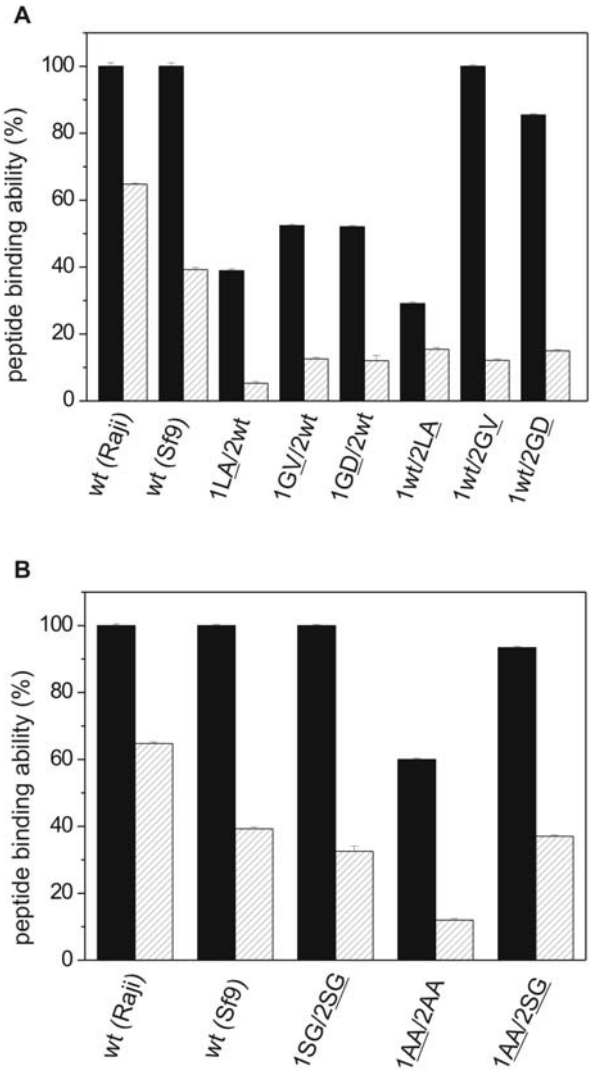

Figure 4-17. Stability of TAP variants at 37°C. Microsomes expressing TAP C-loop single mutants (**A**) or chimeras (**B**) were incubated for 15 min at 37°C in the presence of 3 mM ATP (black bar) or 1 unit apyrase (hatched bar) in 50 µl AP buffer. In parallel, microsomes were also incubated at 4°C under identical condition for 15 min. Then the mixtures were cooled down to 4°C and incubated with 1 µM radiolabeled R9LQK peptides for 15 min. Specific peptide binding was calculated after subtracting the background binding. Setting the peptide-binding ability of the samples at 4°C as 100%, the retained peptide-binding capacity of each mutant after incubation at 37°C was depicted. The results are the average of triplicate samples.

4.3 Role of the acidic residue downstream of the Walker B motif

4.3.1 Introduction

NBDs of ABC transporters catalyze ATP hydrolysis and energize the substrate transport. The NBDs contain three highly conserved sequences: the Walker A and B motifs and the C-loop, which are essential for ATPase activity. In addition, an acidic residue which is a glutamate in most of cases is also highly conserved downstream of the Walker B motif. Based on biochemical studies of glutamate to glutamine mutants (referred to as EQ mutants in this work) of isolated NBD or full-length ABC transporters (Moody et al., 2002; Orelle et al., 2003), this glutamate was proposed to be the catalytic base for the enzymatic cleavage of the phosphoanhydride bond. This hypothesis is in concert with the prediction derived from the structure alignment of several ATPases and ABC transporters (Geourjon et al., 2001; Muneyuki et al., 2000).

ATP hydrolysis was shown to be strictly controlled by peptide binding and peptide transport indicating an allosteric crosstalk between the transmembrane domain and nucleotide-binding domains (Gorbulev et al., 2001). It is believed that during the substrate transport process extensive communications occur between the substrate-binding site and NBDs of ABC transporters. However, only few studies have experimentally addressed the link between ATP hydrolysis and substrate-binding sites. In fact, peptide binding to TAP is considered to be an ATP-independent process (van Endert et al., 1994).

Several studies have shown that catalytic transition states can also be stabilized by mutation of the conserved glutamate in the NBD instead of using ATPase inhibitors (Janas et al., 2003; Moody et al., 2002; Payen et al., 2003). Thus mutation of this residue in TAP can be helpful to i) address the coupling process between the ATP binding/hydrolysis and the peptide binding and ii) gain more insights in the role of the acidic residue in the ATP hydrolysis process. In this study, we have exchanged the conserved acidic residues in NBD1 and NBD2 of TAP and expressed the TAP EQ mutants in insect cells using a baculovirus dual expression system. The effects of the mutations on peptide binding were assessed. Furthermore, we also studied the influence of nucleotide on the peptide-binding ability of the mutants. Finally, the effects of mutations on the transport activity of the TAP were examined.

4.3.2 Expression of TAP EQ mutants

The glutamate downstream to Walker B motif is highly conserved in human ABC transporters (see Appendix 9.2). However, exceptions were found for the ABCC subfamily, with CFTR and MRP1 as representatives. In this subfamily, the glutamate is invariably substituted by an aspartate in NBD1. Surprisingly, TAP1 and TAP2 (ABCB2 and ABCB3) also show this sequence arrangement, thereby distinguishing themselves from other ABCB subfamily members. In order to investigate the function of the acidic residues in the TAP complex, the aspartate in TAP1 (VLILDD) was mutated to asparagine and glutamine (VLILDN, VLILDQ); while the glutamate in TAP2 (VLILDE) was exchanged to glutamine (VLILDQ). The single mutant subunit was constructed into a baculovirus dual expression system together with either wild type or the mutated opposite subunit to form a heterodimeric transporter. Mutants harboring either single or double mutations were expressed in Sf9 cells, which are termed 1DN/2wt, 1DQ/2wt and 1wt/2EQ for single mutants, 1DN/2EQ, and 1DQ/2EQ for double mutants. All TAP constructs are summarized as EQ mutants despite of the aspartate in TAP1.

The expression levels of the TAP EQ mutants in microsomes isolated from infected cells were determined by SDS-PAGE and Western blotting, using the monoclonal antibodies 148.3 and 435.4 to detect TAP1 and TAP2, respectively. Microsomes from insect cells infected with a tapasin baculovirus construct were used as a negative control.

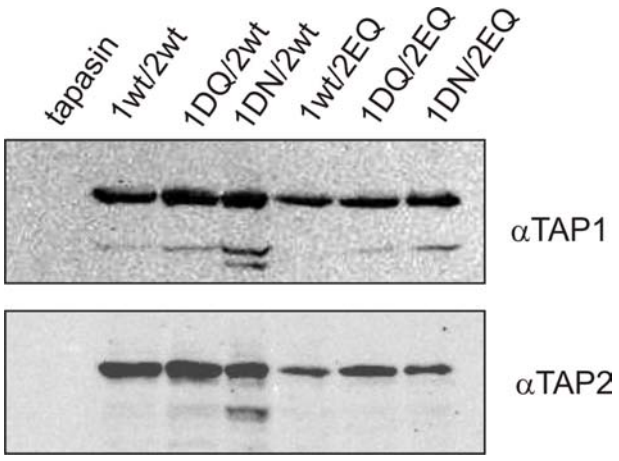

Figure 4-18. Expression of TAP EQ mutants. Microsomal proteins (5 µg) from baculovirus infected Sf9 insect cells were separated with SDS-PAGE (9%) and analysed by Western-blot with anti-TAP1 (148.3) or anti-TAP2 (435.3) antibody. As negative control microsomes containing tapasin were used.

As shown in Fig. 4-18, all EQ mutants were expressed in Sf9 cells at a comparable level to the wild type protein.

4.3.3 Peptide binding of EQ mutants at 4°C

The effect of mutations on the peptide-binding ability of TAP was examined. Microsomes containing TAP variants were incubated with increasing concentrations of radiolabeled R9LQK at 4°C for 15 min. The mixture was added to filter plates followed by the standard procedure as described in section 3.4.5. As shown in Fig. 4-19, the data were fitted by the Langmuir (1:1) binding equation and the peptide dissociation constants K_d as well as the maximal peptide-binding capacity B_{max} of each protein were obtained. All the constants are summarized in Tab. 4-3. The B_{max} value of each construct indicates the amount of functional TAP complexes presented in the experiments. The K_d values of all TAP proteins are quite similar, demonstrating that substitution of the putative catalytic base of TAP1 and TAP2 does not alter the peptide-binding affinity.

At 4°C, EQ mutants of several nucleotide-binding domains of ABC transporters can be arrested in a dimeric transition state upon ATP binding, resulting in a sandwich dimer containing two ATPs (Janas et al., 2003; Moody et al., 2002; Verdon et al., 2003). It was postulated that such an ATP-driven dimerization step mediates the structural rearrangement of the transmembrane domains (Locher et al., 2002; Moody et al., 2002; Smith et al., 2002b). Here we addressed the question, whether nucleotide binding to TAP EQ mutants induces any changes in the peptide-binding site located in the transmembrane domain. Thus, the peptide-binding affinity of all constructs was determined in the presence of 3 mM ATP or ADP. The results are depicted in Fig. 4-19 and the obtained constants are summarized in Tab. 4-3. Consistent with previous observations, wild type TAP binds peptide with the same affinity in the presence or absence of nucleotides (Neumann and Tampé, 1999; Uebel et al., 1995). In contrast to our expectation, nucleotides did not show significant influence on the peptide-binding affinity of all five mutated proteins. These results suggest that the peptide-binding affinity of the TAP complex was not changed in the ATP-ATP dimeric state of the NBDs.

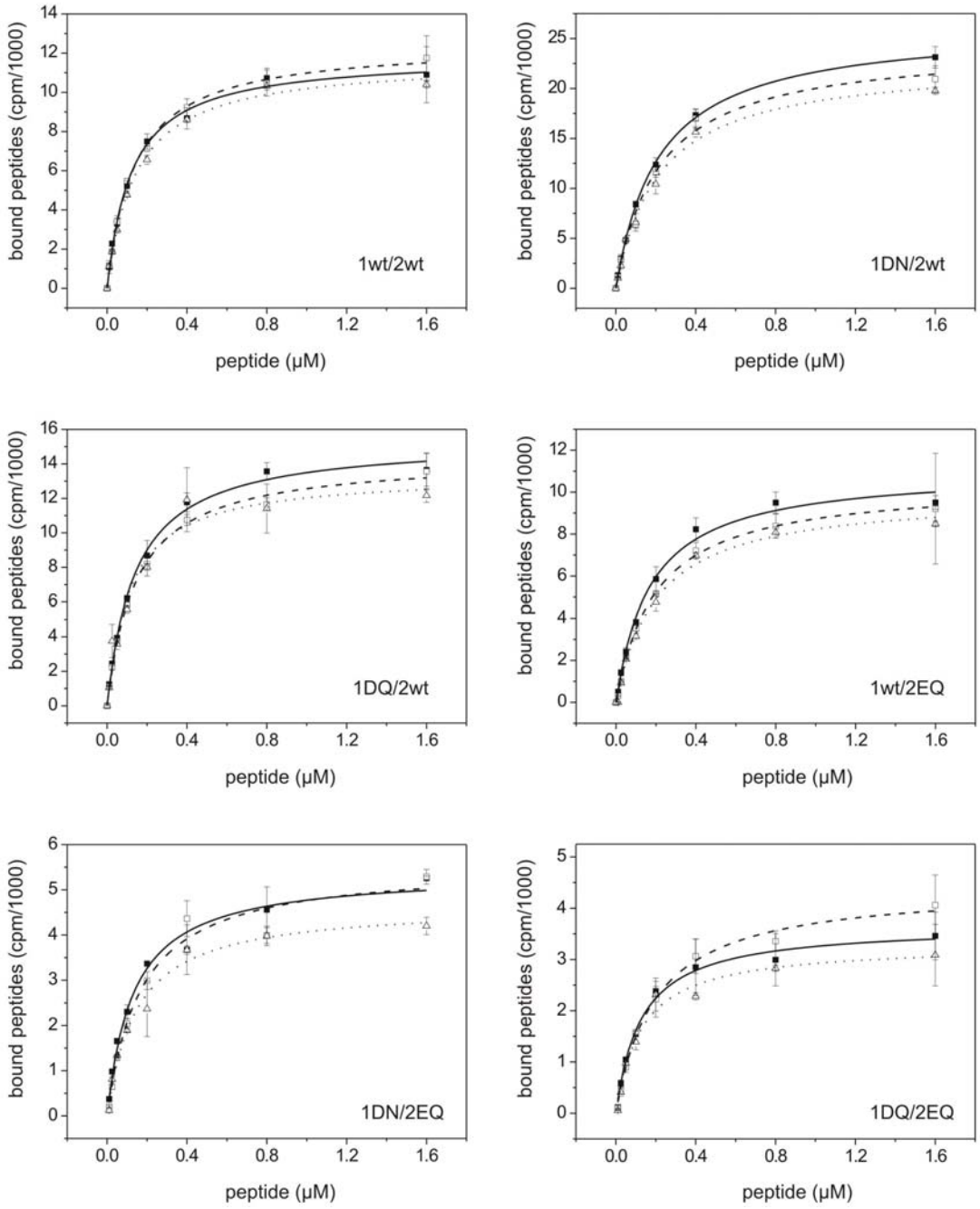

Figure 4-19. Peptide binding of EQ mutants at 4°C. Microsomes (15µg protein) containing TAP mutants were incubated with an increasing concentration of radiolabeled R9LQK in 50 µl AP buffer in the absence or presence of 3 mM ATP/ADP at 4°C for 15 min. Free peptides were removed by washing three times with 150 µl ice cold AP buffer and microsome-associated peptides were determined by γ-counting. Specifically bound peptides in the absence of nucleotides (—— ■), or presence of 3 mM ATP (---- □) or 3 mM ADP (····· △) are plotted against the peptide concentration and fitted by the Langmuir (1:1) binding equation. Data resemble the mean of triplicate measurements.

Table 4-3. Summary of peptide binding constants of TAP EQ mutants at 4°C.

Protein	No nucleotide		ATP		ADP	
	K_d (μM)	B_{max} (cpm/1000)	K_d (μM)	B_{max} (cpm/1000)	K_d (μM)	B_{max} (cpm/1000)
1wt/2wt	0.123±0.010	11.8±0.2	0.138±0.009	12.4±0.2	0.142±0.012	11.6±0.3
1DN/2wt	0.215±0.007	26.3±0.2	0.216±0.027	24.3±1.0	0.215±0.021	22.7±0.8
1DQ/2wt	0.142±0.012	15.4±0.2	0.145±0.010	14.3±0.3	0.200±0.026	13.4±0.8
1wt/2EQ	0.131±0.018	11.0±0.3	0.168±0.010	10.4±0.1	0.146±0.018	9.8±0.3
1DN/2EQ	0.127±0.018	5.3±0.2	0.95±0.035	5.5±0.3	0.128±0.022	4.6±0.2
1DQ/2EQ	0.190±0.014	3.6±0.1	0.130±0.019	4.4±0.1	0.190±0.024	3.3±0.2

4.3.4 Peptide binding of EQ mutants at 27°C

EQ mutants of Mdl1 NBD were shown to be arrested in a dimeric transition state containing one ATP and one ADP after being incubated under ATP hydrolysis condition (Janas et al., 2003). This ATP-ADP dimeric state occurs after the ATP-ATP dimeric state in the ATP hydrolysis cycle. Since in the ATP-ATP dimeric state, the peptide-binding site of TAP remains the same as in its ground state, a question arises: is the peptide-binding site of TAP complex altered in the ATP-ADP dimeric state? To trap TAP EQ mutants in an ATP-ADP dimeric state, microsomes containing TAP EQ mutants were incubated at 27°C with 20 nM peptides R9LQK in the presence of nucleotides for 30 min. Then radiolabeled R9LQK with increasing concentrations were added to the microsomes to determine their peptide-binding ability at 27°C. Although peptide transport can occur under experimental condition, it doesn't disturb the peptide-binding assay because R9LQK without a glycosylation sequence cannot accumulate inside the microsomes. The results are shown in Fig. 4-20 and all affinity constants were summarized in Table 4-4.

Similar to the results at 4°C, nucleotides did not significantly affect peptide dissociation constants of all six TAP variants at 27°C. In contrast, B_{max} values of TAP complexes differed in the presence or absence of nucleotides (Fig. 4-21). In the presence of nucleotides, wild type TAP showed a higher B_{max} than in the absence of nucleotides.

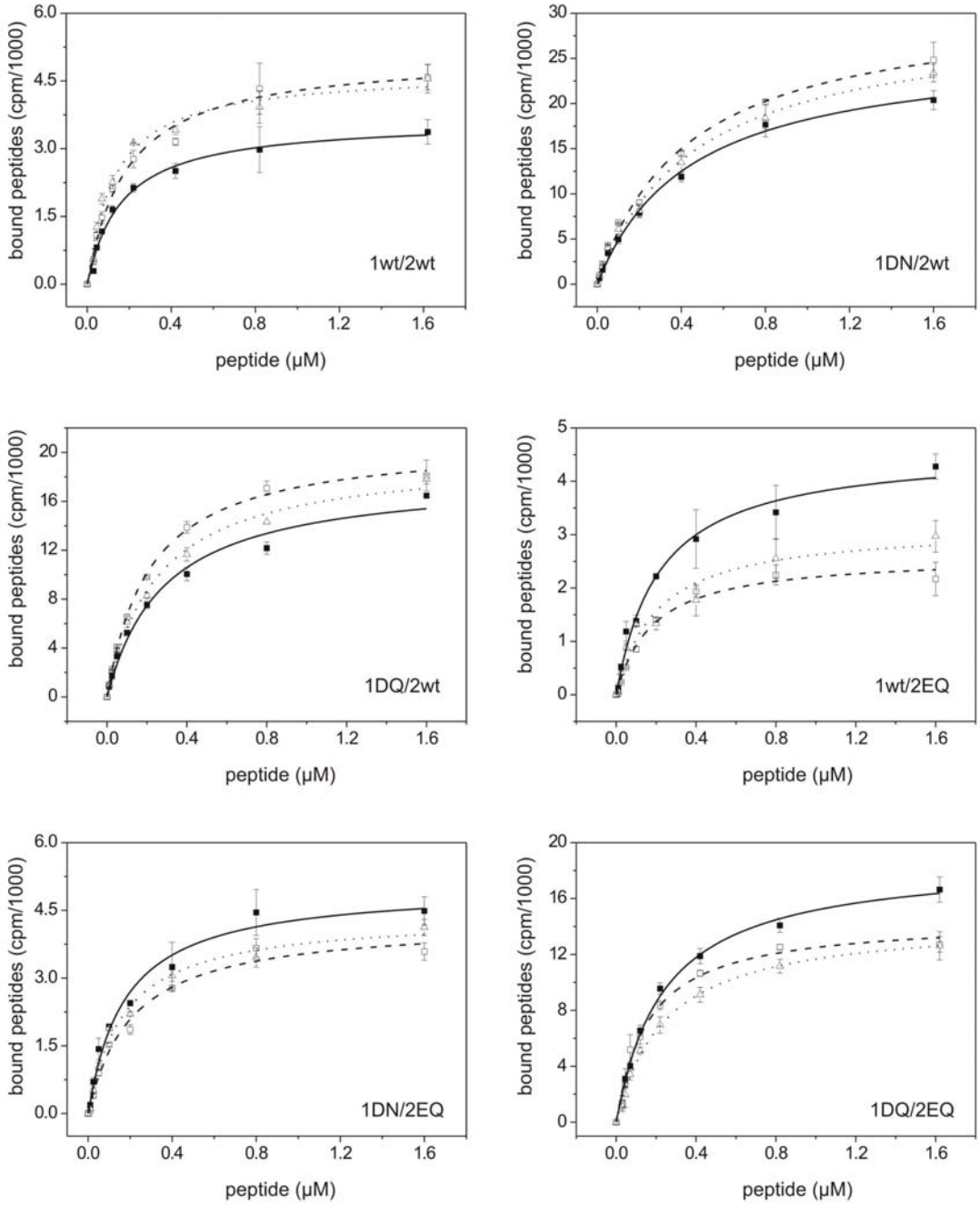

Figure 4-20. Peptide binding of EQ mutants at 27°C. Microsomes (15 µg protein) containing TAP mutants were incubated with 20 nM R9LQK in the absence of nucleotides (—— ■) or in the presence of 3 mM ATP (---- □), 3 mM ADP (····· △) at 27°C in 45µL AP buffer for 30 min. Afterwards, 5 µl increasing concentrations of iodinated R9LQK was added to the mixture, which were incubated at 27°C for 5 min. Free peptides were removed by washing three times with 150 µl ice cold AP buffer and microsome-associated peptides were determined by γ-counting. Specifically bound peptides are plotted against the peptide concentration and fitted by a Langmuir (1:1) binding equation. Data resemble the mean of triplicate measurements.

Table 4-4. Summary of peptide binding constants of TAP EQ mutants at 27°C.

Protein	No nucleotide		ATP		ADP	
	K_d (µM)	B_{max} (cpm/1000)	K_d (µM)	B_{max} (cpm/1000)	Kd (µM)	B_{max} (cpm/1000)
1wt/2wt	0.106±0.010	3.4±0.1	0.128±0.027	4.8±0.2	0.089±0.010	4.4±0.1
1DN/2wt	0.442±0.040	26.3±1.0	0.430±0.052	31.1±1.4	0.463±0.050	29.6±1.4
1DQ/2wt	0.282±0.051	18.1±1.1	0.213±0.018	21.0±0.4	0.180±0.012	19.8±0.8
1wt/2EQ	0.209±0.034	4.6±0.2	0.230±0.027	2.7±0.1	0.221±0.051	3.1±0.3
1DN/2EQ	0.190±0.0353	5.0±0.2	0.220±0.023	4.2±0.2	0.191±0.023	4.4±0.2
1DQ/2EQ	0.190±0.038	17.7±0.5	0.130±0.033	13.7±0.6	0.192±0.022	13.6±0.3

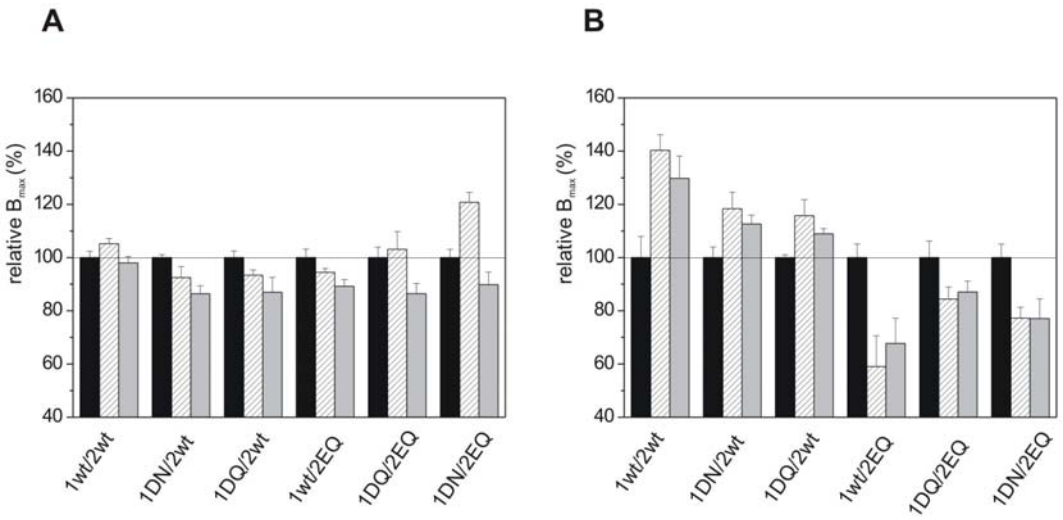

Figure 4-21. Effect of nucleotides on the peptide binding ability of EQ mutants. B_{max} of each TAP mutant derived from Fig. 4-19 and Fig. 4-20 are shown. The B_{max} value of each TAP variants in the absence of nucleotides was set to 100%. The ratios of the B_{max} in the presence of 3 mM ATP (hatched) or 3 mM ADP (gray) to the sample in the absence of nucleotides (black) are depicted.

Similar results were observed for single TAP1 mutants (1DN/2wt, 1DQ/2wt). It was previously shown that binding of nucleotides stabilizes TAP at high temperature (van Endert, 1999). Since incubation of microsomes at 27°C for 30 min denatures TAP gradually, the higher B_{max} in the presence of nucleotides could be due to their increased stability. Strikingly, both ATP and ADP caused a reduced B_{max} value by 20% for TAP2

single mutation (1wt/2EQ) and TAP mutants with double mutations (1DN/2EQ and 1DQ/2EQ). Such negative regulatory effect was only observed at 27°C (Fig. 4-20). This data suggested that part of TAP complexes with mutant TAP2 subunits might turn to a conformation in which peptide binding is abolished.

In addition, the peptide dissociation constants determined at 4°C or 27°C are quite similar for all TAP variants except for TAP1DN/2wt. This mutant showed a two-fold increased K_d value at 27°C compare to 4°C. This might be due to too high concentration of TAP complex (ligand) in the reaction. In this case, the prerequisite condition ([substrate]>>[ligand]) to fit the data by the Langmuir (1:1) binding equation is not met.

4.3.5 Peptide binding kinetics

As another means of evaluating the influence of nucleotide on peptide binding, a fluorescence quenching assay was applied to study peptide-binding kinetics (Neumann and Tampé, 1999). Fluorescein is very sensitive to the polarity or pH of the environment. Thus the time-dependent change of fluorescence emission was analyzed during the binding and dissociation of fluorescein-labeled peptide to TAP. When microsomes are added to the solution containing fluorescein-labeled peptide RRYC(Fluo)KSTEL, a decrease of the fluorescence signal is observed. Adding a 400-fold molar excess of non-labeled peptide (competitor) releases bound fluorescein-labeled peptides, leading to a time-dependent increase of the fluorescence signal. A typical experiment is shown in Fig. 4-22A. The association and dissociation, represented by the decrease and recovery of the fluorescence signal, can be fitted by monoexponential function (Fig. 4-22B) and the dissociation rate constant k_{dis} can be deduced.

To investigate the effect of the mutation on peptide-binding kinetics, the mutant 1DQ/2EQ was selected and compared with wild type TAP. The dissociation rate constants k_{dis} for wt and 1DQ/2EQ mutants under different conditions are presented in Table 4-5. At 4°C, peptide dissociation rate constants of wild type TAP and 1DQ/2EQ are quite similar in the presence or absence of nucleotides. Thus, we can conclude that at 4°C neither the binding of nucleotides nor mutation of the glutamate (aspartate) affects the peptide dissociation rate of TAP.

At 27°C, peptide dissociation rate constant of wt TAP increases to different extent varying from 2.5 to 6 fold depending on the presence or absence of nucleotides. This result

demonstrated that increasing temperature accelerated peptide dissociation from TAP. In comparison to the value with ADP or no nucleotides, k_{dis} decreases by approximate 50% in the presence of ATP or ATP•Mg^{2+}. The Mg^{2+} cation did not show an influence on the peptide binding rate, indicating that both ATP binding and hydrolysis slowed down the peptide dissociation from TAP to the same extent.

As for the TAP 1DQ/2EQ at 27°C, the k_{dis} also increases by a factor of 3 to12. Similar to wild type TAP, ATP binding and/or hydrolysis also slow down the dissociation of peptides from 1DQ/2EQ. In addition, mutants show nearly identical k_{dis} values as the wt TAP under ATP binding/hydrolysis conditions (ATP/ATP•Mg^{2+}). Dissociation rate constants of 1DQ/EQ were slightly larger than that of wt TAP in the presence of ADP or no nucleotides, suggesting that the mutant 1DQ/2EQ undergoes relatively faster peptide dissociation under these conditions. Taken together, we concluded that ATP binding and/or hydrolysis induce a slower dissociation rate at high temperature for both wt TAP and mutant 1DQ/2EQ. Moreover, the k_{dis} constants of wt TAP and 1DQ/2EQ do not show drastic differences under all conditions, indicating that the mutation does not have a strong influence on the peptide dissociation rate.

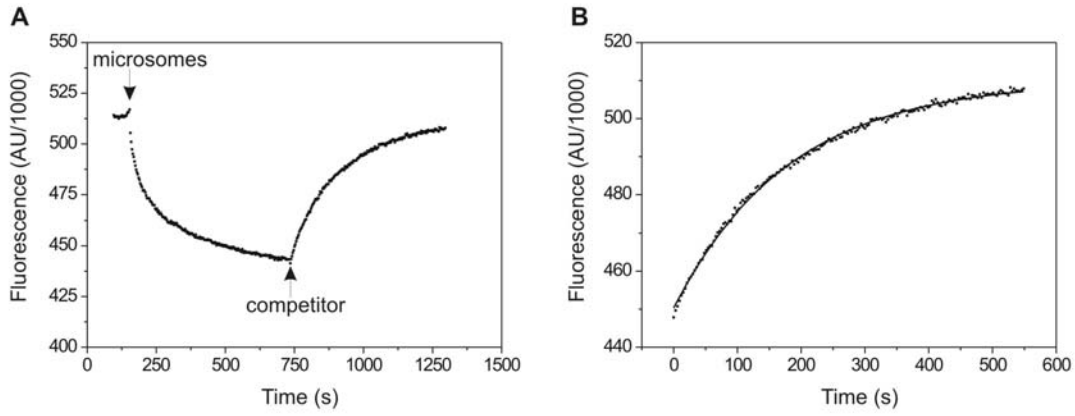

Figure 4-22. Peptide binding kinetics studied by fluorescence quenching. A, The fluorescence emission was recorded at 470/515 nm (excitation/emission) after mixing TAP-containing microsomes with 20 nM RRYC(Fluo)KSTEL in the presence or absence of nucleotides at 4°C or 27°C (see Methods). The concentrations of TAP and total protein were 2 nM and 100 µg/ml, respectively. Dissociation of bound peptide from the TAP complexes was induced by adding a 400-fold molar excess of non-labeled RRYQKSTEL. **B,** The time-dependent change of fluorescence signal was fitted with monoexponential function (Section 3.4.6) to obtain the dissociation rate constants (solid line).

Table 4-5. Peptide binding dissociation rate constants.*

Protein	Condition	k_{dis} ($s^{-1}\times10^3$)	
		4°C	27°C
wt	-	5.62±0.54	30.40±1.71
	ATP	7.52±0.36	18.52±1.50
	ATP•Mg^{2+}	5.26±0.72	16.64±2.16
	ADP	5.59±0.27	37.31±1.08
1DQ/2EQ	-	5.26±0.65	45.45±3.73
	ATP	6.41±0.82	19.92±3.14
	ATP•Mg^{2+}	5.32±0.38	17.89±2.31
	ADP	4.44±0.32	61.34±1.25

*Numbers listed are the average calculated from triple experiments

4.3.6 Peptide transport activity of TAP mutants

To study the effect of the EQ mutation on the function of TAP, peptide uptake by microsomes from Sf9 cells expressing wild type and mutant TAP was determined at 32°C for 2 min. The total amount of TAP in each TAP variant was normalized by peptide-binding assays in order to compare their activity. As shown in Fig. 4-23, substitution of the aspartate residue in TAP1 (1DN/2wt) with asparagine does not show any effect on peptide transport activity. In comparison, a glutamate at this position (1DQ/2wt) leads to a decrease in peptide translocation by 40%. The equivalent mutation at TAP2 (1wt/2EQ) showed similar reduced activity. Surprisingly, although the transport activity was more severely impaired in the constructs containing double mutations at both subunits (1DN/2EQ and 1DQ/2EQ), the transport activity of these two variants still retained 30% of the wild type level. In summary, all the TAP EQ mutants except for TAP 1DN/2wt show a reduced transport activity. However, the activities of the TAP constructs bearing double mutations are not completely abolished. These results demonstrate that the acidic residue adjacent to Walker B site is not essential for TAP function.

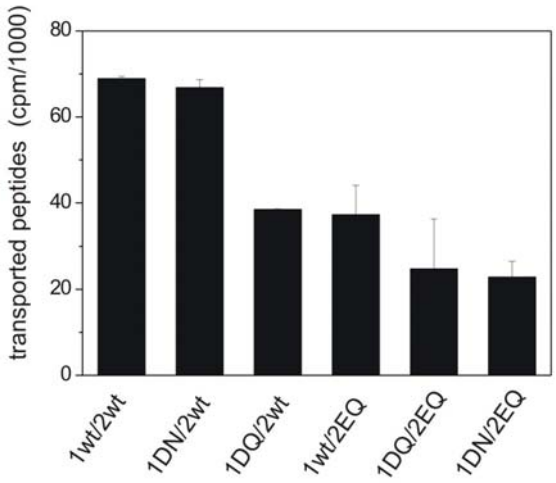

Figure 4-23. Peptide transport activity of TAP EQ mutants. Microsomes containing different mutants were incubated with 1 µM radiolabeled RRYQNSTEL in the presence of 3 mM ATP or ADP at 32°C for 2 min. Transported peptides were recovered by Con A sepharose and the radioactivity was quantified by γ-counting. ATP-dependent peptide transport was calculated by subtracting the radioactivity of the ATP samples from the ADP samples. The amount of TAP mutants in the reaction was normalized by their peptide-binding sites. Data resemble the mean of triplicate measurements.

4.3.7 Effect of EQ mutations on peptide transport kinetics

Peptide transport by TAP consists of three steps (Abele and Tampé, 1999; Lankat-Buttgereit and Tampé, 2002): i) ATP binding to TAP; ii) peptide binding to TAP; iii) peptide transport.

So far, no kinetic data has been reported for ATP binding to ABC transporters, which occurs likely within the millisecond time. At the concentration of 3 mM of ATP, peptide transport is predominantly controlled by peptide binding and subsequent transport process. Thus we propose a two-step transport process: i) binding of peptide to TAP that is already preloaded with ATP; ii) translocation of peptide through the ER membrane.

$$TAP + Pep^{cytosol} \underset{k2}{\overset{k1}{\rightleftharpoons}} TAP^{*}Pep \xrightarrow{k3} TAP + Pep^{ER}$$

The initial peptide transport rates of wild type and mutant (1DN/2EQ) TAP were determined at increasing concentrations of peptide RRYQNSTEL at 32°C. Data of both

TAP variants could be fitted by Michaelis-Menten equation and the results are depicted in Fig 4-24. To distinguish the K_m value for the two substrates (peptides and nucleotides), we defined here the K_m value for peptides as $K_{m,\,pep}$. Interestingly, the calculated $K_{m,\,pep}$ of wild type (1.43 µM) is around two times higher than that of 1DN/2EQ (0.65 µM).

Since the peptide-binding affinities ($K_d=k_2/k_1$) of both proteins in the presence of ATP are quite similar, the difference in the K_m values can be explained by the reduced *k3* value for the TAP mutant 1DN/2EQ. In the Michaelis-Menten model, the *k3* is the turnover number, which is directly related to the activity of an enzyme. The calculated *k3* for wt TAP (0.140 s^{-1}) is 4 times higher than mutant 1DN/2EQ (0.034 s^{-1}), which is in good agreement with the ratio from transport activity. In summary, by kinetic analysis we showed the turnover number of TAP complex is reduced by a factor of 4 after eliminating the acidic residue downstream of both Walker B sites.

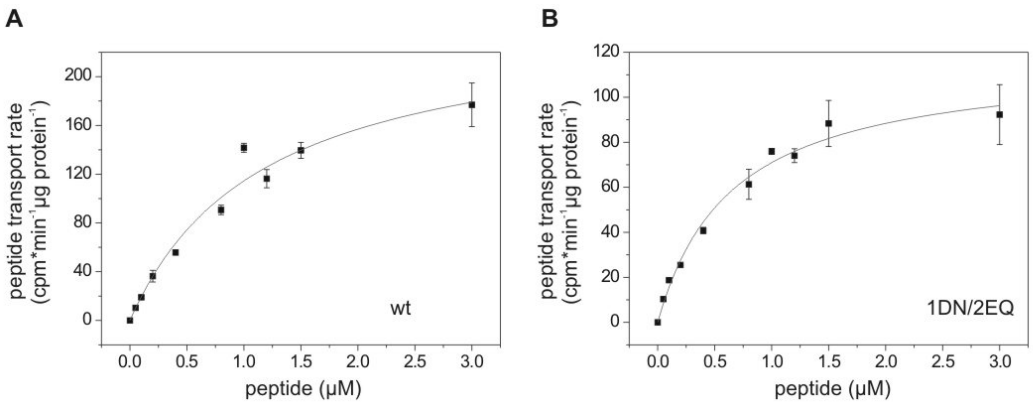

Figure 4-24. Peptide transport kinetics of TAP complexes. Microsomes (100 µg protein) containing TAP wide type (**A**) or 1DN/2EQ (**B**) were incubated with 3 mM ATP or ADP at increasing concentrations of RRYQNSTEL at 32°C for 2 min. Transported peptides were recovered by concanavalin A sepharose, and the radioactivity was quantified by γ-counting. ATP-dependent transported peptides were calculated by subtracting the signal of ADP samples from the ATP samples. The data were fitted with the Michaelis-Menten equation $V=V_{max}*C/(K_{m,pep}+C)$ leading to a $K_{m,pep}$ value of 1.434±0.118µM for wild type TAP and 0.650±0.099 µM for TAP 1DN/2EQ. Data points were derived from triplicate measurements.

4.3.8 Effect of divalent cations on peptide transport

It is well known that divalent cations are an essential cofactor for ATPases in enzymatic cleavage of the phosphoanhydride bond (Cohn, 1990; O'Rourke, 1993). Mg^{2+}

serves this role in most biological systems (Cohn, 1990; O'Rourke, 1993). Other divalent cations (e.g. Mn^{2+}, Ca^{2+}) can substitute for Mg^{2+} in this respect, albeit to different extent (Cohn, 1990; Morbach et al., 1993; Urbatsch et al., 1994). Thus, we were interested in determining whether the acidic residues of TAP1 (D668) and TAP2 (E632) may be involved in forming a complex with cations, as well as whether mutations affect the selectivity of cations. To address these questions, the peptide transport efficiency in the presence of different divalent cations was analyzed. As shown in Fig 4-25, wild type TAP transported peptides most efficiently in the presence of Mn^{2+}. The ability of other cations to support peptide transport decreases in the following order: Mg^{2+}>Co^{2+}>Ni^{2+}. Cu^{2+} and Zn^{2+} failed to catalyze the ATP hydrolysis by TAP. 1DQ/2EQ follows similar rules in choosing a cation as the wild type protein with a slight preference for Co^{2+} over Mg^{2+}. However, the whole specificity profile for selecting cations was not changed by introducing neutral residues, indicating the acidic residue is not involved in complexing the divalent cation.

Although ABC transporters show a reduced ATP-binding in the absence of cation (Cai et al., 2002; Chen et al., 2003b), submilimolar concentrations of ATP were sufficient to bind isolated EQ NBDs and subsequently induce the dimerization in the absence of cation (Janas et al., 2003; Moody et al., 2002; Verdon et al., 2003). Peptide transport of TAP 1DQ/2EQ is dependent on divalent cations, suggesting that ATP-binding alone is not able to support the peptide translocation. TAP must undergo ATP hydrolysis to pump the peptides through the ER membrane.

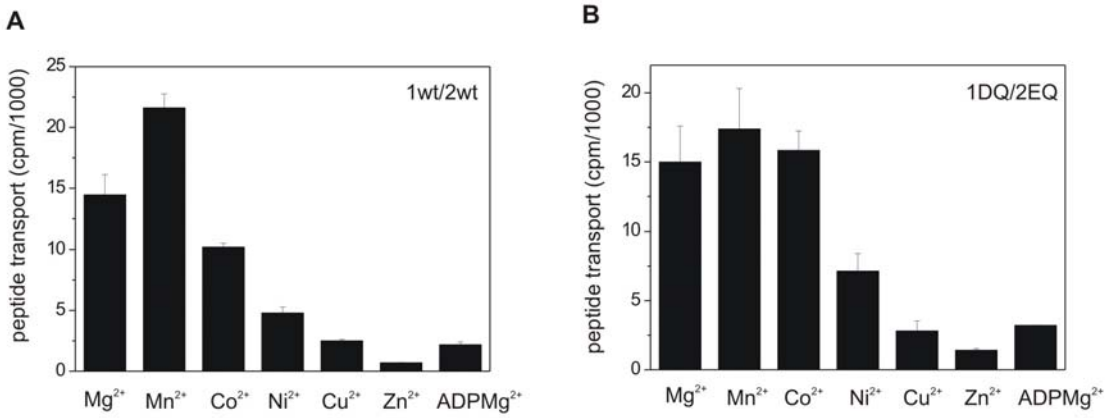

Figure 4-25. Effect of divalent cations on peptide transport. Microsomes (200 µg protein) containing (**A**) TAP wt or (**B**) 1DQ/2EQ were incubated with 1 µM radiolabeled RRYQNSTEL in the presence of 3 mM ATP or ADP and 5 mM divalent cations ($MgCl_2$, $CoCl_2$, $MnCl_2$, $NiCl_2$, $CuCl_2$ and $ZnSO_4$) in 50 µl PBS buffer, pH 7.0 at 32°C for 2 min. Transported peptides were recovered by Con A sepharose and the radioactivity was quantified by γ-counting. Data resemble the mean of triplicate measurements.

5. Discussion

5.1 Two catalytically active NBDs of TAP

In the last decade, major advances have been made in the study of the mechanism of peptide transport by TAP: (i) the peptide specificity and the peptide-binding mechanism of TAP were deciphered in detail (Neumann et al., 2002; Neumann and Tampé, 1999; Uebel et al., 1997); (ii) the importance of the nucleotide-binding domains of TAP for peptide transport was shown by mutation analysis (Alberts et al., 2001; Karttunen et al., 2001; Knittler et al., 1999; Lapinski et al., 2001; Saveanu et al., 2001); and (iii) the allosteric coupling between peptide binding, ATP hydrolysis and peptide transport was observed with reconstituted TAP (Gorbulev et al., 2001). However, the contribution of each subunit in the TAP complex to ATP hydrolysis was not characterized up to now.

By using the technique of BeF_x trapping of 8-azido-[α-^{32}P]ATP followed by photolabeling, immunoprecipitation and separation of the TAP subunits by high resolution SDS-PAGE, we analyzed the ATPase activity of TAP1 and TAP2 for the first time. Using the ATPase inhibitor BeF_x formation of a stable complex consisting of Mg•ADP•BeF_x bound to NBD was achieved. For myosin, a trapping of MgADP by BeF_x longer than 3 days is reported (Maruta et al., 1993). Restricted by the instability of TAP, we showed that the trapped TAP complex is at least stable for 45 min. We showed that BeF_x trapping of TAP is peptide-specific. High affinity peptides induced nucleotide trapping of both subunits of TAP in a concentration-dependent manner. This reflects the peptide-stimulated ATPase activity of the TAP complex reported in earlier work (Gorbulev et al., 2001). Although these previous results demonstrated that peptide binding correlates with ATP hydrolysis, we now provide evidence that ATP hydrolysis at both subunits is induced by peptides with an EC50 corresponding to the affinity of the peptide. These observations are in line with the model that peptide binding to TAP is responsible for a dramatic structural rearrangement (Neumann et al., 2002) that triggers ATP hydrolysis by the NBDs of TAP1 and TAP2 resulting in peptide translocation. The low amount of trapping in the absence of peptide or in the presence of low affinity peptides could result from a low intrinsic ATPase activity of TAP. However, in the presence of US6, which blocks ATP binding, no reduction of background ATPase activity could be observed excluding an intrinsic ATPase activity of TAP (Kyritsis et al., 2001). Therefore, background trapping probably caused a

backward reaction, in which 8-azido-[α-^{32}P]ADP produced by other ATPases is bound and trapped at TAP. This point is supported by the observation that trapping of 8-azido-ADP results in the same labeling efficiency of TAP as with 8-azido-ATP in the presence of the viral inhibitor ICP47, which blocks peptide binding to TAP.

The trapped state can be formed independently of ATP hydrolysis, as indicated in the studies of Pgp, MRP6, and myosin, which were trapped from an ADP binding state (backward reaction) by vanadate or metal fluorides in the absence of ATP hydrolysis (Cai et al., 2002; Sauna et al., 2001b; Werber et al., 1992). With low efficiency, BeF_x also traps TAP from an ADP binding state. Importantly, however, the trapping of 8-azido-ADP is not affected by peptides. These observations are in line with studies on Pgp showing that trapping without ATP hydrolysis is energetically less favorable. Substrate-induced trapping of Pgp is only achieved after ATP hydrolysis and is strongly inhibited in presence of ADP (Sauna et al., 2001a; Sauna et al., 2001b). Surprisingly, the trapping efficiency of TAP by orthovanadate is very low in comparison to BeF_x. Similar results are reported for MRP6, where BeF_x traps ADP very efficiently and vanadate could only trap ADP in presence of Ni^{2+} (Cai et al., 2002). The trapping efficiencies of phosphate analogs can be discussed by comparing the x-ray structures of myosin in complex with Mg•ADP•BeF_4^{2-}, Mg•ADP•AlF_4^-, and Mg•ADP•Vi (Fisher et al., 1995; Smith and Rayment, 1996). The Vi/AlF_4^+-inhibited complexes reflecting most probably the myosin•Mg•ADP-Pi transition state were very similar, and the distance between Al/V and the bridging oxygen of the γ-phosphate group of ADP was 2.0 Å for AlF_4^- and 2.1 Å for Vi. However, in the BeF_x-trapped state, which resembles the ground state before ATP hydrolysis occurs, the distance between BeF_x and the bridging oxygen was only 1.6 Å. Based on this knowledge, the differences in trapping MgADP to TAP were probably caused by small structural differences in the ATP-binding pocket, in which Mg•ADP•BeF_x fits well forming a stable complex.

The crystal structure of the monomeric NBD of TAP1 is highly similar to other NBDs of ABC transporters (Gaudet and Wiley, 2001). The structure of the E171Q mutant of MJ0796 and the orientation of the NBDs of the vitamin B12 transporter BtuCD resemble the Rad50 dimer in which the ATP binding pocket is formed from the Walker A and B sequences of one subunit and the C-loop of the other subunit (Hopfner et al., 2000; Locher et al., 2002; Smith et al., 2002b). We propose that this dimer structure represents a

physiological intermediate that occurs transiently during the transport cycle when ATP is bound. Therefore, in the trapped state, the NBDs of TAP should be closely associated resembling the structure of the NBD dimer. This could explain that, in the trapped state, TAP neither binds nor exchanges nucleotides. This observation is in agreement with soluble expressed NBDs of the structural and functional TAP homolog MDL1p, a homodimeric ABC peptide transporter located in the inner mitochondrial membrane. The NBDs of MDL1p form stable BeF_x-trapped dimers after ATP hydrolysis. The BeF_x-trapped NBD dimer contains two ADP molecules, which cannot be exchanged by nucleotides (Janas et al., 2003). With the structure of the NBD dimer in mind, it is surprising that both TAP subunits show different labeling efficiency. At 4°C, TAP2 shows stronger 8-azido-ATP photolabeling than TAP1. This difference reflects the 2-fold higher affinity of TAP2 (2.7 µM) for 8-azido-ATP than TAP1 (4.6 µM) as reported recently (Lapinski et al., 2003). However, in the BeF_x-trapped state, TAP1 is more strongly photocross-linked than TAP2. The possibility that trapped 8-azido-ADP bound to the Walker A site of TAP2 photoreacts with the C-loop of TAP1 is very unlikely, because it was shown that trapped 8-azido-[α-^{32}P]ADP is photocrosslinked to a tyrosine residue of P-gp, which is highly conserved throughout ABC transporters and forms π- π interactions with the adenine ring (Gaudet and Wiley, 2001; Hung et al., 1998; Sankaran et al., 1997; Smith et al., 2002b). Furthermore, it is very unlikely that the different signals of trapped nucleotide arise from different ATPase activities of both subunits during peptide transport. In this case TAP1 should hydrolyze more ATP than TAP2, which is in contrast to the cooperativity between both NBDs as reported for other ABC transporter (Davidson and Sharma, 1997; Liu et al., 1997; Senior and Bhagat, 1998). Therefore, kinetic or structural differences between both ATP-binding sites must likely be the reason for the different labeling efficiencies. One possibility is that two ATPs are hydrolyzed within the dimer during peptide transport; TAP2 might release ADP faster than TAP1 resulting in a lower trapping yield. Another possibility is that the two nucleotide-binding sites differ slightly resulting in a more stable Mg•ADP•BeF_x complex for TAP1 than for TAP2.

In this study, we demonstrate that BeF_x traps ADP in TAP1 and TAP2 after peptide-stimulated ATP hydrolysis. However, we could not decide whether one or two nucleotides are fixed within the heterodimeric TAP complex at the same time. Principally, two possibilities are found for the trapped state of ABC transporters: (i) both subunits have

tightly bound nucleotides in the trapped state, or (ii) only one nucleotide is associated with the ABC transporter after trapping. In the case of the chloride channel CFTR, an occlusion of NBD1 with 8-azido-[α-^{32}P]ATP is observed that can be enhanced under vanadate trapping conditions that also strongly traps 8-azido-[α-^{32}P]ADP to NBD2 (Szabo et al., 1999). Consequently, in the trapped state, one ADP and one ATP are bound to NBD2 and NBD1 of CFTR, respectively. In contrast, only one ADP is bound to P-gp and the maltose permease in the vanadate-trapped state (Chen et al., 2001; Qu and Sharom, 2001). These differences in trapping are also reflected in the effect of mutations of the highly conserved lysine in Walker A sequence. Mutation of any NBD of the classic ABC transporters TAP, P-gp, and maltose permease has severe effects on transport or ATPase activity, whereas the same mutation in NBD1 of CFTR does not inhibit significantly the gating (Alberts et al., 2001; Karttunen et al., 2001; Knittler et al., 1999; Lapinski et al., 2001; Saveanu et al., 2001). A high and low affinity substrate-binding site has been proposed for several drug ABC transporters during the transport process (Sauna and Ambudkar, 2000; van Veen et al., 2000). Interestingly, the amount of peptide-binding sites and the peptide affinity of TAP are not altered in the BeF_x-trapped intermediate. These data suggest that the peptide has already been translocated across the membrane.

In summary, we provide direct evidence that both NBDs of the TAP complex are active in ATP hydrolysis during the peptide transport process. In line with previous studies, the asymmetric pattern of photolabeling under BeF_x-trapping conditions indicates the distinctive properties of TAP1 and TAP2 with respect to ATP binding and hydrolysis (Alberts et al., 2001; Karttunen et al., 2001; Knittler et al., 1999; Lapinski et al., 2001; Saveanu et al., 2001). Combining the newly established BeF_x trapping of TAP with mutations influencing ATP hydrolysis or peptide transport, the exact role of the two NBDs in TAP function can be addressed.

5.2 Non-equivalent C-signature motifs in TAP

Recent studies have provided some evidence that both TAP subunits act asymmetrically in the transport cycle (Alberts et al., 2001; Karttunen et al., 2001; Lapinski et al., 2001; Saveanu et al., 2001). However, the origin for this functional non-equivalence is still an open question. Therefore we investigated the contribution of the ABC signature

motif to the functional asymmetry of the TAP subunits by single-site mutants and chimeras of the C-loop.

Single-site mutations of the C-loop in TAP1 or TAP2 effect TAP function to a different degree reflecting the asymmetry of both TAP subunits. Exchanging the leucine or glycine (LSGGQ) in TAP1 fully abolished peptide transport. However, TAP complexes with equivalent mutations in TAP2 (LAAGQ) showed still residual peptide transport activity. Accordingly, mutations in ATP-binding site I (formed by Walker A and B motifs of TAP1 and C-loop of TAP2) are tolerated to a certain extent, whereas TAP complexes with the same mutations in site II are inactive. These findings are in agreement with Walker A mutations of TAP1 (site I) are still able to transport peptides, although with very low efficiency, whereas equivalent mutations at site II interrupt peptide translocation (Karttunen et al., 2001; Lapinski et al., 2003). As all our C-loop mutants do neither alter the peptide nor ATP binding, we conclude that these mutations influence the ATP activity of TAP. These results are supported by the recent finding that an exchange the invariant glycine to alanine in the C-loop of TAP1 does not influence peptide binding but abrogates peptide transport via the TAP complex (Hewitt and Lehner, 2003). In addition, analogous P-gp mutants of the invariant glycine in the N- or C-terminal NBD show ATP binding, but not ATPase activity (Szakacs et al., 2001). Furthermore, in the maltose permease (MalK subunit), the pheromone transporter Ste6p, and CFTR, the exchange of the invariant glycine decreases the ATPase as well as transport activity (Browne et al., 1996; Ketchum et al., 2001; Li et al., 1996; Panagiotidis et al., 1993). The exchange of the invariant glycine of the C-loop (LSGGQ) reduces the ATPase activity of all ABC-transporters studied so far. Nevertheless, there are some subtle differences in the consequences induced by the mutations, which are marked by a total loss or strong decrease in catalytic activity. TAP mutants of the invariant glycine are non-equivalent, implying that the degenerated ATP-binding site I is less crucial for the transport function than site II. We conclude that C-loop mutants of TAP2, which contains a mutated ATP-binding site I but an intact site II, are still able to form an active NBD-dimer but with a strong decreased ATPase activity reflected in the strongly decreased transport rate. The equivalent mutation in the C-loop of TAP1 (a mutated site II) leads to an inactive transport complex. This model is supported by mutational studies of GlcV, the NBD of the glucose transporter of *Sulfolobus solfataricus*. The G144A mutant (LSGGQ) that cannot form homodimers, and the E166A mutant

(putative catalytic base) are both ATPase inactive (Verdon et al., 2003). However, mixtures of both GlcV mutants can form dimers with 20% ATPase activity of wt GlcV, demonstrating that one active ATP binding site is sufficient for ATP hydrolysis.

To decipher the origin of the asymmetry of the NBDs of TAP, we exchanged the C-loops of TAP1 and TAP2. Comparable to the single-site mutants, all C-loop chimeras showed similar peptide and ATP binding activities. Strikingly, the C-loop controls the peptide transport efficiency: the chimera with two canonical C-loops showed the highest transport rate whereas the chimera with two degenerated C-loop sequences the lowest. TAP complexes with mixed C-loops transport peptides with almost identical efficiency. Based on the crystal structures of NBD dimers (Chen et al., 2003a; Hopfner et al., 2000; Smith et al., 2002b), it was postulated that the serine of the C-loop forming a hydrogen bond to the γ-phosphate of ATP is essential for ABC-protein function. This serine in the C-loop is conserved in all human ABC-proteins, except for TAP2. However, here we provide evidence that this serine is not essential for TAP1 function. This observation is also supported by BeF_x-trapping experiments, which demonstrated that both ATP-binding sites of TAP hydrolyze ATP in a peptide-specific manner, although the C-loop of TAP2 does not contain a serine residue (Chen et al., 2003b). The serine of the canonical C-loop may be at least partially involved in the timing of ATP hydrolysis and hence the asymmetry of TAP1 and TAP2. Similar results are most recently obtained for P-glycoprotein (Tombline et al., 2004). Mutation of the serine in the C-loop of P-glycoprotein to alanine in one of each NBD reduces ATPase activity to 66% and the double mutant possesses 3% ATPase activity of wt P-glycoprotein. In GlcV the serine of the C-loop is not essential for ATP hydrolysis (Verdon et al., 2003). The S142A mutant hydrolyzes ATP with 50% of the activity of wt GlcV. However, any other substitution of this highly conserved serine leads to an inactive protein. Furthermore, mutation of this serine residue to asparagine, isoleucine or arginine in the ATP-binding site II of CFTR results in cystic fibrosis (Cutting et al., 1990; Kerem et al., 1990). The same mutations in pheromone transporter STE6p drastically reduce secretion of mating a-factor (Browne et al., 1996). Also the conservative mutation, serine to cysteine reduces the ATPase activity of P-glycoprotein to 22% of wt P-glycoprotein (Loo et al., 2002). The glycine residue (LSGGQ) is expected to have minor effects on the asymmetry because this residue is divergent not only in human ABC-transporters (Fig. 4-8C) but also between human (LAAGQ) and rodent (LAVGQ) TAP2.

The TAP mutants described herein provide information about the architecture of the C-loops. Exchange of the highly conserved glycine of the C-loop (LSGGQ) has severe effects on the transport activity. The monomeric structure of the GlcV mutant (G144A) shows within a resolution of 1.5 Å no conformational changes in the C-loop (Verdon et al., 2003). By modeling the GlcV (G144A) dimer on the dimeric MJ0796 structure, it became evident that the methyl group of alanine causes steric hindrance with an oxygen of the γ-phosphate of ATP as well as the side chain of serine in the Walker A motif of the opposite NBD (Verdon et al., 2003). Therefore, introducing any side chain at the position of the invariant glycine of the C-loop is believed to inhibit NBD dimer formation by steric hindrance. In the C-loop, the hydroxyl group of the serine forms a hydrogen bond with the γ- phosphate of ATP (Chen et al., 2003a; Smith et al., 2002b). Introduction of an alanine at this position does not seem to weaken the NBD dimer affinity, because transient GlcV dimers of S142A mutants could be detected by gel filtration in the presence of MgATP (Verdon et al., 2003). This finding supports the idea that the serine to alanine mutation in the C-loop reduces the ATPase activity, which prolongs dimer formation. Accordingly, we suggest that the peptide transport rate of TAP containing two degenerated C-loops is lowered by decreasing the rate of ATP hydrolysis and not the rate of dimer formation. The leucine of the C-loop points to a hydrophobic, buried environment. These hydrophobic interactions seem to stabilize the structure of the C-loop as introducing alanine instead of leucine drastically decreases the peptide transport activity of TAP.

In summary, the C-loop is an essential motif that is involved in the functional asymmetry of the NBDs of the TAP complex. The substitutions of the invariant glycine or the leucine of the C-loop demonstrated the asymmetric behaviour of both ATP binding sites. These finding reveals that ATP-binding site II is more important than site I for catalytic activity of TAP. The serine residue in the C-loop is not essential for transport function. Moreover, the serine to alanine substitution induces an asymmetric behaviour of both NBDs potentially by slowing down the ATP hydrolysis rate. This may result in a prolonged NBD dimer formation.

5.3 Role of the acidic residue downstream of the Walker B motif

EQ mutants of TAP were generated to identify a transition state with a low peptide-binding affinity induced by ATP binding or hydrolysis. At 4°C, nucleotides showed no influence on the peptide-binding sites, while nucleotides binding to all TAP complexes containing mutated TAP2 induced a partial reduction of B_{max} at 27°C. In addition, mutation of the putative catalytic base at both sites does not abolish the function of the TAP complex.

It was proposed that transporters may employ a central binding site that is alternately exposed to each side of the membrane (Mitchell, 1957). Extended from this notion, an alternating access/binding site model has been proposed to explain the conformational coupling between the ABC domains and substrate-binding sites. In detail, it is believed that ABC transporters have to couple two distinct activities in order to mediate active extrusion of substrates: i) conformational changes in the nucleotide-binding domains induced by the binding and /or hydrolysis of ATP. ii) reorientation of substrate-binding sites in the transmembrane domains with alternate exposure to each face of the membrane. Such alternating changes in the substrate-binding affinity facilitate the substrate binding to and release from the transporter (Davidson, 2002; Urbatsch et al., 2003; van Veen et al., 2000). A drastic decrease in substrate-binding affinity of MRP1, Pgp and LmrA in the transition state trapped by vanadate is an important support for this model (Qian et al., 2001; Sauna and Ambudkar, 2001; van Veen et al., 2000).

So far, such a low affinity peptide-binding site of TAP has not been identified. In contrast to Pgp, TAP retains a high affinity peptide-binding site in a BeF_x-trapped state. Previous studies have shown that EQ mutation of the NBDs arrest these proteins in two dimeric transition states, which sandwich two ATP or one ATP and one ADP, respectively (Janas et al., 2003; Moody et al., 2002; Verdon et al., 2003). Thus, we anticipated that TAP EQ mutants would shift from a high to low substrate-binding site in one of the transition states according to the alternating binding site model.

In contrast to our expectation, peptide-binding ability seems not affected in the ATP sandwich state of the TAP complex. At 4°C, neither the K_d nor the B_{max} has been changed by the nucleotides for all TAP constructs (Tab. 4-3), demonstrating binding of ATP or ADP does not influence the substrate-binding domain of these proteins. So far, biochemical studies on isolated EQ NBD mutants reveals that they all form dimers after

ATP binding at 4°C and ATP hydrolysis is not required for this process (Janas et al., 2003; Moody et al., 2002; Orelle et al., 2003; Verdon et al., 2003). Accordingly, our results suggest that peptide-binding sites of double EQ mutants remain in a high affinity state when their NBDs are trapped in the dimeric conformation. Thus, we conclude that ATP-induced dimerization of the NBDs does not induce the shift of the peptide-binding site from a high to a low affinity state. Nevertheless, we cannot exclude that the trapped dimerization state of the double EQ mutants (1DN/2EQ and 1DQ/2EQ) was still too transient to be probed by this assay. Moreover, it should be noted that so far the NBD dimerization upon ATP binding has only been observed in the studies of isolated NBDs, and direct evidence supporting the dimeric state in the full-length ABC transporters is still missing.

Next, the peptide-binding affinity of TAP complexes in the second NBD dimeric state was investigated. The EQ mutant of NBDs of the MDL1 was shown to be locked in this state after hydrolysis of one of the two bound ATPs (Janas et al., 2003). After incubation of the TAP variants under transport condition to convert TAP into the ATP-ADP dimeric state, TAP complexes containing mutated TAP2 (1wt/2EQ, 1DN/2EQ and 1DQ/2EQ) exhibited a reduced peptide-binding sites by 20 %. This suggests that a fraction of proteins was not accessible to peptides upon interaction with nucleotides. Surprisingly, nucleotides at saturating concentrations could not induce a more drastic reduction. Two reasons might contribute to such a subtle effect: i) 20 nM of peptides failed to trigger the ATP hydrolysis of all proteins and further induces a complete response; ii) the trapped state is not stable and a large portion of TAP complexes still rest in the states which expose a high affinity site for peptides. Further experiments are needed to clarify these points.

Since the 1wt/2EQ mutant behaves differently from its equivalent TAP1 mutants, it is tempting to speculate that only the EQ mutation in TAP2 is sufficient to trap the TAP complex in a low-affinity or peptide-inaccessible state in the presence of nucleotides. In the case of Pgp, it is believed that there are two ATP hydrolysis events in one full catalytic cycle. The first ATP hydrolysis event occurs randomly at one of the NBDs and induces a drastic decrease of substrate binding, while the second ATP hydrolysis sets the transporter back to the ground state (Sauna and Ambudkar, 2001). LmrA also contains two ATP hydrolysis events in one cycle, each hydrolysis event can trigger the transmembrane domain shifting from high to low affinity state (van Veen et al., 2000). Despite of the

difference in these two findings, they both supported the notion that the ATP hydrolysis at either of the two NBDs has the potential to induce the conformation change in the transmembrane domain. By contrast, the NBDs of MRP1 displayed a distinct function in the ATP hydrolysis cycle (Hou et al., 2000; Hou et al., 2003). Only ATP binding and hydrolysis by NBD2 was required for MRP1 to switch from a high to low affinity substrate-binding site (Payen et al., 2003; Qian et al., 2001). The different behaviors of TAP1 and TAP2 single mutants suggested that the TAP complex alters its substrate-binding site by a mechanism similar to that of MRP1.

So far, ATP has been found to be absolutely required for the dimer formation of the EQ mutants of isolated NBDs of ABC transporters. It was surprising to observe that ADP also induced the alteration of the peptide-binding site in the TAP2 mutants. Thus, it is not clear whether ADP binding also induces a dimer formation of NBD in the full-length transporter or the dimerization of the NBDs does not occur concomitantly with the alteration of the peptide-binding site. Further investigations are required to identify how ATP and ADP induce conformational changes of the NBDs of the EQ mutants (1wt/2EQ, 1DQ/2EQ and 1DN/2EQ) and subsequently the alteration of the peptide-binding site.

Effects of mutating the putative catalytic base on the function of ABC transporters are not consistent. In most of the cases, the ATPase activity of isolated EQ NBDs almost abolished the ATPase activity (Janas et al., 2003; Moody et al., 2002; Orelle et al., 2003; Urbatsch et al., 2000). In cases of full-length ABC transporters, e.g. Pgp and BmrA, mutation one of the sites was sufficient to fully inhibit the substrate transport (Orelle et al., 2003; Sauna et al., 2002). By contrast, Verdon et al. also showed that the EQ mutants of soluble GlcV retains 20% of ATPase activity (Verdon et al., 2003). Together with the observation of the TAP double mutants, it indicates that the acidic residue downstream of the Walker B motif is not essential for the function of some ABC transporters.

Surprisingly, the TAP 1DN/2wt mutant still maintains full activity. This observation was again in line with the studies on MRP1, in which substitution of the aspartate in the NBD1 of MRP1 with a series of residues (e.g. serine, leucine, asparagine) only slightly decreases the drug transport activity (Payen et al., 2003). It should be noted that although TAP belongs to ABCB subfamily, TAP1 and TAP2 share common features with ABCC family members in respect to the highly conserved sequences: i) an aspartate downstream of the Walker B in the NBD1; ii) a non-conserved C-loops in the NBD2 (see

appendix 9.2). These biochemical coincidences indicate that TAP might share common mechanism of ATP hydrolysis with the ABCC family members. Notably, the partial activity of EQ mutants also suggests that these proteins are not trapped in a stable transition state triggered by ATP binding and/or hydrolysis, which is likely the reason for the observed subtle reduction of B_{max}.

In parallel, it was observed that peptide transport by TAP double EQ mutants depends on the presence of divalent cations as strictly as for the wild type protein. According to the structure of BtuCD, it was proposed that the two NBDs dimerize upon ATP binding, which act as the power stroke for the substrate translocation (Locher et al., 2002; Smith et al., 2002b). From this model, one can anticipate that peptide translocation by TAP EQ double mutants is only due to ATP binding even though removal of the acidic residues completely diminishes the catalytic activity. However, here we observed that TAP 1DQ/2EQ mutant transport peptides in a divalent cation-dependent manner. It should be stressed that a divalent cation was not absolutely required for the EQ mutants to carry out ATP binding and subsequent dimerization (Janas et al., 2003; Moody et al., 2002; Verdon et al., 2003). Thus we conclude that TAP EQ utilizes the divalent cation for ATP hydrolysis rather than only ATP binding.

In summary, the putative catalytic bases are not essential for ATP hydrolysis by TAP transporter. Double EQ mutants bind peptides in the presence of ATP at 4 °C indicating that ATP binding, followed by dimerization of the NBDs does not affect the peptide-binding site. These mutants bearing mutated TAP2 tend to switch to a conformation in which the peptide-binding sites are not accessible during the ATP hydrolysis cycle. Further studies on the TAP EQ proteins may reveal more information about the stage of catalytic process in which the peptide-binding site is altered.

Finally, based on the knowledge about other ABC-transporters as well as our findings we propose the following working model for TAP: Peptide and ATP bind independently to TAP. In the absence of peptide the NBDs are fixed in a monomeric state by interactions between TMD and NBD. Binding of peptide weakens these interactions allowing the ATP-loaded NBDs to dimerize. The NBD-dimer is stabilized preferentially by interactions within the ATP binding site II. Two ATPs are then hydrolyzed sequentially at both ATP-binding sites. Peptide is delivered to the ER probably after the first ATP hydrolysis at ATP-binding site II. The introduction of a negative charge by ATP hydrolysis

or the release of inorganic phosphate forces the dissociation of the NBDs, which reset the protein for the next cycle. For efficient transport, ATP hydrolysis at both nucleotide-binding sites takes place to destabilize the NBD-dimer. Therefore, two ATP are hydrolysed per transported peptide under normal condition. However, ATP hydrolysis at ATP binding site II is sufficient to dissociate the NBD-dimer albeit with a much slower dissociation rate constant. This explains why mutation at ATP-binding site I but not at site II could retain residual peptide transport activity.

6. Abbreviations

ABC	ATP binding cassette
ADP	adenosine diphosphate
ATP	adenosine triphosphate
CFTR	cystic fibrosis transmembrane conductance regulator
CTL	cytotoxic T-lymphocyte
DTT	1,4-dithio-DL-threitol
EDTA	ethylenediaminetetraacetic acid
EGTA	ethylene glycol-bis(2-aminoethylether)-*N,N,N′,N′*-tetraacetic acid
ER	endoplasmic reticulum
HEPES	*N*-(2-hydroxyethylpiperazine)-*N′*-2-ethanesulfonic acid
ICD	intracellular domain
IPTG	isopropyl β-D-thiogalactopyranoside
MDL	multi-drug resistance like protein
MHC	major histocompatibility complex
MRP	multi-drug resistant protein
NBD	nucleotide-binding domain
PAGE	polyacrylamide gel electrophoreseis
PBS	phosphate-buffered saline
Pgp	P-glycoprotein
SDS	sodium dodecyl sulphate
Sf9	*Spodoptera frugiperda* 9
SUR	sulfonylurea receptor
TAP	transporter associated with antigen processing
TCR	T-cell receptor
TGN	*trans*-Golgi network
TMD	transmembrane domain
Tris	*tris* (hydroxymethyl)aminomethane
wt	wild type

7. Summary

The transporter associated with antigen processing (TAP) plays a pivotal role in the adaptive immune response against virus-infected or malignantly transformed cells. As member of the ABC transporter family, TAP hydrolyzes ATP to energize the transport of antigenic peptides from the cytosol into the lumen of the endoplasmic reticulum. TAP forms a heterodimeric complex composed of TAP1 and TAP2 (ABCB2/3). Both subunits contain a hydrophobic transmembrane domain and a hydrophilic nucleotide-binding domain. The aim of this work was to study the ATP hydrolysis event of the TAP complex and gain further insights into the mechanism of peptide transport process.

To analyze ATP hydrolysis of each subunit I developed a method of trapping 8-azido-nucleotides to TAP in the presence of phosphate transition state analogs followed by photocross-linking, immunoprecipitation, and high-resolution SDS-PAGE. Strikingly, trapping of both TAP subunits by beryllium fluoride is peptide-specific. The peptide concentration required for half-maximal trapping is identical for TAP1 and TAP2 and directly correlates with the peptide-binding affinity. Only background levels of trapping were observed for low affinity peptides or in the presence of the herpes simplex viral protein ICP47, which specifically blocks peptide binding to TAP. Importantly, the peptide-induced trapped state is reached after ATP hydrolysis and not in a backward reaction of ADP binding and trapping. In the trapped state, TAP can neither bind nor exchange nucleotides, whereas peptide binding is not affected. In summary, these data support the model that peptide binding induces a conformation that triggers ATP hydrolysis in both subunits of the TAP complex within the catalytic cycle.

The role of the ABC signature motif (C-loop) on the functional non-equivalence of the NBDs was investigated. The C-loops of TAP transporter contain a canonical C-loop (LSGGQ) for TAP1 and a degenerated ABC signature motif (LAAGQ) for TAP2. Mutation of the leucine or glycine (LSGGQ) in TAP1 fully abolished peptide transport. TAP complexes with equivalent mutations in TAP2 showed however still residual peptide transport activity. To elucidate the origin of the asymmetry of the NBDs of TAP, we further examined TAP complexes with exchanged C-loops. Strikingly, the chimera with two canonical C-loops showed the highest transport rate whereas the chimera with two degenerated C-loops had the lowest transport rate, demonstrating that the ABC signature

motifs control the peptide transport efficiency. All single-site mutants and chimeras showed similar activities in peptide or ATP binding, implying that these mutations affect the ATPase activity of TAP. In addition, these results prove that the serine of the C-loop is not essential for TAP function, but rather coordinates, together with other residues of the C-loop, the ATP hydrolysis in both nucleotide-binding sites.

To study the coupling between the ATP binding/hydrolysis and the peptide binding, the putative catalytic bases of the TAP complex were mutated to generate the so-called EQ mutants. The mutations did not influence the peptide-binding ability. Dimerization of the NBDs of EQ mutants upon ATP binding does not alter the peptide binding property. At 27°C, both ATP and ADP could induce the loss of peptide-binding ability (B_{max}) only in the variants bearing a mutated TAP2. Further studies are required to deduce at which stage in the catalytic cycle the peptide-binding site is affected. In addition, mutation of the putative catalytic base of both subunits showed a magnesium-dependent peptide transport activity, demonstrating these mutants did not abolish the ATP hydrolysis. Thus, the function of this acidic residue as the catalytic base is not likely to be universe for all ABC transporters.

8. Zusammenfassung

Der menschliche Organismus ist in seiner Umgebung einer Vielzahl von Pathogenen ausgesetzt. Aufgrund dieses Selektionsdrucks hat sich im Laufe der Evolution bei den Vertebraten das adaptive Immunsystem entwickelt. Dieses lässt sich in die humorale und die zelluläre Immunität unterteilen. Die humorale Immunantwort beschränkt sich auf die Produktion von Antikörpern durch B-Lymphozyten. Auftretende antigene Strukturen werden durch diese Immunglobuline markiert und nachfolgend beseitigt.

Die zelluläre Immunantwort hingegen wird über T-Lymphozyten vermittelt. Innerhalb der Zelle werden Proteine durch das Proteasom degradiert. Die generierten Peptide werden im Komplex mit MHC I (*major histocompatibility complex class I*) Molekülen den $CD8^+$-T-Lymphozyten präsentiert. Die Erkennung eines antigenen Peptids (z.B. viraler oder Tumor-assoziierter Herkunft) führt zur Zerstörung einer infizierten oder entarteten Zelle. Der Prozess der Generierung und MHC I-vermittelten Präsentation von Peptiden wird als Antigenprozessierung bezeichnet. TAP (*transporter associated with antigen processing*) erfüllt im Rahmen dieses Prozesses eine wichtige Aufgabe. Die durch das Proteasom produzierten Peptide werden von TAP aus dem Zytoplasma in das Lumen des Endoplasmatischen Retikulums (ER) transportiert. Nachfolgend werden diese Peptide auf MHC I Moleküle geladen und über den Golgi-Apparat auf der Zelloberfläche präsentiert.

TAP gehört zur Familie der ABC (*ATP binding cassette*)-Transporter, welche ATP-abhängig ein breites Spektrum an Substanzen über eine Membran transportieren. TAP formt einen Heterodimer bestehend aus TAP1 und TAP2. Jede Untereinheit wird aus einer N-terminale Transmembrandomäne (TMD) gefolgt von einer Nukleotidbindungsdomäne (NBD) gebildet. TAP1 und TAP2 werden auch als sogenannte *half-size transporter* bezeichnet. Die TMDs beider Untereinheiten bilden zusammen die Peptidbindungsstelle und formen die Translokationspore. TAP transportiert vornehmlich Peptide mit einer Länge von 8-16 Aminosäuren. Die Bindungsselektivität der Peptide wird durch die ersten drei N-terminalen und die letzte C-terminale Aminosäure bestimmt.

Die zytoplasmatischen NBDs sind die Motordomänen von ABC-Transportern, die ATP hydrolysieren und die für den Transport benötigte Energie bereitstellen. Beide NBDs enthalten die für die Bindung und Hydrolyse von ATP essentiellen Walker A-, Walker B- und C-*Loop*-Motive. Diese Motive sind unter allen ABC-Transportern hoch konserviert.

Die in der Walker B-Sequenz befindlichen Aminosäuren Asp688 (TAP1) und Glu632 (TAP2) werden als katalytische Basen bezeichnet, da sie wahrscheinlich ein Wassermolekül polarisieren, welches infolge dessen das □-Phosphat des ATPs nukleophil angreift.

Im Verlauf dieser Arbeit erschienen einige biochemische und biophysikalische Publikationen, die zeigten, dass die NBDs von ABC-Transportern in Anwesenheit von ATP Dimere bilden. Dabei werden an der Grenzfläche der zwei NBDs zwei Moleküle ATP komplexiert. An der Bindung eines ATP Moleküls sind die Walker A/B Motive und der C-*Loop* der benachbarten NBD beteiligt. Allerdings geht aus diesen Arbeiten nicht hervor, ob beide Motordomänen während des Substrattransportes katalytisch aktiv sind. Daher steht im Fokus der Forschung die Frage nach dem molekularen Mechanismus der Interaktionen beider NBDs innerhalb eines Transportzyklus. Frühere Studien an TAP hatten gezeigt, dass der Peptidtransport strikt mit der Peptidbindung und der Hydrolyse von ATP gekoppelt ist. Für den Peptidtransport ist die Anwesenheit beider NBDs essentiell. Allerdings wurde die ATPase-Aktivität der einzelnen NBDs bisher nicht nachgewiesen. Deswegen wurde im ersten Teil dieser Doktorarbeit der Frage nachgegangen, ob beide NBDs von TAP während des Transportprozesses katalytisch aktiv sind.

Aus diesem Grund wurde im Rahmen dieser Arbeit zuerst eine Methode etabliert, um die katalytische Aktivität der einzelnen Untereinheiten zu analysieren. Dabei werden 8-azido-Nukleotide mittels ATPase Inhibitoren fest an TAP gebunden. Diese Gruppe von ATPase-Inhibitoren stellen Phosphatanaloga (z.B. BeF_x, ScF_x oder V_i) dar, welche die Position des abgespaltenen □-Phosphats des ATP einnehmen, wodurch sich ein stabiler Komplex aus Mg•8-Azido-ADP und einem Phosphatanalogon bildet. Die Komplexierung der Nukleotide mittels dieser Inhibitoren erfolgt nur nach ATP-Hydrolyse, womit eine Möglichkeit besteht, die katalytische Aktivität der einzelnen Untereinheiten zu verfolgen. Nach der Bindung des 8-Azido-Nukleotids wird durch die Bestrahlung der Probe mit UV-Licht eine kovalente Verknüpfung mit der NBD erzielt. Die TAP-Untereinheiten werden daraufhin immunpräzipitiert, durch hochauflösende PAGE separiert und über Autoradiographie visualisiert.

Mit dem Inhibitor BeF_x konnte 8-Azido-ADP effizient in den NBDs sowohl von TAP1 als auch TAP2 fest gebunden werden. Die Komplexierung von ADP durch BeF_x wird durch die Anwesenheit von Peptid stimuliert. Somit scheint sowohl TAP1 als auch TAP2 peptid-

abhängig ATP zu hydrolysieren. Dabei korreliert die halbmaximale Stimulation der ATPase-Aktivität beider Untereinheit mit der Peptidaffinität. In Abwesenheit von Peptiden oder in Gegenwart des viralen TAP-Inhibitors ICP47 (Inhibition der Peptidbindung) wurde bei beiden NBDs nur eine geringe Hintergrund-Aktivität detektiert. In dem Mg•ADP•BeF_x komplexierten Zustand kann TAP weder Nukleotide binden noch austauschen. Allerdings ist die Peptidbindung in diesem fixierten Zustand nicht beeinflusst. Basierend auf diesen Daten kann festgestellt werden, dass beide Untereinheiten des Peptidtransporters ATP in einer peptidabhängigen Weise hydrolysieren.

Studien an Walker A Mutanten zeigen, dass beide Untereinheiten von TAP während des Transportprozesses asymmetrisch agieren. Ein Grund für diese funktionelle Asymmetrie könnte in den unterschiedlichen Sequenzen der C-*Loops* von TAP1 und TAP2 liegen. Während TAP1 (LSGGQ) die kanonische C-*Loop*-Sequenz besitzt, weist TAP2 (LAAGQ) einen sogenannten degenerierten C-*Loop* auf. Um den Einfluss der unterschiedlichen C-*Loops* auf die funktionelle Asymmetrie von TAP aufzuklären, wurden im Rahmen dieser Arbeit Mutationsstudien an den C-*Loops* durchgeführt. Zum einen wurden Aminosäurenreste ausgetauscht, welche sowohl in TAP1 (LSGGQ, mutierte Aminosäurenseitenketten sind unterstrichen) als auch TAP2 (LAAGQ) vorhanden sind. Die generierten C-*Loop*-Mutanten (1LA/2wt, 1GV/2wt, 1GD/2wt, 1wt/2LA, 1wt/2GV und 1wt/2GD) werden in gleichem Maße in Sf9-Insektenzellen exprimiert wie das Wildtyp-Protein (wt-TAP). Weiterhin konnten keine signifikanten Unterschiede bezüglich der Peptidaffinität und der ATP-Bindung festgestellt werden. Allerdings weisen die Mutanten im Vergleich zum wt-TAP eine veränderte Transportaktivität auf. TAP-Komplexe, bei denen das Leucin bzw. Glycin in TAP1 (LSGGQ) mutiert wurde, zeigen keinen Peptidtransport. Dagegen besitzen TAP-Komplexe mit den entsprechenden Mutationen in TAP2 (LAAGQ) eine erniedrigte Transportaktivität. Dadurch wird jedoch verdeutlich, dass TAP1 und TAP2 funktional nicht identisch sind.

Durch den Austausch der C-*Loops* zwischen TAP1 und TAP2 konnte gezeigt werden, dass die C-*Loops* zumindest teilweise für die funktionelle Asymmetrie der beiden Untereinheiten verantwortlich sind. Dabei transportieren TAP-Chimären mit zwei kanonischen C-*Loops* (LSGGQ) Peptide mit einer höheren Effizienz als TAP-Komplexe mit einem kanonischen C-*Loop* (LSGGQ) und einem degenerierten C-*Loop* (LAAGQ). Im Vergleich dazu transportieren TAP-Chimären mit zwei degenerierten C-*Loops* Peptide mit

geringster Effizienz. Die Peptidbindungs- und Nukleotidbindungseffizienz der TAP-Chimären wurden nicht beeinflusst, so dass diese Mutationen wahrscheinlich ausschließlich die ATPase Tätigkeit verändern. Desweiteren belegen diese Mutationsstudien, dass das konservierte Serin des C-*Loops* (LSGGQ) für die katalytische Aktivität nicht essentiell ist. Dieses Serin kommt in allen menschlichen ABC-Transportern außer TAP2 vor und bildet eine Wasserstoffbrücke zum □-Phosphat von ATP aus. Folglich beeinflussen Mutationen des hoch konservierten Serins des C-*Loops* die ATP-Hydrolysegeschwindigkeit und Mutationen des Leucins und Glycins (LSGGQ) die Dimerisierung der NBDs während des Transportzyklus. Offensichtlich destabilisieren Mutationen im kanonischen C-*Loop* von TAP1 das NBD-Dimer stärker als die äquivalenten Mutationen in TAP2. Folglich trägt die ATP-Bindungsstelle II (Walker A/B-Motiv von TAP2 und C-*Loop* von TAP1) mehr zur Dimerbildung bei als die ATP-Bindungsstelle I.

Es wird vermutet, dass die TMD von ABC-Transportern während des katalytischen Zyklus Konformationsänderungen durchlaufen, wodurch die Substrataffinität stark verringert wird. Diese strukturelle Änderung erleichtert die Freisetzung des Substrats auf der gegenüberliegenden Seite der Membran. Im letzten Teil dieser Arbeit wurde daher versucht, einen Zustand von TAP zu identifizieren, der induziert durch ATP-Bindung oder ATP–Hydrolyse eine erniedrigte Peptidaffinität aufweist. Da im TAP-Komplex ein solcher Zustand bisher nicht nachgewiesen werden konnte, wurden im Walker B-Motiv die sauren Aminosäuren Asp688 in TAP1 und Glu632 in TAP2 gegen Asparagin bzw. Glutamin ersetzt. Studien an anderen ABC-Transportern oder isolierten NBDs haben gezeigt, dass die Mutation der katalytischen Base zu einem Glutamin die ATP-Hydrolyse inhibiert und sich in Gegenwart von ATP ein stabiler NBD-Dimer bildet. Es wird postuliert, dass solch ein NBD-Dimer einen Übergangszustand im Transportzyklus von TAP mit stark erniedrigter Substratspezifität darstellt. Die Einzel- oder Doppelmutation der Aminosäuren Asp688 und Glu632 beeinflussen im Vergleich zum wt-TAP weder Expressionsrate noch Peptidaffinität. Überraschenderweise transportieren alle Mutanten Peptide. Selbst die Doppelmutanten, bei denen beide katalytischen Basen zu Asparagin oder Glutamin mutiert wurden, zeigten im Vergleich zu wt-TAP noch eine 30%ige Transportaktivität. Auch bei diesen Mutanten ist der Peptidtransport von der ATP-Hydrolyse abhängig, da divalente Kationen einen essentiellen Kofaktor darstellen. Daher scheint zumindest in TAP das

katalytische Wassermolekül nicht nur durch die postulierte Base sondern auch durch andere Aminosäureseitenketten polarisiert werden zu können.

Die Hydrolyse des ATPs und nicht die Dimerisierung der Motordomänen liefert die Energie für den Peptidtransport, da bei diesen TAP-Mutanten unter Bedingungen, unter denen ATP-Hydrolyse nicht möglich ist, durch Zugabe von ATP keine Änderung der Peptid-Affinität festgestellt werden konnte.

9. Appendix

9.1 Sequence alignment of human ABC transporters

9.1.1 Walker A

```
ABCA1-N         LVKVYRDGMK--VAVDGLALNFYEGQITSFLGHNGAGKTTTMSILTGLFPPTSGTAYILG 961
ABCA2-N         LTKVYKDDKK--LALNKLSLNLYENQVVSFLGHNGAGKTTTMSILTGLFPPTSGSATIYG 1053
ABCA3-N         LSKVFRVGNKDRAAVRDLNLNLYEGQITVLLGHNGAGKTTTLSMLTGLFPPTSGRAYISG 594
ABCA4-N         LVKIFEPCGR--PAVDRLNITFYENQITAFLGHNGAGKTTTLSILTGLLPPTSGTVLVGG 991
ABCA5-N         IQKTYRKKGENVEALRNLSFDIYEGQITALLGHSGTGKSTLMNILCGLCPPSDGFASIYG 542
ABCA6-N         VKKEYKGKSGKVEALKGLLFDIYEGQITAILGHSGAGKSSLLNILNGLSVPTEGSVTIYN 542
ABCA7-N         LEKRFPGSPQ--PALRGLSLDFYQGHITAFLGHNGAGKTTTLSILSGLFPPSGGSAFILG 869
ABCA8-N         VTKEYKGKPDKIEALKDLVFDIYEGQITAILGHSGAGKSTLLNILSGLSVPTKGSVTIYN 544
ABCA9-N         LKKEYAGKCERVEALKGVVFDIYEGQITALLGHSGAGKTTLLNILSGLSVPTSGSVTVYN 545
ABCA10-N        VIKEYNGKTGKVEALQGIFFDIYEGQITAILGHNGAGKSTLLNILSGLSVSTEGSATIYN 455
ABCA12-N        VTKIYG----SKVAVDNLNLNFYEGHITSLLGPNGAGKTTTISMLTGLFGASAGTIFVYG 1406

ABCA1-C         -RKPAVDRICVGIPPGECFGLLGVNGAGKSSTFKMLTGDTTVTRGDAFLNKNS--ILSNI 1981
ABCA2-C         GRILAVDRLCLGVRPGECFGLLGVNGAGKTSTFKMLTGDESTTGGEAFVNGHS--VLKEL 2123
ABCA3-C         VPLLAVDRLSLAVQKGECFGLLGFNGAGKTTTFKMLTGEESLTSGDAFVGGHR--ISSDV 1451
ABCA4-C         -SSPAVDRLCVGVRPGECFGLLGVNGAGKTTTFKMLTGDTTVTSGDATVAGKS--ILTNI 2007
ABCA5-C         VKKVATKYISFCVKKGEILGLLGPNGAGKSTIINILVGDIEPTSGQVFLGDYSSETSE-D 1369
ABCA6-C         KKKIAARNISFCVQEGEILGLLGPNGAGKSSSIRMISGITKPTAGEVELKG--------C 1349
ABCA7-C         -RMPAVDRLCLGIPPGECFGLLGVNGAGKTSTFRMVTGDTLASRGEAVLAGHS--VAREP 1862
ABCA8-C         KNKIATRNVSFCVRKGEVLGLLGHNGAGKSTSIKVITGDTKPTAGQVLLKGSG------G 1314
ABCA9-C         KKKIATRNVSFCVKKGEVIGLLGHNGAGKSTTIKMITGDTKPTAGQVILKGSG------G 1357
ABCA10-C        KKKIAIRNVSFCVKKGEVLGLLGHNGAGKSTSIKMITGCTKPTAGVVVLQGSRASVRQQH 1276
ABCA12-C        KKIIAVNNISIGIPAGECFGLLGVNGAGKTTIFKMLTGDIIPSSGNILIRNKTG-SLGHV 2326

ABCB1-N         PDN-IKGNLEFRNVHFSYPSRKEVKILKGLNLKVQSGQTVALVGNSGCGKSTTVQLMQRL 72
ABCB2           PLH-LEGLVQFQDVSFAYPNRPDVLVLQGLTFTLRPGEVTALVGPNGSGKSTVAALLQNL 614
ABCB3           PTT-LQGVVKFQDVSFAYPNRPDRPVLKGLTFTLRPGEVTALVGPNGSGKSTVAALLQNL 519
ABCB4-N         PDS-IKGNLEFNDVHFSYPSRANVKILKGLNLKVQSGQTVALVGSSGCGKSTTVQLIQRL 75
ABCB6           RFQ--KGRIEFENVHFSYAD--GRETLQDVSFTVMPGQTLALVGPSGAGKSTILRLLFRF 639
ABCB7           QITPQTATVAFDNVHFEYIE--GQKVLSGISFEVPAGKKVAIVGGSGSGKSTIVRLLFRF 521
ABCB8           KEQ-LRGSVTFQNVCFSYPCRPGFEVLKDFTLTLPPGKIVALVGQSGGGKTTVASLLERF 506
ABCB9           PDH-LEGRVDFENVTFTYRTRPHTQVLQNVSFSLSPGKVTALVGPSGSGKSSCVNILENF 512
ABCB10          EKS-FQGALEFKNVHFAYPARPEVPIFQDFSLSIPSGSVTALVGPSGSGKSTVLSLLLRL 543
ABCB11-N        ---------EFHNVTFHYPSRPEVKILNDLNMVIKPGEMTALVGPSGAGKSTALQLIQRF 51
ABCB1-C         PNT-LEGNVTFGEVVFNYPTRPDIPVLQGLSLEVKKGQTLALVGSSGCGKSTVVQLLERF 175
ABCB4-C         PDK-FEGNITFNEVVFNYPTRANVPVLQGLSLEVKKGQTLALVGSSGCGKSTVVQLLERF 95
ABCB11-C        -----------VDCKFTYPSRPDSQVLNGLSVSISPGQTLAFVGSSGCGKSTSIQLLERF 49
```


ABCC1-N GALVAVVGQVGCGKSSLLSALLAEMDKVEGHVAIKGS---------- 707
ABCC2-N GQLVAVIGPVGSGKSSLISAMLGEMENVHGHITIKGT---------- 700
ABCC3-N GALVAVVGPVGCGKSSLVSALLGEMEKLEGKVHMKGS---------- 690
ABCC4-N GELLAVVGPVGAGKSSLLSAVLGELAPSHGLVSVHGR---------- 474
ABCC5-N GKLVGICGSVGSGKTSLISAILGQMTLLEGSIAISGT---------- 624
ABCC6-N GCLLAVVGPVGAGKSSLLSALLGELSKVEGFVSIEGA---------- 692
ABCC7-N GQLLAVAGSTGAGKTSLLMMIMGELEPSEGKIKHSGR---------- 487
ABCC8-N GQLTMIVGQVGCGKSSLLLAALGEMQKVSGAVFWSSLPDSEIGEDPSPERETATDLDIRK 765
ABCC9-N GQLTMIVGQVGCGKSSLLLAILGEMQTLEGKVHWSNVNES----EPSFEATRS-----RN 748
ABCC10-N GMLVGIVGKVGCGKSSLLAAIAGELHRLRGHVAVRGLSKG---------- 637
ABCC11-N GMMLGVCGNTGSGKSSLLSAILEEMHLLEGSVGVQGS---------- 573
ABCC12-N GKILGICGNVGSGKSSLLAALLGQMQLQKGVVAVNGT---------- 542
ABCC1-C ETAPPSSWPQVGRVEFRNYCLRYREDLDFVLRHINVTINGGEKVGIVGRTGAGKSSLTLG 1339
ABCC2-C -KRPPPDWPSKGKIQFNNYQVRYRPELDLVLRGITCDIGSMEKIGVVGRTGAGKSSLTNC 1346
ABCC3-C GSRPPEGWPPRGEVEFRNYSVRYRPGLDLVLRDLSLHVHGGEKVGIVGRTGAGKSSMTLC 1335
ABCC4-C --RPPPAWPHEGVIIFDNVNFMYSPGGPLVLKHLTALIKSQEKVGIVGRTGAGKSSLISA 1087
ABCC5-C NKAPSPDWPQEGEVTFENAEMRYRENLPLVLKKVSFTIKPKEKIGIVGRTGSGKSSLGMA 1239
ABCC6-C TCAAQPPWPQGGQIEFRDFGLRYRPELPLAVQGVSFKIHAGEKVGIVGRTGAGKSSLASG 1311
ABCC7-C HVKKDDIWPSGGQMTVKDLTAKYTEGGNAILENISFSISPGQRVGLLGRTGSGKSTLLSA 1256
ABCC8-C PSLIPKNWPDQGKIQIQNLSVRYDSSLKPVLKHVNALISPGQKIGICGRTGSGKSSFSLA 1390
ABCC9-C PSQVPEHWPQEGEIKIHDLCVRYENNLKPVLKHVKAYIKPGQKVGICGRTGSGKSSLSLA 1358
ABCC10-C LQLGTG-WLTQGGVEFQDVVLAYRPGLPNALDGVTFCVQPGEKLGIVGRTGSGKSSLLLV 1264
ABCC11-C GTSCPQGWPQHGEIIFQDYHMKYRDNTPTVLHGINLTIRGHEVVGIVGRTGSGKSSLGMA 1187
ABCC12-C VGTCPKDWPSCGEITFRDYQMRYRDNTPLVLDSLNLNIQSGQTVGIVGRTGSGKSSLGMA 1166
ABCD1 VDVEQGIICENIPIVTPSGE-VVVASLNIRVEEGMHLLITGPNGCGKSSLFRILGGLWPT 526
ABCD2 IDVDHGIICENVPIITPAGE-VVASRLNFKVEEGMHLLITGPNGCGKSSLFRILSGLWPV 530
ABCD3 IIADNIIKFDHVPLATPNGD-VLIRDLNFEVRSGANVLICGPNGCGKSSLFRVLGELWPL 492
ABCD4 EPADTAFLLERVSISAPSSDKPLIKDLSLKISEGQSLLITGNTGTGKTSLLRVLGGLWTS 440
ABCF1-N AAENDFSVSQAEMSSRQAMLENASDIKLEKFSISAHGKELFVNADLYIVAGRRYGLVGPN 300
ABCF2-N G--------------VLASHPNSTDVHIINLSLTFHGQELLSDTKLELNSGRRYGLIGLN 120
ABCF3-N R-------------LESSGKNKSYDVRIENFDVSFGDRVLLAGADVNLAWGRRYGLVGRN 212
ABCE1-N G--------------ALSIVNLPSNLEKETTHRYCANAFKLHRLPIPRP-GEVLGLVGTN 112
ABCF1-N GKGKTTLLKHIANRALSIPPNIDVLLCEQEVVADETPAVQAVLRADTKRLKLLEEERRLQ 360
ABCF2-N GIGKSMLLSAIGKREVPIPEHIDIYHLTREMPPSDKTPLHCVMEVDTERAMLEKEAERLA 180
ABCF3-N GLGKTTLLKMLATRSLRVPAHISLLHVEQEVAGDDTPALQSVLESDSVREDLLRRERELT 272
ABCE1-N GIGKSAALKILAGKQKPNLG----------KYDDPPDWQEILTYFRGSELQNYFTKILE 161
ABCF1-C GYQGQKP-LFKNLDFGIDMDSRICIVGPNGVGKSTLLLLLTGKLTPTHGEMRKNHRLKIG 653
ABCF2-C KYTKDGPCIYNNLEFGIDLDTRVALVGPNGAGKSTLLKLLTGELLPTDGMIRKHSHVKIG 463
ABCF3-C YYD-PKHVIFSRLSVSADLESRICVVGENGAGKSTMLKLLLGDLAPVRGIRHAHRNLKIG 558
ABCE1-C TDS----------------EIMVMLGENGTGKTTFIRMLAGRLKPDEGGEVPVLNVSYK 412
ABCG1 RFSSLPRRAAVNIEFRDLSYSVPEGP---WWRKKGYKTLLKGISGKFNSGELVAIMGPSG 117
ABCG4 RFSHLPKRSAVDIEFVELSYSVREGP---CWRKRGYKTLLKCLSGKFCRRELIGIMGPSG 105
ABCG2 SNDLKAFTEGAVLSFHNICYRVKLKSGFLPCRKPVEKEILSNINGIMKPG-LNAILGPTG 83
ABCG5 ATAPEPHSLGILHASYSVSHRVRPWWDITSCRQQWTRQILKDVSLYVESGQIMCILGSSG 89
ABCG8 LNYQVDLASQVPWFEQLAQFKMPWTS---PSCQNSCELGIQNLSFKVRSGQMLAIIGSSG 108
ABCG1 AGKSTLMNILAG-YRE-TGMKGAVLINGLPRDLRCFRKVSCYIMQDDMLLPHLTVQEAMM 175
ABCG4 AGKSTFMNILAG-YRE-SGMKGQILVNGRPRELRTFRKMSCYIMQDDMLLPHLTVLEAMM 163
ABCG2 GGKSSLLDVLAA-RKDPSGLSGDVLINGAPR-PANFKCNSGYVVQDDVVMGTLTVRENLQ 141
ABCG5 SGKTTLLDAMSGRLGRAGTFLGEVYVNGRALRREQFQDCFSYVLQSDTLLSSLTVRETLH 149
ABCG8 CGRASLLDVITGRGHGGKIKSGQIWINGQPSSPQLVRKCVAHVRQHNQLLPNLTVRETLA 168

9.1.2 Walker B and C-loop

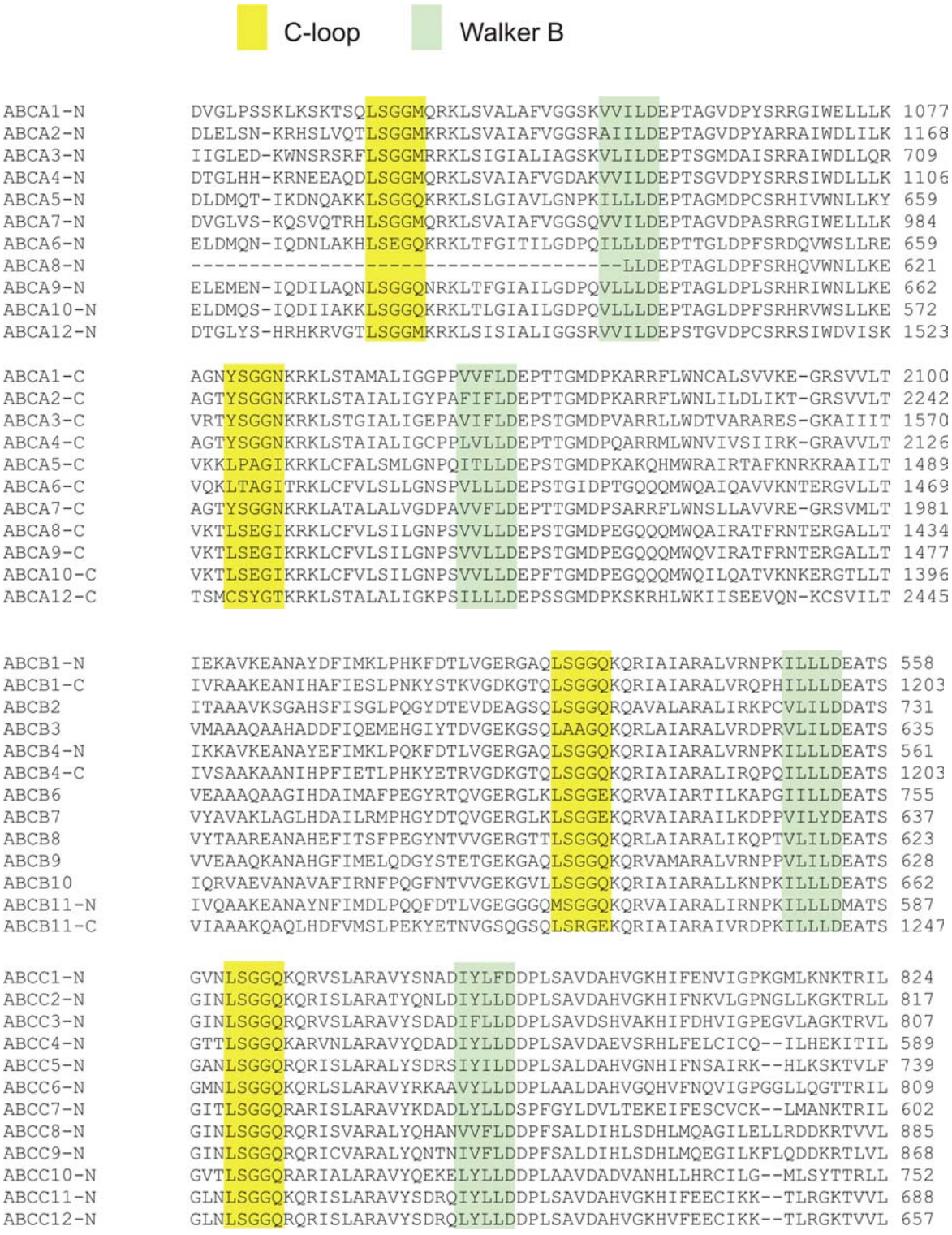


ABCC1-C WTSLELAHLKDFVSALPDKLDHECAEGGENLSVGQRQLVCLARALLRKTKILVLDEATAA 1459
ABCC2-C WKALELAHLKSFVASLQLGLSHEVTEAGGNLSIGQRQLLCLGRALLRKSKILVLDEATAA 1466
ABCC3-C WWALELSHLHTFVSSQPAGLDFQCSEGGENLSVGQRQLVCLARALLRKSRILVLDEATAA 1455
ABCC4-C WNALQEVQLKETIEDLPGKMDTELAESGSNFSVGQRQLVCLARAILRKNQILIIDEATAN 1206
ABCC5-C WDALERTHMKECIAQLPLKLESEVMENGDNFSVGERQLLCIARALLRHCKILILDEATAA 1359
ABCC6-C WAALETVQLKALVASLPGQLQYKCADRGEDLSVGQKQLLCLARALLRKTQILILDEATAA 1431
ABCC7-C WKVADEVGLRSVIEQFPGKLDFVLVDGGCVLSHGHKQLMCLARSVLSKAKILLLDEPSAH 1375
ABCC8-C WEALEIAQLKLVVKALPGGLDAIITEGGENFSQGQRQLFCLARAFVRKTSIFIMDEATAS 1510
ABCC9-C WEALEIAQLKNMVKSLPGGLDAVVTEGGENFSVGQRQLFCLARAFVRKSSILIMDEATAS 1478
ABCC10-C WQALKQCHLSEVITSMGG-LDGELGEGGRSLSLGQRQLLCLARALLTDAKILCIDEATAS 1383
ABCC11-C WDALERTFLTKAISKFPKKLHTDVVENGGNFSVGERQLLCIARAVLRNSKIILIDEATAS 1307
ABCC12-C WQVLERTFMRDTIMKLPEKLQAEVTENGENFSVGERQLLCVARALLRNSKIILLDEATAS 1286
ABCD1 HLHHILQREGGWEAMCDW--KDVLSGGEKQRIGMARMFYHRPKYALLDECTSAVSIDVEG 641
ABCD2 HLYHIVQREGGWDAVMDW--KDVLSGGEKQRMGMARMFYHKPKYALLDECTSAVSIDVEG 645
ABCD3 QLGHILEREGGWDSVQDW--MDVLSGGEKQRMAMARLFYHKPQFAILDECTSAVSVDVEG 607
ABCD4 GLSNLVARTEGLDQQVDWNWYDVLSPGEMQRLSFARLFYLQPKYAVLDEATSALTEEVES 560
ABCF1-N GQLEQ--GDDTAAERLEKVYEELRATGAAAAEAKARRILAGLGFDPEMQNRPTQKFSGGW 418
ABCF2-N -------HEDAECEKLMELYERLEELDADKAEMRASRILHGLGFTPAMQRKKLKDFSGGW 233
ABCF3-N AQIAAGRAEGSEAAELAEIYAKLEEIEADKAPARASVILAGLGFTPKMQQQPTREFSGGW 332
ABCE1-N DDLKAIIKPQYVARFLRLAKGTVGSILDRKDETKTQAIVCQQLDLTHLKERNVEDLSGGE 221
ABCF1-N RMRVSLARALFMEPTLLMLDEPTNHLDLNAVIWLNNYLQGWR---KTLLIVSHDQGFLDD 475
ABCF2-N RMRVALARALFIRPFMLLLDEPTNHLDLDACVWLEEELKTFK---RILVLVSHSQDFLNG 290
ABCF3-N RMRLALARALFARPDLLLLDEPTNMLDVRAILWLENYLQTWP---STILVVSHDRNFLNA 389
ABCE1-N LQRFACAVVCIQKADIFMFDEPSSYLDVKQRLKAAITIRSLINPDRYIIVVEHDLSVLDY 281
ABCF1-C FFNQQYAEQLRMEETPTEYLQRGFNLP--YQDARKCLGRFGLESHAHTIQICKLSGGQKA 711
ABCF2-C RYHQHLQEQLDLDLSPLEYMMKCYPEIKEKEEMRKIIGRYGLTGKQQVSPIRNLSDGQKC 523
ABCF3-C YFSQHHVEQLDLNVSAVELLARKFPGR-PEEEYRHQLGRYGISGELAMRPLASLSGGQKS 617
ABCE1-C PQKISPKSTGSVRQLLHEKIRDAYTHP---QFVTDVMKPLQIEN-IIDQEVQTLSGGELQ 468
ABCF1-C RVVFAELACREPDVLILDEPTNNLDIESIDALGEAIN----EYKGAVIVVSHDARLITET 767
ABCF2-C RVCLAWLAWQNPHMLFLDEPTNHLDIETIDALADAIN----EFEGGMMLVSHDFRLIQQV 579
ABCF3-C RVAFAQMTMPCPNFYILDEPTNHLDMETIEALGRALN----NFRGGVILVSHDERFIRLV 673
ABCE1-C RVRLRLCLGKPADVYLIDEPSAYLDSEQRLMAARVVKRFILHAKKTAFVVEHDFIMATYL 528
ABCG1 VSAHLKLQEKDE--GRREMVKEILTALGLLSCANTRTG-----SLSGGQRKRLAIALELV 228
ABCG4 VSANLKLSEKQE--VKKELVTEILTALGLMSCSHTRTA-----LLSGGQRKRLAIALELV 216
ABCG2 FSAALRLATTMTNHEKNERINRVIEELGLDKVADSKVGTQFIRGVSGGERKRTSIGMELI 201
ABCG5 YTALLAIRRGNPG-SFQKKVEAVMAELSLSHVADRLIGNYSLGGISTGERRRVSIAAQLL 208
ABCG8 FIAQMRLPRTFSQAQRDKRVEDVIAELRLRQCADTRVGNMYVRGLSGGERRRVSIGVQLL 228
ABCG1 NNPPVMFFDEPTSGLDSASCFQVVSLMKGLAQGGRSIICTIHQPSAKLFELFDQLYVLSQ 288
ABCG4 NNPPVMFFDEPTSGLDSASCFQVVSLMKSLAQGGRTIICTIHQPSAKLFEMFDKLYILSQ 276
ABCG2 TDPSILSLDEPTTGLDSSTANAVLLLLKRMSKQGRTIIFSIHQPRYSIFKLFDSLTLLAS 261
ABCG5 QDPKVMLFDEPTTGLDCMTANQIVVLLVELARRNRIVVLTIHQPRSELFQLFDKIAILSF 268
ABCG8 WNPGILILDEPTSGLDSFTAHNLVKTLSRLAKGNRLVLISLHQPRSDIFRLFDLVLLMTS 288

9.2 Vector maps

9.2.1 pFastBacDual

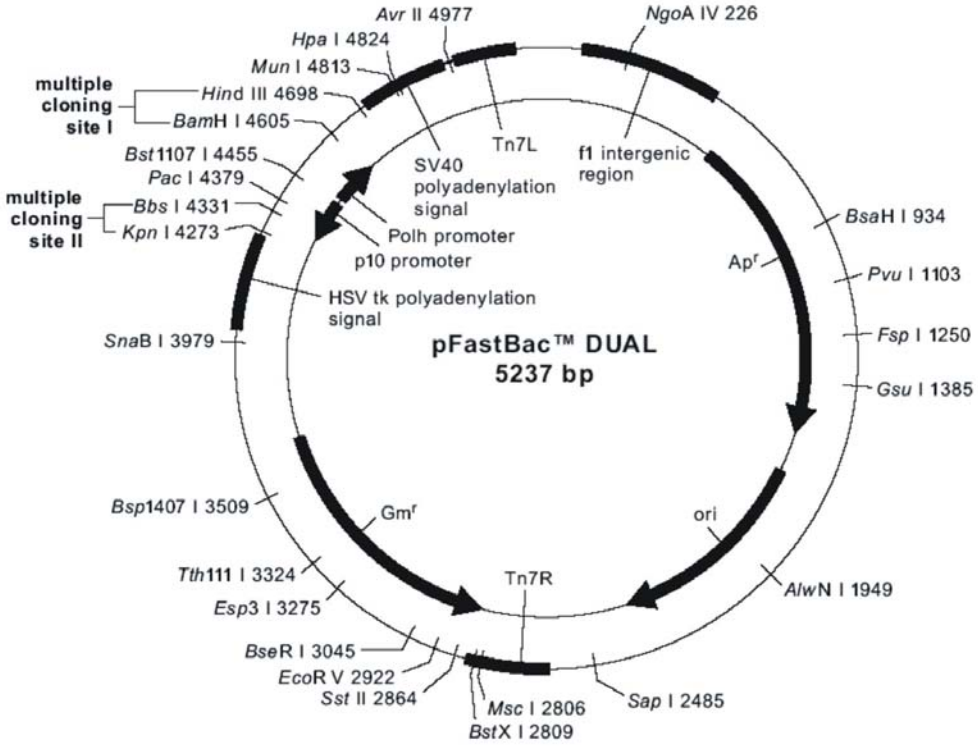

pFastBac™ DUAL polyhedrin promoter region and MCS I:

4515 +1

5´ - - -AAATAAGTAT TTTACTGTTT TCGTAACAGT TTTGTAATAA AAAAACCTAT AAATATTCCG GATTATTCAT

polyhedrin promoter

BamH I | Rsr II | BssH II | EcoR I | Stu I | Sal I | Sst I | Spe I | Not I | Nsp V | Xba I

ACCGTCCCAC CATCGGGCGC GGATCCCGGT CCGAAGCGCG CGGAATTCAA AGGCCTACGT CGACGAGCTC ACTAGTCGCG GCCGCTTTCG AATCTAGAGC

Pst I | Hind III

CTGCAGTCTC GACAAGCTTG TCGAGAAGTA CTAGAGGATC ATAATC 3´

+1 corresponds to the transcriptional start for the polyhedrin promoter.
ATT corresponds to the original translational start codon. The ATG was mutated to an ATT.
An in-frame ATG codon must be provided by the cloned gene to initiate translation.
Stop codons are shown in bold.

pFastBac™ DUAL p10 promoter region and MCS II:

4417 +1

5´ - AAA TAAGAATTAT TATCAAATCA TTTGTATATT AATTAAAATA CTATACTGTA AATTACATTT TATTTACAAT

p10 promoter

Bbs I | Sma I | Xho I | Nco I | Nhe I | Pvu II | Nsi I | Sph I | Kpn I

CACTCGACGA AGACTTGATC ACCCGGGATC TCGAGCCATG GTGCTAGCAG CTGATGCATA GCATGCGGTA CCGGGAGATG GGGGAGGCTA ACTGAAACAC 3´

+1 corresponds to the transcriptional start for the p10 promoter and corresponds to position 4420 on the map.
Digestion at the *Bbs* I site generates a *Bam*H I compatible overhang. An in-frame ATG codon must be provided by the cloned gene to initiate translation when the *Bbs* I, *Sma* I or *Xho* I sites are used for cloning. When cloning into the *Nco* I site, or sites downstream of the *Nco* I site, make sure the reading frame of the cloned gene is in frame relative to the ATG sequence of the *Nco* I site.
Stop codons are shown in bold.

9.2.2 pSL1180

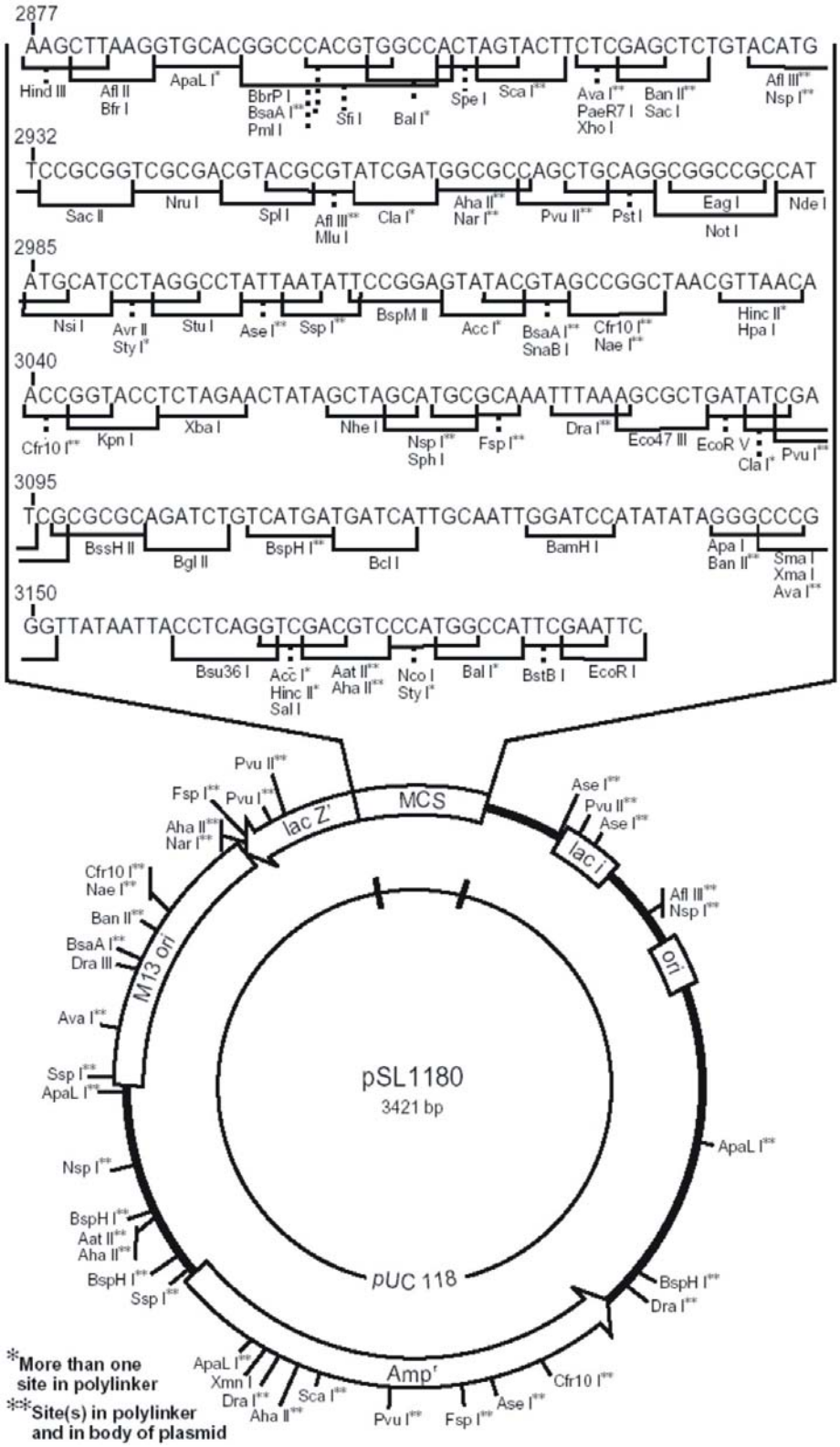
2877
AAGCTTAAGGTGCACGGCCCACGTGGCCACTAGTACTTCTCGAGCTCTGTACATG
Hind III
Afl II
Bfr I
ApaL I*
BbrP I
BsaA I**
Pml I
Sfi I
Bal I*
Spe I
Sca I**
Ava I**
PaeR7 I
Xho I
Ban II**
Sac I
Afl III**
Nsp I**
2932
TCCGCGGTCGCGACGTACGCGTATCGATGGCGCCAGCTGCAGGCGGCCGCCAT
Sac II
Nru I
Spl I
Afl III**
Mlu I
Cla I*
Aha II**
Nar I**
Pvu II**
Pst I
Eag I
Not I
Nde I
2985
ATGCATCCTAGGCCTATTAATATTCCGGAGTATACGTAGCCGGCTAACGTTAACA
Nsi I
Avr II
Sty I*
Stu I
Ase I**
Ssp I**
BspM II
Acc I*
BsaA I**
SnaB I
Cfr10 I**
Nae I**
Hinc II*
Hpa I
3040
ACCGGTACCTCTAGAACTATAGCTAGCATGCGCAAATTTAAAGCGCTGATATCGA
Cfr10 I**
Kpn I
Xba I
Nhe I
Nsp I**
Sph I
Fsp I**
Dra I**
Eco47 III
EcoR V
Cla I*
Pvu I**
3095
TCGCGCGCAGATCTGTCATGATGATCATTGCAATTGGATCCATATATAGGGCCCG
BssH II
Bgl II
BspH I**
Bcl I
BamH I
Apa I
Ban II**
Sma I
Xma I
Ava I**
3150
GGTTATAATTACCTCAGGTCGACGTCCCATGGCCATTCGAATTC
Bsu36 I
Acc I*
Hinc II*
Sal I
Aat II**
Aha II**
Nco I
Sty I*
Bal I*
BstB I
EcoR I
Pvu II**
Fsp I**
Pvu I**
Aha II**
Nar I**
lac Z'
MCS
Ase I**
Pvu II**
Ase I**
lac i
Afl III**
Nsp I**
ori
Cfr10 I**
Nae I**
Ban II**
BsaA I**
Dra III
M13 ori
Ava I**
Ssp I**
ApaL I**
pSL1180
3421 bp
ApaL I**
Nsp I**
BspH I**
Aat II**
Aha II**
BspH I**
Ssp I**
pUC 118
BspH I**
Dra I**
*More than one site in polylinker
**Site(s) in polylinker and in body of plasmid
ApaL I**
Xmn I
Dra I**
Aha II**
Sca I**
Amp^r
Pvu I**
Fsp I**
Ase I**
Cfr10 I**

10. Reference

Abele, R. and Tampé, R. (1999) Function of the transport complex TAP in cellular immune recognition. *Biochim Biophys Acta*, **1461**, 405-419.

Ackerman, A.L., Kyritsis, C., Tampé, R. and Cresswell, P. (2003) Early phagosomes in dendritic cells form a cellular compartment sufficient for cross presentation of exogenous antigens. *Proc Natl Acad Sci U S A*, **100**, 12889-12894.

Ahn, K., Gruhler, A., Galocha, B., Jones, T.R., Wiertz, E.J., Ploegh, H.L., Peterson, P.A., Yang, Y. and Fruh, K. (1997) The ER-luminal domain of the HCMV glycoprotein US6 inhibits peptide translocation by TAP. *Immunity*, **6**, 613-621.

Ahn, K., Meyer, T.H., Uebel, S., Sempe, P., Djaballah, H., Yang, Y., Peterson, P.A., Fruh, K. and Tampé, R. (1996) Molecular mechanism and species specificity of TAP inhibition by herpes simplex virus ICP47. *EMBO J*, **15**, 3247-3255.

Aki, M., Shimbara, N., Takashina, M., Akiyama, K., Kagawa, S., Tamura, T., Tanahashi, N., Yoshimura, T., Tanaka, K. and Ichihara, A. (1994) Interferon-gamma induces different subunit organizations and functional diversity of proteasomes. *J Biochem (Tokyo)*, **115**, 257-269.

Akiyama, K., Yokota, K., Kagawa, S., Shimbara, N., Tamura, T., Akioka, H., Nothwang, H.G., Noda, C., Tanaka, K. and Ichihara, A. (1994) cDNA cloning and interferon gamma down-regulation of proteasomal subunits X and Y. *Science*, **265**, 1231-1234.

Alberts, P., Daumke, O., Deverson, E.V., Howard, J.C. and Knittler, M.R. (2001) Distinct functional properties of the TAP subunits coordinate the nucleotide-dependent transport cycle. *Curr Biol*, **11**, 242-251.

Aleksandrov, L., Aleksandrov, A.A., Chang, X.B. and Riordan, J.R. (2002) The First Nucleotide Binding Domain of Cystic Fibrosis Transmembrane Conductance Regulator Is a Site of Stable Nucleotide Interaction, whereas the Second Is a Site of Rapid Turnover. *J Biol Chem*, **277**, 15419-15425.

Androlewicz, M.J., Anderson, K.S. and Cresswell, P. (1993) Evidence that transporters associated with antigen processing translocate a major histocompatibility complex class I-binding peptide into the endoplasmic reticulum in an ATP-dependent manner. *Proc Natl Acad Sci U S A*, **90**, 9130-9134.

Androlewicz, M.J., Ortmann, B., van Endert, P.M., Spies, T. and Cresswell, P. (1994) Characteristics of peptide and major histocompatibility complex class I/beta 2-microglobulin binding to the transporters associated with antigen processing (TAP1 and TAP2). *Proc Natl Acad Sci U S A*, **91**, 12716-12720.

Arora, S., Lapinski, P.E. and Raghavan, M. (2001) Use of chimeric proteins to investigate the role of transporter associated with antigen processing (TAP) structural domains in peptide binding and translocation. *Proc Natl Acad Sci U S A*, **98**, 7241-7246.

Attaya, M., Jameson, S., Martinez, C.K., Hermel, E., Aldrich, C., Forman, J., Lindahl, K.F., Bevan, M.J. and Monaco, J.J. (1992) Ham-2 corrects the class I antigen-processing defect in RMA-S cells. *Nature*, **355**, 647-649.

Balakrishnan, L., Venter, H., Shilling, R.A. and Van Veen, H.W. (2003) Reversible transport by the ABC multidrug export pump LmrA: ATP synthesis at the expense of downhill ethidium uptake. *J Biol Chem*.

Beinert, D., Neumann, L., Uebel, S. and Tampé, R. (1997) Structure of the viral TAP-inhibitor ICP47 induced by membrane association. *Biochemistry*, **36**, 4694-4700.

Bochtler, M., Ditzel, L., Groll, M., Hartmann, C. and Huber, R. (1999) The proteasome. *Annu Rev Biophys Biomol Struct*, **28**, 295-317.

Bouabe, H. and Knittler, M.R. (2003) The distinct nucleotide binding states of the transporter associated with antigen processing (TAP) are regulated by the nonhomologous C-terminal tails of TAP1 and TAP2. *Eur J Biochem*, **270**, 4531-4546.

Browne, B.L., McClendon, V. and Bedwell, D.M. (1996) Mutations within the first LSGGQ motif of Ste6p cause defects in a-factor transport and mating in Saccharomyces cerevisiae. *J Bacteriol*, **178**, 1712-1719.

Cai, J., Daoud, R., Alqawi, O., Georges, E., Pelletier, J. and Gros, P. (2002) Nucleotide binding and nucleotide hydrolysis properties of the ABC transporter MRP6 (ABCC6). *Biochemistry*, **41**, 8058-8067.

Chang, G. and Roth, C.B. (2001) Structure of MsbA from E. coli: a homolog of the multidrug resistance ATP binding cassette (ABC) transporters. *Science*, **293**, 1793-1800.

Chen, J., Lu, G., Lin, J., Davidson, A.L. and Quiocho, F.A. (2003a) A tweezers-like motion of the ATP-binding cassette dimer in an ABC transport cycle. *Mol Cell*, **12**, 651-661.

Chen, J., Sharma, S., Quiocho, F.A. and Davidson, A.L. (2001) Trapping the transition state of an ATP-binding cassette transporter: evidence for a concerted mechanism of maltose transport. *Proc Natl Acad Sci U S A*, **98**, 1525-1530.

Chen, M., Abele, R. and Tampé, R. (2003b) Peptides induce ATP hydrolysis at both subunits of the transporter associated with antigen processing. *J Biol Chem*, **278**, 29686-29692.

Cohn, M. (1990) Structural and chemical properties of ATP and its metal complexes in solution. *Ann N Y Acad Sci*, **603**, 151-164.

Collins, E.J., Garboczi, D.N. and Wiley, D.C. (1994) Three-dimensional structure of a peptide extending from one end of a class I MHC binding site. *Nature*, **371**, 626-629.

Cutting, G.R., Kasch, L.M., Rosenstein, B.J., Zielenski, J., Tsui, L.C., Antonarakis, S.E. and Kazazian, H.H., Jr. (1990) A cluster of cystic fibrosis mutations in the first nucleotide-binding fold of the cystic fibrosis conductance regulator protein. *Nature*, **346**, 366-369.

Daumke, O. and Knittler, M.R. (2001) Functional asymmetry of the ATP-binding-cassettes of the ABC transporter TAP is determined by intrinsic properties of the nucleotide binding domains. *Eur J Biochem*, **268**, 4776-4786.

Davidson, A.L. (2002) Mechanism of coupling of transport to hydrolysis in bacterial ATP-binding cassette transporters. *J Bacteriol*, **184**, 1225-1233.

Davidson, A.L. and Sharma, S. (1997) Mutation of a single MalK subunit severely impairs maltose transport activity in Escherichia coli. *J Bacteriol*, **179**, 5458-5464.

DeMars, R., Rudersdorf, R., Chang, C., Petersen, J., Strandtmann, J., Korn, N., Sidwell, B. and Orr, H.T. (1985) Mutations that impair a posttranscriptional step in expression of HLA-A and -B antigens. *Proc Natl Acad Sci U S A*, **82**, 8183-8187.

Dick, L.R., Aldrich, C., Jameson, S.C., Moomaw, C.R., Pramanik, B.C., Doyle, C.K., DeMartino, G.N., Bevan, M.J., Forman, J.M. and Slaughter, C.A. (1994) Proteolytic processing of ovalbumin and beta-galactosidase by the proteasome to a yield antigenic peptides. *J Immunol*, **152**, 3884-3894.

Diederichs, K., Diez, J., Greller, G., Muller, C., Breed, J., Schnell, C., Vonrhein, C., Boos, W. and Welte, W. (2000) Crystal structure of MalK, the ATPase subunit of the trehalose/maltose ABC transporter of the archaeon Thermococcus litoralis. *EMBO J*, **19**, 5951-5961.

Eggers, M., Boes-Fabian, B., Ruppert, T., Kloetzel, P.M. and Koszinowski, U.H. (1995) The cleavage preference of the proteasome governs the yield of antigenic peptides. *J Exp Med*, **182**, 1865-1870.

Ehring, B., Meyer, T.H., Eckerskorn, C., Lottspeich, F. and Tampé, R. (1996) Effects of major-histocompatibility-complex-encoded subunits on the peptidase and proteolytic activities of human 20S proteasomes. Cleavage of proteins and antigenic peptides. *Eur J Biochem*, **235**, 404-415.

Falk, K. and Rotzschke, O. (2002) The final cut: how ERAP1 trims MHC ligands to size. *Nat Immunol*, **3**, 1121-1122.

Fetsch, E.E. and Davidson, A.L. (2002) From the Cover: Vanadate-catalyzed photocleavage of the signature motif of an ATP-binding cassette (ABC) transporter. *Proc Natl Acad Sci U S A*, **99**, 9685-9690.

Fisher, A.J., Smith, C.A., Thoden, J.B., Smith, R., Sutoh, K., Holden, H.M. and Rayment, I. (1995) X-ray structures of the myosin motor domain of Dictyostelium discoideum complexed with MgADP.BeFx and MgADP.AlF4. *Biochemistry*, **34**, 8960-8972.

Fruh, K., Ahn, K., Djaballah, H., Sempe, P., van Endert, P.M., Tampe, R., Peterson, P.A. and Yang, Y. (1995) A viral inhibitor of peptide transporters for antigen presentation. *Nature*, **375**, 415-418.

Fruh, K., Gossen, M., Wang, K., Bujard, H., Peterson, P.A. and Yang, Y. (1994) Displacement of housekeeping proteasome subunits by MHC-encoded LMPs: a newly discovered mechanism for modulating the multicatalytic proteinase complex. *Embo J*, **13**, 3236-3244.

Gaczynska, M., Rock, K.L., Spies, T. and Goldberg, A.L. (1994) Peptidase activities of proteasomes are differentially regulated by the major histocompatibility complex-encoded genes for LMP2 and LMP7. *Proc Natl Acad Sci U S A*, **91**, 9213-9217.

Galocha, B., Hill, A., Barnett, B.C., Dolan, A., Raimondi, A., Cook, R.F., Brunner, J., McGeoch, D.J. and Ploegh, H.L. (1997) The active site of ICP47, a herpes simplex virus-encoded inhibitor of the major histocompatibility complex (MHC)-encoded

peptide transporter associated with antigen processing (TAP), maps to the NH2-terminal 35 residues. *J Exp Med*, **185**, 1565-1572.

Gaudet, R. and Wiley, D.C. (2001) Structure of the ABC ATPase domain of human TAP1, the transporter associated with antigen processing. *EMBO J*, **20**, 4964-4972.

Geourjon, C., Orelle, C., Steinfels, E., Blanchet, C., Deleage, G., Di Pietro, A. and Jault, J.M. (2001) A common mechanism for ATP hydrolysis in ABC transporter and helicase superfamilies. *Trends Biochem Sci*, **26**, 539-544.

Gorbulev, S., Abele, R. and Tampé, R. (2001) Allosteric crosstalk between peptide-binding, transport, and ATP hydrolysis of the ABC transporter TAP. *Proc Natl Acad Sci U S A*, **98**, 3732-3737.

Gromme, M. and Neefjes, J. (2002) Antigen degradation or presentation by MHC class I molecules via classical and non-classical pathways. *Mol Immunol*, **39**, 181-202.

Gromme, M., van der Valk, R., Sliedregt, K., Vernie, L., Liskamp, R., Hammerling, G., Koopmann, J.O., Momburg, F. and Neefjes, J. (1997) The rational design of TAP inhibitors using peptide substrate modifications and peptidomimetics. *Eur J Immunol*, **27**, 898-904.

Guermonprez, P., Saveanu, L., Kleijmeer, M., Davoust, J., Van Endert, P. and Amigorena, S. (2003) ER-phagosome fusion defines an MHC class I cross-presentation compartment in dendritic cells. *Nature*, **425**, 397-402.

Hammond, C., Braakman, I. and Helenius, A. (1994) Role of N-linked oligosaccharide recognition, glucose trimming, and calnexin in glycoprotein folding and quality control. *Proc Natl Acad Sci U S A*, **91**, 913-917.

Hammond, S.A., Johnson, R.P., Kalams, S.A., Walker, B.D., Takiguchi, M., Safrit, J.T., Koup, R.A. and Siliciano, R.F. (1995) An epitope-selective, transporter associated with antigen presentation (TAP)-1/2-independent pathway and a more general TAP-1/2-dependent antigen-processing pathway allow recognition of the HIV-1 envelope glycoprotein by CD8+ CTL. *J Immunol*, **154**, 6140-6156.

Henderson, R.A., Michel, H., Sakaguchi, K., Shabanowitz, J., Appella, E., Hunt, D.F. and Engelhard, V.H. (1992) HLA-A2.1-associated peptides from a mutant cell line: a second pathway of antigen presentation. *Science*, **255**, 1264-1266.

Hengel, H., Koopmann, J.O., Flohr, T., Muranyi, W., Goulmy, E., Hammerling, G.J., Koszinowski, U.H. and Momburg, F. (1997) A viral ER-resident glycoprotein inactivates the MHC-encoded peptide transporter. *Immunity*, **6**, 623-632.

Hewitt, E.W., Gupta, S.S. and Lehner, P.J. (2001) The human cytomegalovirus gene product US6 inhibits ATP binding by TAP. *EMBO J*, **20**, 387-396.

Hewitt, E.W. and Lehner, P.J. (2003) The ABC-transporter signature motif is required for peptide translocation but not peptide binding by TAP. *Eur J Immunol*, **33**, 422-427.

Higgins, C.F. (1992) ABC transporters: from microorganisms to man. *Annu Rev Cell Biol*, **8**, 67-113.

Higgins, C.F. (2001) ABC transporters: physiology, structure and mechanism--an overview. *Res Microbiol*, **152**, 205-210.

Hill, A.B., Barnett, B.C., McMichael, A.J. and McGeoch, D.J. (1994) HLA class I molecules are not transported to the cell surface in cells infected with herpes simplex virus types 1 and 2. *J Immunol*, **152**, 2736-2741.

Hopfner, K.P., Karcher, A., Shin, D.S., Craig, L., Arthur, L.M., Carney, J.P. and Tainer, J.A. (2000) Structural biology of Rad50 ATPase: ATP-driven conformational control in DNA double-strand break repair and the ABC-ATPase superfamily. *Cell*, **101**, 789-800.

Hou, Y., Cui, L., Riordan, J.R. and Chang, X. (2000) Allosteric interactions between the two non-equivalent nucleotide binding domains of multidrug resistance protein MRP1. *J Biol Chem*, **275**, 20280-20287.

Hou, Y.X., Riordan, J.R. and Chang, X.B. (2003) ATP binding, not hydrolysis, at the first nucleotide-binding domain of multidrug resistance-associated protein MRP1 enhances ADP.Vi trapping at the second domain. *J Biol Chem*, **278**, 3599-3605.

Houde, M., Bertholet, S., Gagnon, E., Brunet, S., Goyette, G., Laplante, A., Princiotta, M.F., Thibault, P., Sacks, D. and Desjardins, M. (2003) Phagosomes are competent organelles for antigen cross-presentation. *Nature*, **425**, 402-406.

Hrycyna, C.A., Ramachandra, M., Ambudkar, S.V., Ko, Y.H., Pedersen, P.L., Pastan, I. and Gottesman, M.M. (1998) Mechanism of action of human P-glycoprotein ATPase activity. Photochemical cleavage during a catalytic transition state using orthovanadate reveals cross-talk between the two ATP sites. *J Biol Chem*, **273**, 16631-16634.

Hughes, E.A. and Cresswell, P. (1998) The thiol oxidoreductase ERp57 is a component of the MHC class I peptide-loading complex. *Curr Biol*, **8**, 709-712.

Hung, L.W., Wang, I.X., Nikaido, K., Liu, P.Q., Ames, G.F. and Kim, S.H. (1998) Crystal structure of the ATP-binding subunit of an ABC transporter. *Nature*, **396**, 703-707.

Hunter, W.M. and Greenwood, F.C. (1964) A radio-immunoelectrophoretic assay for human growth hormone. *Biochem J*, **91**, 43-56.

Janas, E., Hofacker, M., Chen, M., Gompf, S., van der Does, C. and Tampé, R. (2003) The ATP hydrolysis cycle of the nucleotide-binding domain of the mitochondrial ATP-binding cassette transporter Mdl1p. *J Biol Chem*, **278**, 26862-26869.

Karpowich, N., Martsinkevich, O., Millen, L., Yuan, Y.R., Dai, P.L., MacVey, K., Thomas, P.J. and Hunt, J.F. (2001) Crystal structures of the MJ1267 ATP binding cassette reveal an induced-fit effect at the ATPase active site of an ABC transporter. *Structure (Camb)*, **9**, 571-586.

Karttunen, J.T., Lehner, P.J., Gupta, S.S., Hewitt, E.W. and Cresswell, P. (2001) Distinct functions and cooperative interaction of the subunits of the transporter associated with antigen processing (TAP). *Proc Natl Acad Sci U S A*, **98**, 7431-7436.

Karttunen, J.T., Trowsdale, J. and Lehner, P.J. (1999) Antigen presentation: TAP dances with ATP. *Curr Biol*, **9**, R820-824.

Kelly, A., Powis, S.H., Kerr, L.A., Mockridge, I., Elliott, T., Bastin, J., Uchanska-Ziegler, B., Ziegler, A., Trowsdale, J. and Townsend, A. (1992) Assembly and function of the two ABC transporter proteins encoded in the human major histocompatibility complex. *Nature*, **355**, 641-644.

Kerem, B.S., Zielenski, J., Markiewicz, D., Bozon, D., Gazit, E., Yahav, J., Kennedy, D., Riordan, J.R., Collins, F.S., Rommens, J.M. and et al. (1990) Identification of mutations in regions corresponding to the two putative nucleotide (ATP)-binding folds of the cystic fibrosis gene. *Proc Natl Acad Sci U S A*, **87**, 8447-8451.

Ketchum, C.J., Schmidt, W.K., Rajendrakumar, G.V., Michaelis, S. and Maloney, P.C. (2001) The yeast a-factor transporter Ste6p, a member of the ABC superfamily, couples ATP hydrolysis to pheromone export. *J Biol Chem*, **276**, 29007-29011.

Kisselev, A.F., Akopian, T.N., Woo, K.M. and Goldberg, A.L. (1999) The sizes of peptides generated from protein by mammalian 26 and 20 S proteasomes.

Implications for understanding the degradative mechanism and antigen presentation. *J Biol Chem*, **274**, 3363-3371.

Kleijmeer, M.J., Kelly, A., Geuze, H.J., Slot, J.W., Townsend, A. and Trowsdale, J. (1992) Location of MHC-encoded transporters in the endoplasmic reticulum and cis-Golgi. *Nature*, **357**, 342-344.

Knittler, M.R., Alberts, P., Deverson, E.V. and Howard, J.C. (1999) Nucleotide binding by TAP mediates association with peptide and release of assembled MHC class I molecules. *Curr Biol*, **9**, 999-1008.

Koch, J., Guntrum, R., Heintke, S., Kyritsis, C. and Tampé, R. (2004) Functional dissection of the transmembrane domains of the transporter associated with antigen processing (TAP). *J Biol Chem*, **279**, 10142-10147.

Koopmann, J.O., Post, M., Neefjes, J.J., Hammerling, G.J. and Momburg, F. (1996) Translocation of long peptides by transporters associated with antigen processing (TAP). *Eur J Immunol*, **26**, 1720-1728.

Kyritsis, C., Gorbulev, S., Hutschenreiter, S., Pawlitschko, K., Abele, R. and Tampé, R. (2001) Molecular mechanism and structural aspects of transporter associated with antigen processing inhibition by the cytomegalovirus protein US6. *J Biol Chem*, **276**, 48031-48039.

Lacaille, V.G. and Androlewicz, M.J. (1998) Herpes simplex virus inhibitor ICP47 destabilizes the transporter associated with antigen processing (TAP) heterodimer. *J Biol Chem*, **273**, 17386-17390.

Laemmli, U.K. (1970) Cleavage of structural proteins during the assembly of the head of bacteriophage T4. *Nature*, **227**, 680-685.

Lankat-Buttgereit, B. and Tampé, R. (2002) The transporter associated with antigen processing: function and implications in human diseases. *Physiol Rev*, **82**, 187-204.

Lapinski, P.E., Neubig, R.R. and Raghavan, M. (2001) Walker A lysine mutations of TAP1 and TAP2 interfere with peptide translocation but not peptide binding. *J Biol Chem*, **276**, 7526-7533.

Lapinski, P.E., Raghuraman, G. and Raghavan, M. (2003) Nucleotide interactions with membrane-bound transporter associated with antigen processing proteins. *J Biol Chem*, **278**, 8229-8237.

Lehner, P.J., Karttunen, J.T., Wilkinson, G.W. and Cresswell, P. (1997) The human cytomegalovirus US6 glycoprotein inhibits transporter associated with antigen processing-dependent peptide translocation. *Proc Natl Acad Sci U S A*, **94**, 6904-6909.

Li, Z.S., Szczypka, M., Lu, Y.P., Thiele, D.J. and Rea, P.A. (1996) The yeast cadmium factor protein (YCF1) is a vacuolar glutathione S-conjugate pump. *J Biol Chem*, **271**, 6509-6517.

Lindquist, J.A., Jensen, O.N., Mann, M. and Hammerling, G.J. (1998) ER-60, a chaperone with thiol-dependent reductase activity involved in MHC class I assembly. *EMBO J*, **17**, 2186-2195.

Liu, C.E., Liu, P.Q. and Ames, G.F. (1997) Characterization of the adenosine triphosphatase activity of the periplasmic histidine permease, a traffic ATPase (ABC transporter). *J Biol Chem*, **272**, 21883-21891.

Locher, K.P., Lee, A.T. and Rees, D.C. (2002) The E. coli BtuCD structure: a framework for ABC transporter architecture and mechanism. *Science*, **296**, 1091-1098.

Loo, T.W., Bartlett, M.C. and Clarke, D.M. (2002) The "LSGGQ" motif in each nucleotide-binding domain of human P- glycoprotein is adjacent to the opposing walker A sequence. *J Biol Chem*, **277**, 41303-41306.

Madden, D.R. (1995) The three-dimensional structure of peptide-MHC complexes. *Annu Rev Immunol*, **13**, 587-622.

Maruta, S., Henry, G.D., Sykes, B.D. and Ikebe, M. (1993) Formation of the stable myosin-ADP-aluminum fluoride and myosin-ADP-beryllium fluoride complexes and their analysis using 19F NMR. *J Biol Chem*, **268**, 7093-7100.

Matsuo, M., Kioka, N., Amachi, T. and Ueda, K. (1999) ATP binding properties of the nucleotide-binding folds of SUR1. *J Biol Chem*, **274**, 37479-37482.

Meyer, T.H., van Endert, P.M., Uebel, S., Ehring, B. and Tampé, R. (1994) Functional expression and purification of the ABC transporter complex associated with antigen processing (TAP) in insect cells. *FEBS Lett*, **351**, 443-447.

Mitchell, P. (1957) A general theory of membrane transport from studies of bacteria. *Nature*, **180**, 134-136.

Momburg, F., Roelse, J., Howard, J.C., Butcher, G.W., Hammerling, G.J. and Neefjes, J.J. (1994) Selectivity of MHC-encoded peptide transporters from human, mouse and rat. *Nature*, **367**, 648-651.

Moody, J.E., Millen, L., Binns, D., Hunt, J.F. and Thomas, P.J. (2002) Cooperative, ATP-dependent association of the nucleotide binding cassettes during the catalytic cycle of ATP-binding cassette transporters. *J Biol Chem*, **277**, 21111-21114.

Morbach, S., Tebbe, S. and Schneider, E. (1993) The ATP-binding cassette (ABC) transporter for maltose/maltodextrins of Salmonella typhimurium. Characterization of the ATPase activity associated with the purified MalK subunit. *J Biol Chem*, **268**, 18617-18621.

Morrice, N.A. and Powis, S.J. (1998) A role for the thiol-dependent reductase ERp57 in the assembly of MHC class I molecules. *Curr Biol*, **8**, 713-716.

Mourez, M., Hofnung, M. and Dassa, E. (1997) Subunit interactions in ABC transporters: a conserved sequence in hydrophobic membrane proteins of periplasmic permeases defines an important site of interaction with the ATPase subunits. *EMBO J*, **16**, 3066-3077.

Muneyuki, E., Noji, H., Amano, T., Masaike, T. and Yoshida, M. (2000) F(0)F(1)-ATP synthase: general structural features of 'ATP-engine' and a problem on free energy transduction. *Biochim Biophys Acta*, **1458**, 467-481.

Nandi, D., Jiang, H. and Monaco, J.J. (1996) Identification of MECL-1 (LMP-10) as the third IFN-gamma-inducible proteasome subunit. *J Immunol*, **156**, 2361-2364.

Neefjes, J.J., Dierx, J. and Ploegh, H.L. (1993a) The effect of anchor residue modifications on the stability of major histocompatibility complex class I-peptide interactions. *Eur J Immunol*, **23**, 840-845.

Neefjes, J.J., Momburg, F. and Hammerling, G.J. (1993b) Selective and ATP-dependent translocation of peptides by the MHC- encoded transporter. *Science*, **261**, 769-771.

Neumann, L., Abele, R. and Tampé, R. (2002) Thermodynamics of peptide binding to the transporter associated with antigen processing (TAP). *J Mol Biol*, **324**, 965-973.

Neumann, L., Kraas, W., Uebel, S., Jung, G. and Tampé, R. (1997) The active domain of the herpes simplex virus protein ICP47: a potent inhibitor of the transporter associated with antigen processing. *J Mol Biol*, **272**, 484-492.

Neumann, L. and Tampé, R. (1999) Kinetic analysis of peptide binding to the TAP transport complex: evidence for structural rearrangements induced by substrate binding. *J Mol Biol*, **294**, 1203-1213.

Nijenhuis, M. and Hammerling, G.J. (1996) Multiple regions of the transporter associated with antigen processing (TAP) contribute to its peptide binding site. *J Immunol*, **157**, 5467-5477.

Nijenhuis, M., Schmitt, S., Armandola, E.A., Obst, R., Brunner, J. and Hammerling, G.J. (1996) Identification of a contact region for peptide on the TAP1 chain of the transporter associated with antigen processing. *J Immunol*, **156**, 2186-2195.

Orelle, C., Dalmas, O., Gros, P., Di Pietro, A. and Jault, J.M. (2003) The Conserved Glutamate Residue Adjacent to the Walker-B Motif Is the Catalytic Base for ATP Hydrolysis in the ATP-binding Cassette Transporter BmrA. *J Biol Chem*, **278**, 47002-47008.

O'Rourke, B. (1993) Ion channels as sensors of cellular energy. Mechanisms for modulation by magnesium and nucleotides. *Biochem Pharmacol*, **46**, 1103-1112.

Pamer, E. and Cresswell, P. (1998) Mechanisms of MHC class I--restricted antigen processing. *Annu Rev Immunol*, **16**, 323-358.

Panagiotidis, C.H., Reyes, M., Sievertsen, A., Boos, W. and Shuman, H.A. (1993) Characterization of the structural requirements for assembly and nucleotide binding of an ATP-binding cassette transporter. The maltose transport system of Escherichia coli. *J Biol Chem*, **268**, 23685-23696.

Park, S., Ajtai, K. and Burghardt, T.P. (1999) Inhibition of myosin ATPase by metal fluoride complexes. *Biochim Biophys Acta*, **1430**, 127-140.

Paulsson, K. and Wang, P. (2003) Chaperones and folding of MHC class I molecules in the endoplasmic reticulum. *Biochim Biophys Acta*, **1641**, 1-12.

Payen, L.F., Gao, M., Westlake, C.J., Cole, S.P. and Deeley, R.G. (2003) Role of carboxylate residues adjacent to the conserved core Walker B motifs in the catalytic cycle of multidrug resistance protein 1 (ABCC1). *J Biol Chem*, **278**, 38537-38547.

Peterson, J.R., Ora, A., Van, P.N. and Helenius, A. (1995) Transient, lectin-like association of calreticulin with folding intermediates of cellular and viral glycoproteins. *Mol Biol Cell*, **6**, 1173-1184.

Pfander, R., Neumann, L., Zweckstetter, M., Seger, C., Holak, T.A. and Tampé, R. (1999) Structure of the active domain of the herpes simplex virus protein ICP47 in water/sodium dodecyl sulfate solution determined by nuclear magnetic resonance spectroscopy. *Biochemistry*, **38**, 13692-13698.

Powis, S.J., Townsend, A.R., Deverson, E.V., Bastin, J., Butcher, G.W. and Howard, J.C. (1991) Restoration of antigen presentation to the mutant cell line RMA-S by an MHC-linked transporter. *Nature*, **354**, 528-531.

Qian, Y.M., Qiu, W., Gao, M., Westlake, C.J., Cole, S.P. and Deeley, R.G. (2001) Characterization of binding of leukotriene C4 by human multidrug resistance protein 1: evidence of differential interactions with NH2- and COOH-proximal halves of the protein. *J Biol Chem*, **276**, 38636-38644.

Qu, Q. and Sharom, F.J. (2001) FRET analysis indicates that the two ATPase active sites of the P-glycoprotein multidrug transporter are closely associated. *Biochemistry*, **40**, 1413-1422.

Ritz, U., Momburg, F., Pircher, H.P., Strand, D., Huber, C. and Seliger, B. (2001) Identification of sequences in the human peptide transporter subunit TAP1 required for transporter associated with antigen processing (TAP) function. *Int Immunol*, **13**, 31-41.

Rock, K.L. and Goldberg, A.L. (1999) Degradation of cell proteins and the generation of MHC class I-presented peptides. *Annu Rev Immunol*, **17**, 739-779.

Sadasivan, B., Lehner, P.J., Ortmann, B., Spies, T. and Cresswell, P. (1996) Roles for calreticulin and a novel glycoprotein, tapasin, in the interaction of MHC class I molecules with TAP. *Immunity*, **5**, 103-114.

Sankaran, B., Bhagat, S. and Senior, A.E. (1997) Photoaffinity labelling of P-glycoprotein catalytic sites. *FEBS Lett*, **417**, 119-122.

Saric, T., Chang, S.C., Hattori, A., York, I.A., Markant, S., Rock, K.L., Tsujimoto, M. and Goldberg, A.L. (2002) An IFN-gamma-induced aminopeptidase in the ER, ERAP1, trims precursors to MHC class I-presented peptides. *Nat Immunol*, **3**, 1169-1176.

Sauna, Z.E. and Ambudkar, S.V. (2000) Evidence for a requirement for ATP hydrolysis at two distinct steps during a single turnover of the catalytic cycle of human P-glycoprotein. *Proc Natl Acad Sci U S A*, **97**, 2515-2520.

Sauna, Z.E. and Ambudkar, S.V. (2001) Characterization of the catalytic cycle of ATP hydrolysis by human P-glycoprotein. The two ATP hydrolysis events in a single catalytic cycle are kinetically similar but affect different functional outcomes. *J Biol Chem*, **276**, 11653-11661.

Sauna, Z.E., Muller, M., Peng, X.H. and Ambudkar, S.V. (2002) Importance of the conserved Walker B glutamate residues, 556 and 1201, for the completion of the catalytic cycle of ATP hydrolysis by human P-glycoprotein (ABCB1). *Biochemistry*, **41**, 13989-14000.

Sauna, Z.E., Smith, M.M., Muller, M. and Ambudkar, S.V. (2001a) Evidence for the vectorial nature of drug (substrate)-stimulated ATP hydrolysis by human P-glycoprotein. *J Biol Chem*, **276**, 33301-33304.

Sauna, Z.E., Smith, M.M., Muller, M. and Ambudkar, S.V. (2001b) Functionally similar vanadate-induced 8-azidoadenosine 5'-[alpha- (32)P]Diphosphate-trapped transition state intermediates of human P- glycoprotin are generated in the absence and presence of ATP hydrolysis. *J Biol Chem*, **276**, 21199-21208.

Saveanu, L., Daniel, S. and van Endert, P.M. (2001) Distinct functions of the ATP binding cassettes of transporters associated with antigen processing: a mutational analysis of Walker A and B sequences. *J Biol Chem*, **276**, 22107-22113.

Schmitt, L. and Tampé, R. (2000) Affinity, specificity, diversity: a challenge for the ABC transporter TAP in cellular immunity. *Chembiochem*, **1**, 16-35.

Schmitt, L. and Tampé, R. (2002) Structure and mechanism of ABC transporters. *Curr Opin Struct Biol*, **12**, 754-760.

Schneider, E. and Hunke, S. (1998) ATP-binding-cassette (ABC) transport systems: functional and structural aspects of the ATP-hydrolyzing subunits/domains. *FEMS Microbiol Rev*, **22**, 1-20.

Schumacher, T.N., Kantesaria, D.V., Heemels, M.T., Ashton-Rickardt, P.G., Shepherd, J.C., Fruh, K., Yang, Y., Peterson, P.A., Tonegawa, S. and Ploegh, H.L. (1994) Peptide length and sequence specificity of the mouse TAP1/TAP2 translocator. *J Exp Med*, **179**, 533-540.

Senior, A.E. (1998) Catalytic mechanism of P-glycoprotein. *Acta Physiol Scand Suppl*, **643**, 213-218.

Senior, A.E., al-Shawi, M.K. and Urbatsch, I.L. (1995) The catalytic cycle of P-glycoprotein. *FEBS Lett*, **377**, 285-289.

Senior, A.E., al-Shawi, M.K. and Urbatsch, I.L. (1998) ATPase activity of Chinese hamster P-glycoprotein. *Methods Enzymol*, **292**, 514-523.

Senior, A.E. and Bhagat, S. (1998) P-glycoprotein shows strong catalytic cooperativity between the two nucleotide sites. *Biochemistry*, **37**, 831-836.

Serwold, T., Gonzalez, F., Kim, J., Jacob, R. and Shastri, N. (2002) ERAAP customizes peptides for MHC class I molecules in the endoplasmic reticulum. *Nature*, **419**, 480-483.

Sharma, S. and Davidson, A.L. (2000) Vanadate-induced trapping of nucleotides by purified maltose transport complex requires ATP hydrolysis. *J Bacteriol*, **182**, 6570-6576.

Shepherd, J.C., Schumacher, T.N., Ashton-Rickardt, P.G., Imaeda, S., Ploegh, H.L., Janeway, C.A., Jr. and Tonegawa, S. (1993) TAP1-dependent peptide translocation in vitro is ATP dependent and peptide selective. *Cell*, **74**, 577-584.

Smith, C.A. and Rayment, I. (1996) X-ray structure of the magnesium(II).ADP.vanadate complex of the Dictyostelium discoideum myosin motor domain to 1.9 A resolution. *Biochemistry*, **35**, 5404-5417.

Smith, P.C., Karpowich, N., Millen, L., Moody, J.E., Rosen, J., Thomas, P.J. and Hunt, J.F. (2002a) ATP binding to the motor domain from an ABC transporter drives formation of a nucleotide sandwich dimer. *Mol Cell*, **10**, 139-149.

Smith, P.C., Karpowich, N., Millen, L., Moody, J.E., Rosen, J., Thomas, P.J. and Hunt, J.F. (2002b) ATP binding to the motor domain from an ABC transporter drives formation of a nucleotide sandwich dimer. *Mol Cell*, **10**, 139-149.

Spies, T., Cerundolo, V., Colonna, M., Cresswell, P., Townsend, A. and DeMars, R. (1992) Presentation of viral antigen by MHC class I molecules is dependent on a putative peptide transporter heterodimer. *Nature*, **355**, 644-646.

Spies, T. and DeMars, R. (1991) Restored expression of major histocompatibility class I molecules by gene transfer of a putative peptide transporter. *Nature*, **351**, 323-324.

Szabo, K., Szakacs, G., Hegeds, T. and Sarkadi, B. (1999) Nucleotide occlusion in the human cystic fibrosis transmembrane conductance regulator. Different patterns in the two nucleotide binding domains. *J Biol Chem*, **274**, 12209-12212.

Szabo, K., Welker, E., Bakos, Muller, M., Roninson, I., Varadi, A. and Sarkadi, B. (1998) Drug-stimulated nucleotide trapping in the human multidrug transporter MDR1. Cooperation of the nucleotide binding domains. *J Biol Chem*, **273**, 10132-10138.

Szakacs, G., Ozvegy, C., Bakos, E., Sarkadi, B. and Varadi, A. (2001) Role of glycine-534 and glycine-1179 of human multidrug resistance protein (MDR1) in drug-mediated control of ATP hydrolysis. *Biochem J*, **356**, 71-75.

Takada, Y., Yamada, K., Taguchi, Y., Kino, K., Matsuo, M., Tucker, S.J., Komano, T., Amachi, T. and Ueda, K. (1998) Non-equivalent cooperation between the two nucleotide-binding folds of P-glycoprotein. *Biochim Biophys Acta*, **1373**, 131-136.

Tombline, G., Bartholomew, L., Gimi, K., Tyndall, G.A. and Senior, A.E. (2004) Synergy between conserved ABC signature Ser residues in P-glycoprotein catalysis. *J Biol Chem*, **279**, 5363-5373.

Trowsdale, J., Ragoussis, J. and Campbell, R.D. (1991) Map of the human MHC. *Immunol Today*, **12**, 443-446.

Uebel, S., Kraas, W., Kienle, S., Wiesmuller, K.H., Jung, G. and Tampé, R. (1997) Recognition principle of the TAP transporter disclosed by combinatorial peptide libraries. *Proc Natl Acad Sci U S A*, **94**, 8976-8981.

Uebel, S., Meyer, T.H., Kraas, W., Kienle, S., Jung, G., Wiesmuller, K.H. and Tampe, R. (1995) Requirements for peptide binding to the human transporter associated with antigen processing revealed by peptide scans and complex peptide libraries. *J Biol Chem*, **270**, 18512-18516.

Ueda, K., Komine, J., Matsuo, M., Seino, S. and Amachi, T. (1999) Cooperative binding of ATP and MgADP in the sulfonylurea receptor is modulated by glibenclamide. *Proc Natl Acad Sci U S A*, **96**, 1268-1272.

Urban, R.G., Chicz, R.M., Lane, W.S., Strominger, J.L., Rehm, A., Kenter, M.J., UytdeHaag, F.G., Ploegh, H., Uchanska-Ziegler, B. and Ziegler, A. (1994) A subset of HLA-B27 molecules contains peptides much longer than nonamers. *Proc Natl Acad Sci U S A*, **91**, 1534-1538.

Urbatsch, I.L., al-Shawi, M.K. and Senior, A.E. (1994) Characterization of the ATPase activity of purified Chinese hamster P-glycoprotein. *Biochemistry*, **33**, 7069-7076.

Urbatsch, I.L., Julien, M., Carrier, I., Rousseau, M.E., Cayrol, R. and Gros, P. (2000) Mutational analysis of conserved carboxylate residues in the nucleotide binding sites of P-glycoprotein. *Biochemistry*, **39**, 14138-14149.

Urbatsch, I.L., Sankaran, B., Bhagat, S. and Senior, A.E. (1995a) Both P-glycoprotein nucleotide-binding sites are catalytically active. *J Biol Chem*, **270**, 26956-26961.

Urbatsch, I.L., Sankaran, B., Weber, J. and Senior, A.E. (1995b) P-glycoprotein is stably inhibited by vanadate-induced trapping of nucleotide at a single catalytic site. *J Biol Chem*, **270**, 19383-19390.

Urbatsch, I.L., Tyndall, G.A., Tombline, G. and Senior, A.E. (2003) P-glycoprotein catalytic mechanism: studies of the ADP-vanadate inhibited state. *J Biol Chem*, **278**, 23171-23179.

Urlinger, S., Kuchler, K., Meyer, T.H., Uebel, S. and Tampé, R. (1997) Intracellular location, complex formation, and function of the transporter associated with antigen processing in yeast. *Eur J Biochem*, **245**, 266-272.

Ustrell, V., Pratt, G. and Rechsteiner, M. (1995) Effects of interferon gamma and major histocompatibility complex-encoded subunits on peptidase activities of human multicatalytic proteases. *Proc Natl Acad Sci U S A*, **92**, 584-588.

van Endert, P.M. (1999) Role of nucleotides and peptide substrate for stability and functional state of the human ABC family transporters associated with antigen processing. *J Biol Chem*, **274**, 14632-14638.

van Endert, P.M., Saveanu, L., Hewitt, E.W. and Lehner, P. (2002) Powering the peptide pump: TAP crosstalk with energetic nucleotides. *Trends Biochem Sci*, **27**, 454-461.

van Endert, P.M., Tampé, R., Meyer, T.H., Tisch, R., Bach, J.F. and McDevitt, H.O. (1994) A sequential model for peptide binding and transport by the transporters associated with antigen processing. *Immunity*, **1**, 491-500.

van Veen, H.W., Margolles, A., Muller, M., Higgins, C.F. and Konings, W.N. (2000) The homodimeric ATP-binding cassette transporter LmrA mediates multidrug transport by an alternating two-site (two-cylinder engine) mechanism. *EMBO J*, **19**, 2503-2514.

Verdon, G., Albers, S.V., van Oosterwijk, N., Dijkstra, B.W., Driessen, A.J. and Thunnissen, A.M. (2003) Formation of the productive ATP-Mg2+-bound dimer of GlcV, an ABC-ATPase from Sulfolobus solfataricus. *J Mol Biol*, **334**, 255-267.

Werber, M.M., Peyser, Y.M. and Muhlrad, A. (1992) Characterization of stable beryllium fluoride, aluminum fluoride, and vanadate containing myosin subfragment 1-nucleotide complexes. *Biochemistry*, **31**, 7190-7197.

Williams, A., Peh, C.A. and Elliott, T. (2002) The cell biology of MHC class I antigen presentation. *Tissue Antigens*, **59**, 3-17.

Yang, R., Cui, L., Hou, Y.X., Riordan, J.R. and Chang, X.B. (2003) ATP binding to the first nucleotide binding domain of multidrug resistance-associated protein plays a regulatory role at low nucleotide concentration, whereas ATP hydrolysis at the second plays a dominant role in ATP-dependent leukotriene C4 transport. *J Biol Chem*, **278**, 30764-30771.

York, I.A., Chang, S.C., Saric, T., Keys, J.A., Favreau, J.M., Goldberg, A.L. and Rock, K.L. (2002) The ER aminopeptidase ERAP1 enhances or limits antigen presentation by trimming epitopes to 8-9 residues. *Nat Immunol*, **3**, 1177-1184.

York, I.A., Roop, C., Andrews, D.W., Riddell, S.R., Graham, F.L. and Johnson, D.C. (1994) A cytosolic herpes simplex virus protein inhibits antigen presentation to CD8+ T lymphocytes. *Cell*, **77**, 525-535.

Yuan, Y.R., Blecker, S., Martsinkevich, O., Millen, L., Thomas, P.J. and Hunt, J.F. (2001) The crystal structure of the MJ0796 ATP-binding cassette. Implications for the structural consequences of ATP hydrolysis in the active site of an ABC transporter. *J Biol Chem*, **276**, 32313-32321.

Zhou, T., Radaev, S., Rosen, B.P. and Gatti, D.L. (2000) Structure of the ArsA ATPase: the catalytic subunit of a heavy metal resistance pump. *EMBO J*, **19**, 4838-4845.